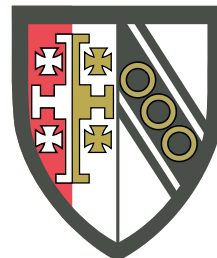


The Interplay of RSV and IFITs

Do they fit together? Ha ha



Michal Varga

Supervisor: Prof. Ian Brierley

Dr. Dalan Bailey

Dr. Trevor Sweeney

Department of Pathology
University of Cambridge

This dissertation is submitted for the degree of
Doctor of Philosophy

Selwyn College

December 2023

Declaration

This thesis is the result of my own work and includes nothing which is the outcome of work done in collaboration except as declared in the preface and specified in the text. I further state that this work is not substantially the same as any work that has already been submitted before for any degree or other qualification except as declared in the preface and specified in the text. It does not exceed the prescribed word limit for the 60,000 (excluding appendices, bibliography, footnotes and tables) by the Degree Committee.

Abstract

Introduction

Methods

Results

Discussion

Acknowledgments

sdfgsdfgsdfg

Table of contents

List of figures

List of tables

Chapter 1

Introducion

1.1 Interferon-Induced Proteins with Tetratricopeptide Re-peats

The interferon-induced proteins with tetratricopeptide repeats (*IFIT*) gene family are interferon-stimulated genes (ISGs) that are activated early in antiviral response. In unstimulated cells, with the exception of some myeloid cell subsets, they are barely detectable; however, upon viral infection their translated products become some of the most abundant proteins in the cell (**Diamond2013TheProteins**). *IFITs* are conserved in higher animals yet absent in the genomes of plants, insect, and yeast.

With regards to their genomic composition, they are composed of two exons, the first encoding the ATG, two additional nucleotides and a 5' untranslated region (UTR), with the second exon containing the rest of the coding sequence and 3'UTR (**deVeer1998IFI60/ISG60/IFIT4Genes**). Most of the IFIT family gene members contain multiple copies of specific sequences in their promoter regions called interferon-stimulated response elements (IRSE), which are targets for downstream effectors of the interferon signalling cascade, enabling the fast activation of IFIT gene transcription (**Lou2009Ifr-9/stat2Stat1**).

Most mammalian IFIT genes are categorised into 4 subgroups named IFIT1, IFIT2, IFIT3, and IFIT5 all with clear orthologous relationships (**Sarkar2004NovelGenes**). Primates, along with some other mammalian species have a duplication of IFIT1 called IFIT1B, which lacks the ISRE in its gene promoter regions. Several rodents including mice and rats have lost the IFIT1 and IFIT5 genes and have duplications of IFIT1B and IFIT3 (**Daugherty2016Evolution-guidedMammals**.) resulting in IFIT1B (typically referred to as IFIT1), IFIT1B-like gene 1, IFIT1B-like 2 gene, IFIT3 and IFIT3B genes. In con-

Introducion

trast, avian species have lost most IFIT genes, with only one left resembling human IFIT5 (**Liu2013Lineage-SpecificFamily**). These variations in IFIT gene numbers are most probably the result of differing evolutionary pressures posed by different viruses affecting their respective host species, although it is evident that maintaining IFIT genes in the genome must be beneficial.

1.1.1 Routes of *IFIT* Expression Activation

1.1.1.1 Interferon Signalling

IFIT induction can be achieved by activating several arms of the innate immune system (Figure ??). The strongest inducers are type I interferons, such as Interferon alpha and beta (IFN α/β). Their signalling is mediated via activation of IFN α/β receptor and the subsequent downstream Janus kinase (JAK), and Signal transducer and activator of transcription (STAT) signal transduction. As a result, interferon-stimulated gene factor 3 (ISGF3), consisting of phosphorylated STAT1 and STAT2 proteins bound to interferon regulatory factor (IRF) IRF9, translocates to the nucleus, binds to the ISRE in the IFIT promoters and induces their transcription (**Der1998IdentificationArrays; Mesev2019DecodingInfection; Schoggins2011Interferon-stimulatedFunctions**).

1.1.1.2 Pattern Recognition Receptors

Another arm of *IFIT* activation is mediated through several pattern recognition receptors (PRRs), which can recognise various pathogen-associated molecular patterns (PAMPs). *IFITs* have been reported to be induced by bacterial PAMPs such as lipopolysaccharide (LPS) from *Neisseria meningitidis* via activation of Toll-like receptor (TLR) 4 (**Zhou2013InterferonDefense**). Interestingly, TLR4 has also been observed to be activated by the glycoprotein of respiratory syncytial virus (RSV) (**Funchal2015RespiratoryNeutrophils**). Other TLRs such as TLR3, TLR7, and TLR9 are capable of sensing PAMPs in the form of foreign nucleic acids in the endosomes. TLRs then interact with their adaptor proteins to in turn activate IRF3, IRF7, and nuclear factor kappa B (NF κ B), all of which have the capability to induce *IFIT* family genes (**Diamond2013TheProteins**). These pathways are often prevalent in lymphocytes, monocytes, and mast cells; however, cytosolic nucleic acid sensors are functional in a broader subset of cells (**Ablasser2011WhereFit**).

1.1 Interferon-Induced Proteins with Tetratricopeptide Repeats

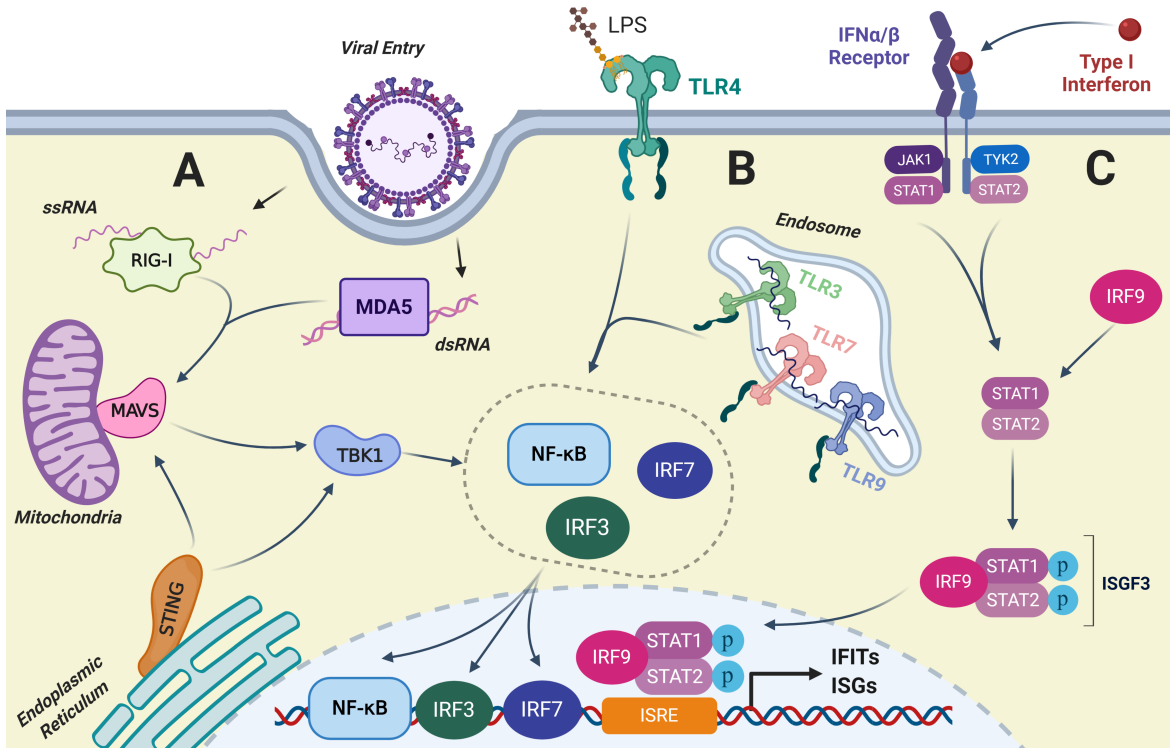


Figure 1.1: Pathways Inducing ISG mRNA Production. Three routes of ISG mRNA production are depicted. Pathway A shows virus releasing its genome upon its entry and subsequent foreign nucleic acid detection by cytosolic sensors RIG-I and MDA5. These detect single-stranded and double-stranded RNA respectively. Both activate MAVS, which in turn activates TBK1. STING protein facilitates this activation by enhancing MAVS and TBK1 interaction. Pathway B shows PAMP detection by TLR receptors. TLR4 recognises LPS in the extracellular space while TLR3, TLR7, and TLR9 detect foreign nucleic acids in endosomes. TBK1, as well as TLR activation, leads to translocation of activated IRF3, IRF7, and NF κ B into the nucleus where they promote ISGs transcription activation. Pathway C depicts type 1 interferon signalling pathway. IFN α / β receptor activation leads to STAT1 and STAT2 activation. Further addition of IRF9 forms ISGF3 complex, which translocates into the nucleus onto ISRE and promotes ISGs transcription activation. ISG, interferon-stimulated genes; RIG-I, retinoic acid-inducible gene-I; MDA5, melanoma differentiation-associated gene 5; MAVS, mitochondrial antiviral signalling protein; TBK1, TANK-binding kinase 1; STING, stimulator of interferon genes; PAMP, pathogen-associated molecular pattern; TLR, toll-like receptor; IRF, interferon regulatory factor; NF κ B, nuclear factor kappa B; IFN, interferon; STAT, signal transducer and activator of transcription; ssRNA, single-stranded RNA; dsRNA, double-stranded RNA; ISGF, interferon-stimulated gene factor; ISRE, interferon-stimulated response elements. The figure was adapted from Diamond and Farzan, (2013) and Natalya Odoardi's BioRender template. Created with BioRender.com.

Introducion

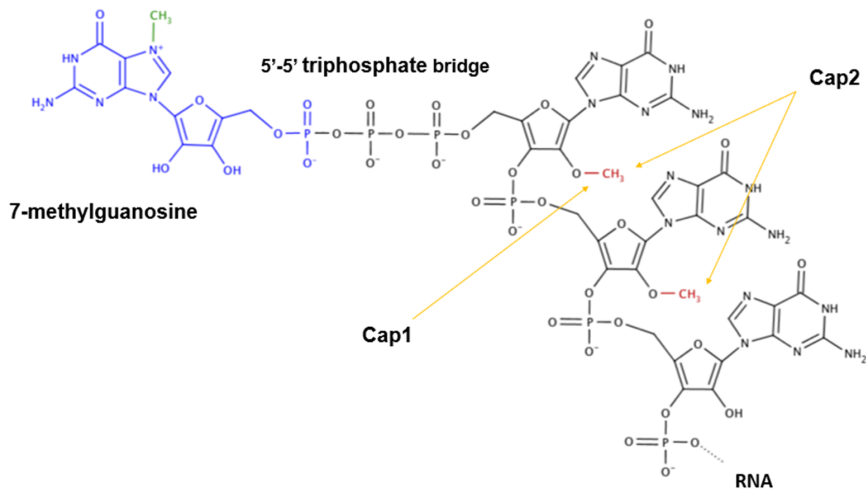
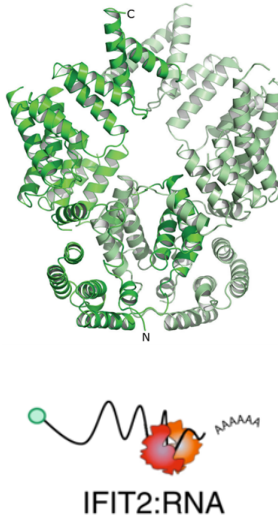


Figure 1.2: Overview of 5'RNA Modifications. Mature mRNA is displayed. Higher eukaryotes modify their mRNA by the initial addition of guanosine (blue) via 5' - 5' triphosphate bridge to the 5' end. Subsequently, the guanosine is methylated into 7-methylguanosine (green) and this modification is referred to as Cap0 structure. Furthermore, the first 2 bases of RNA can be methylated (red) and make either Cap1 or Cap2 structural modification (yellow arrows). The figure was adapted from **Picard-Jean2013RNAGenomes**.

1.1.1.3 Cytosolic Nucleic Acid Sensors

Cytosolic RNA sensors include melanoma differentiation-associated gene 5 (MDA5) and retinoic acid-inducible gene I (RIG-I) (**Vladimer2014IFITs:Proteins**). Both signal through mitochondrial antiviral signalling protein (MAVS), which in turn activates IRF3, IRF7, and NF κ B as their downstream effectors (**Ashley2019Interferon-IndependentCytomegalovirus**). In order to prevent activation by cellular RNA molecules, a precise RNA-recognition mechanism has to be conducted by the sensors. While MDA5 senses long double-stranded RNA (dsRNA) (**Brisse2019ComparativeMDA5**), RIG-I is able to sense differences in the 5' RNA modifications (**Schlee2016DiscriminatingSensing**). During mRNA maturation in higher eukaryotes, 7-methyl guanosine (m7G) is connected by a 5 to 5 triphosphate bridge, which is referred to as capping (**Devarkar2016StructuralRIG-I; Ramanathan2016MRNAApplications**). Several viruses carry uncapped, 5'-triphosphorylated (5'-PPP) or incompletely capped RNA (cap 0), whereas host animals possess cap-1 and cap-2 mRNA moieties (**Choi2018ACaps**), which are all depicted in Figure ???. IFITs can be activated by several signal transduction pathways, each with its own inducers and kinetics. A cross-play of these pathways is what in turn orchestrates IFIT response during viral infection.

1.1 Interferon-Induced Proteins with Tetratricopeptide Repeats



1.1.2 Structural Features of IFIT Proteins

IFITs are composed of multiple copies of tetratricopeptide repeats (TPR). These are motifs comprised of 3-16 tandem repeats of 34 amino acids, which adopt helix-turn-helix confirmations (**DAndrea2003TPRHelix**). TPRs are conserved in all species from bacteria through plants to higher animals and are commonly found in scaffolding proteins (**Vladimer2014IFITs:Proteins**). IFIT TPRs are comprised of degenerate sequences meaning the conservation of the motif is limited. This allows different IFIT proteins to have a broader profile of protein interactors while still maintaining the overall conformation (**Fensterl2015Interferon-InducedPathogenesis**). IFIT proteins are often subjected to post-translational modifications such as ubiquitination or ISGylation (addition of small IFN-induced ubiquitin-like proteins), which may alter IFIT stability and function.

1.1.2.1 IFITs Act as Non-Self RNA Sensors

IFIT1 and IFIT5 both form a positively charged channel with an affinity for 5' ends of single-stranded RNA (ssRNA) molecules in a sequence non-specific manner. IFIT5 can accommodate 5'PPP RNA and effectively acts as a sensor for these molecules (**Abbas2013StructuralProteins; Pichlmair2011IFIT1RNA**). On the other hand, IFIT1 can accommodate m7G, but certain residues inside its channel prevent efficient binding of cap1 and cap2 moieties (**Diamond2014IFIT1:Translation; Mears2018BetterResponse**).

PUT MORE ON IFIT2!! PUT MORE ON IFIT2!! PUT MORE ON IFIT2!! PUT MORE
ON IFIT2!! PUT MORE ON IFIT2!! PUT MORE ON IFIT2!!

Introducion

1.1.2.2 Formation of IFIT Protein Complexes

As shown in Figure ??, all IFIT proteins, apart from IFIT5, can form homo- and heterodimeric and trimeric complexes. IFIT1 homodimerizes via its C-terminal domain (**Abbas2013StructuralProtein**). The same domain has been shown to interact with the C termini of both IFIT2 and IFIT3, although the IFIT1:IFIT3 complex is more thermodynamically stable (**Fleith2018IFIT3RNA**). Compared to IFIT1, IFIT5 has its dimerization motif shielded by its C terminal TPR and thus stays monomeric in solution (**Kumar2014InhibitionMRNAs**). In contrast, IFIT2 and IFIT3 are rarely seen as monomeric in solution and rather stay as their respective homodimers or IFIT2:3 heterodimers. This is predicted to be done by swapping the third TRP domain in their N-terminal domains (Figure ??), which keeps them in a more thermodynamically stable configuration (**Yang2012CrystalMechanisms**). IFIT2 homodimer forms a large positively charged cavity which has a propensity to bind dsRNA and AU-rich RNA molecules (**Vladimer2014IFITs:Proteins**; **Yang2012CrystalMechanisms**). IFIT3 interacts with IFIT1 via its C-terminal domain and this interaction increases the half-life of IFIT1 and its specificity for cap0 RNA. Thus, IFIT3 acts as an enhancer of IFIT1 action (**Fleith2018IFIT3RNA**; **Johnson2018HumanStability**). Recently, it has been shown that IFIT1, IFIT2, and IFIT3 form a heterotrimer, although the precise function of this complex has yet to be elucidated (**Fleith2018IFIT3RNA**). In summary, TPR motifs allow IFITs to have a multitude of possible interaction partners, including themselves. Formation of IFIT homo- and hetero-oligomers influences their function and half-life, allowing for variable possible outcomes to occur following IFIT protein production based on the level of each of the proteins.

1.1.3 Functions of IFIT Proteins

1.1.3.1 Inhibition of Translation and Viral Replication

IFITs can restrict viral replication by several mechanisms. IFIT1 and IFIT5 can physically prevent non-self RNA from interacting with eukaryotic initiation factor (eIF) 4F (**Kumar2014InhibitionMRNAs**). IFIT1 and 2 block the binding of eIF3 to the eIF2–GTP–Met-tRNA ternary complex by interacting with the eIF3E subunit, whereas human IFIT2, and mouse IFIT1 and IFIT2, can block the formation of the 43S–mRNA complex by binding to the eIF3C subunit (**Diamond2014IFIT1:Translation**; **Guo2000CharacterizationVirus**). This is a cap-independent mechanism for viral translation inhibition, however, extensive IFIT expression can negatively influence the whole cellular translation processes via this mechanism and can hinder normal inflammatory responses. Overexpression of IFIT1 in

1.1 Interferon-Induced Proteins with Tetratricopeptide Repeats

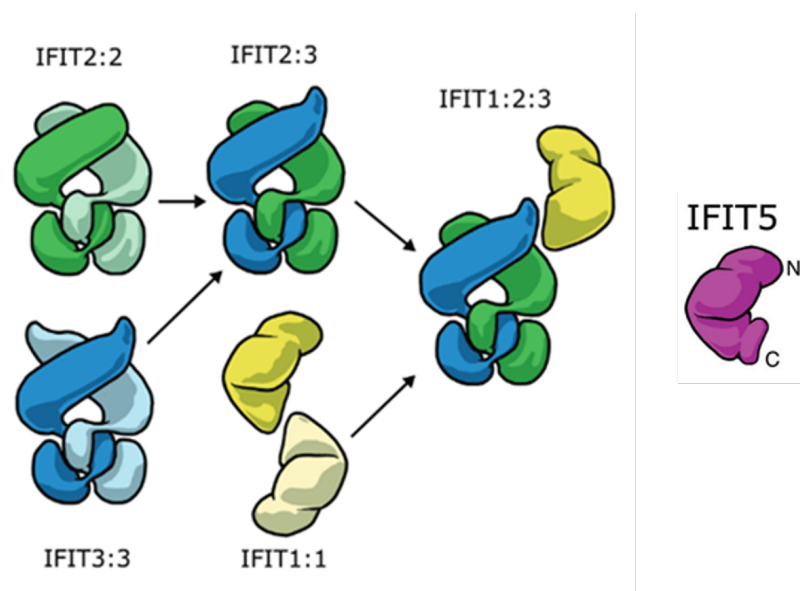


Figure 1.3: IFIT Structures and Multimer Formation. IFIT tertiary and quaternary protein conformations are illustrated. IFIT1 is shown in yellow, IFIT2 in green, IFIT3 in blue, and IFIT5 is highlighted in purple. IFIT1 is able to homodimerise or heterooligomerise with IFIT2 and IFIT3 via its C terminal domain. IFIT5 has the corresponding interaction domain occluded by a helix and thus does not interact with the rest of IFIT proteins. IFIT2 and IFIT3 are capable of forming homodimers or heterodimers by ‘swapping’ TPRs in their N terminal regions. By combining the interactions IFIT1:2:3 heterotrimer is formed. The figure was adapted from [Mears2018BetterResponse](#).

Introducion

human embryonic kidney (HEK) 293T cells inhibited the activation of IRF3 and NF κ B and the transcription of IFN β in response to polyinosinic–polycytidylic acid (poly I:C) (**Li2009ISG56Response**). The previously mentioned affinity of IFIT2 for AU-rich RNA can also regulate cellular translation as a lot of transcripts for cytokines or apoptotic factors are rich in adenine and uracil (**Palanisamy2012ControlMicroRNAs**).

1.1.3.2 Modulation of Innate Immune Response Signalling

IFIT proteins also have the potential to influence innate immune responses by direct interaction with signalling cascade proteins. IFIT3 can potentiate RIG-I signalling by forming a scaffold between MAVS and TANK-binding kinase 1 (TBK1), (**Liu2011IFN-InducedTBK1**), whereas IFIT5 enhances this pathway upstream by recruiting RIG-I to MAVS (**Zhang2013IFIT5Pathways**). IFIT5 has also been reported to help facilitate NF κ B activation via scaffolding its activation kinases (**Zhang2013IFIT5Pathways**). On the other hand, studies show that IFIT1 can both negatively and positively influence RIG-I signalling, upstream of MAVS. IFIT1 interacts with the stimulator of interferon genes (STING), an enhancer of MAVS and TBK1 interaction and it was proposed that these conflicting actions are caused by its multiple binding sites on STING (**Li2009ISG56Response; Reynaud2015IFIT1Interferon**).

1.1.3.3 Effects on Cell Cycle Progression and Apoptosis

IFIT2 and IFIT3 also have roles in cellular homeostasis. IFIT2 overexpression induces the mitochondrial-dependant apoptotic pathway. IFIT2 has been shown to localise on mitochondrial membranes and to directly interact with pro-apoptotic factors which leads to apoptosome formation and subsequent caspase-9 activation (**Chen2017InhibitionApoptosis; Diamond2013TheProteins**). Expression of IFIT3 has been observed to alleviate these effects, most probably by the formation of IFIT2:3 dimers (**Mears2018BetterResponse; Stawowczyk2011TheApoptosis**). IFIT3 has also been observed to have negative effects on proliferation via indirect degradation of cyclin-dependant kinase inhibitor p27. As a result, cell cycle progression halts at G1/S transition checkpoint (**Xiao2006RIG-GProteins**). An overview of the IFIT mechanisms of action is depicted in Figure ??.

Therefore, IFITs not only act as complementary RNA sensors to RIG-I but are also important as mediators of a plethora of other processes. These range from regulation of transcription, activation and inhibition of innate immune signalling, and regulation of cell life cycle. It is again possible that preference for these actions is influenced by the levels of particular IFIT proteins and their interplay. Taking into consideration the above-described

1.1 Interferon-Induced Proteins with Tetratricopeptide Repeats

modes of IFIT expression activation, we can speculate that different stimuli such as viruses or signalling molecules at different concentrations will result in quite diverging actions of IFIT proteins on the phenotype of the cell.

1.1.4 IFIT During Cancer and Sepsis

1.1.5 IFIT Responses to Viral Infections

1.1.5.1 Human IFIT Responses to RNA Viruses

Human IFIT effects on single-stranded RNA viruses have been studied extensively within the past decade. **Rabbani2016Identification3** reported that IFIT1 and IFIT3 restrict human parainfluenza virus 3 (PIV3, negative-sense ssRNA virus), while ectopic expression of IFIT2 and IFIT5 did not affect the viral fitness. *In vitro* IFIT1 knock-down experiments using short hairpin RNA showed marked enhancement of protein expression of human PIV2, PIV5, and mumps virus, all negative-sense ssRNA viruses (**Andrejeva2013ISG56/IFIT1Synthesis; Young2016HumanFamily**). Hantaviruses, a family of negative-sense ssRNA viruses such as Prospect Hill virus (PHV), and Tula virus (TULV), strongly induce IFIT3 expression during the course of their infection (**Matthys2011TheInduction**). Another negative-sense ssRNA virus, which bears a segmented genome, influenza A virus, has been shown to upregulate IFIT1, IFIT2, and IFIT3 in primary macrophages during infection (**Lietzen2011QuantitativeMacrophages**). Human IFIT1 has been observed to be differentially expressed during hepatitis C virus (HCV) infection. HCV was described to suppress IFIT1 upregulation and subsequent experiments showed an inverse relationship between artificial levels of IFIT1 and HCV ability to infect host cells (**Raychoudhuri2011ISG56Replication**).

Introducción

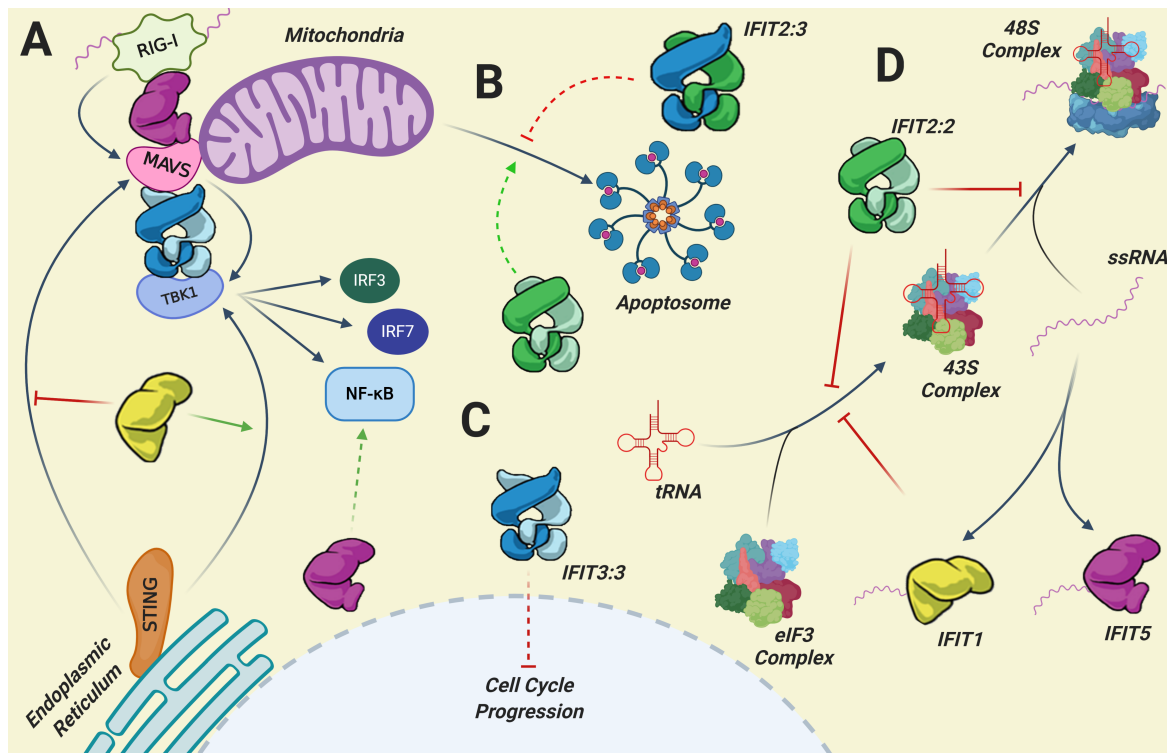


Figure 1.4: Overview of IFIT Mechanisms of Action. IFITs have been described to have multiple actions in cells. Pathway A shows their involvement in innate immune signalling modulation. IFIT5 potentiates RIG-I activation of MAVS by scaffolding the two proteins together. IFIT3:3 further scaffolds MAVS to its effector, TBK1, which induces IRF3, IRF7 and NF κ B nuclear translocation when activated. STING protein also potentiates MAVS and TBK1 interaction. IFIT1 has been observed to inhibit STING interaction with MAVS while potentiating its interaction with TBK1. IFIT5 can also indirectly activate NF κ B. Pathway B shows IFIT2:2 involvement with apoptosisome formation. IFIT2:3 complex reduces the pro-apoptotic activity of IFIT2:2. IFIT3:3 is involved in cell cycle arrest, as depicted in pathway C. Pathway D shows IFIT inhibition of viral replication and cellular translation. IFIT1 and IFIT5 can directly bind to cap0 and 5'PPP mRNA respectively and prevent its translation. IFIT1 and IFIT2 can both prevent 43S complex formation, while IFIT2 can also inhibit 48S complex formation. IFIT, Interferon-Induced Protein with Tetratricopeptide Repeats; RIG-I, retinoic acid-inducible gene I; MAVS, mitochondrial antiviral signalling protein; TBK1, TANK-binding kinase 1; STING, stimulator of interferon genes; IRF, interferon regulatory factor; NF κ B, nuclear factor kappa B; eIF, eukaryotic elongation factor; ssRNA, single-stranded RNA; tRNA, transfer RNA. The figure was adapted from **Mears2018BetterResponse** and **Diamond2013TheProteins**. Created using BioRender.com.

1.1.5.2 Livestock IFIT Responses to Viral Infections

Data on livestock IFIT responses to viral infections is currently limited. Bovine viral diarrhoea virus (BVDV), a positive-sense ssRNA virus has been shown to inhibit IFIT1 and IFIT3 expression in bovine endometrium, compared to IFN Tau treatment, however, levels of IFIT2 and IFIT5 were not assessed (**Cheng2017AcuteEndometrium**). Segmented dsRNA virus Blue tongue 16 has been shown to induce both sheep and goat IFIT1, IFIT2, and IFIT3 proteins in peripheral mononuclear cells, although the level of induction and induction dynamics varied between the species. Although sheep and goat IFIT proteins exhibit high interspecies IFIT protein similarity (97-99% amino acid identity) their functional roles, binding partners, promoter activation, and structure may differ between them. Lastly, porcine reproductive and respiratory syndrome virus was shown to activate IFIT1 and IFIT3 in porcine alveolar macrophages and IFIT1 and IFIT5 in the lung. This further shows that IFIT responses are dependent on cell type and the tissue of origin (**Xiao2010AberrantProfiling**; **Zhou2011MolecularVivo/i**). As presented above, it is clear that there is an abundance of human IFIT response data with regards to RNA viruses, however, there is a need to better define livestock IFIT responses.

1.1.6 Comparison between human and bovine

Structural comparison

Genomic comparison

1.2 Respiratory Syncytial Virus

Human and bovine respiratory syncytial virus (RSV) cause acute respiratory illness in their respective host species and thus cause a large economic burden for the healthcare system and livestock industry alike (**Jha2016RespiratoryVirus**; **Sacco2014RespiratoryCattle**). To date, there is a limited knowledge of how IFITs impact on the replication of RSV.

Bovine and human RSV are enveloped viruses possessing negative-sense ssRNA genome approximately 15 kilobase-pairs in size. Upon viral attachment and entry, the genome is released into the cytoplasm in the form of a ribonucleoprotein i.e. a complex of RSV genome with its nucleoprotein (N protein) (**Noton2015InitiationReplication**). Viral replication also requires the RNA-dependent RNA polymerase (L protein) and the phosphoprotein (P protein), whereas RSV transcription also requires M2-1 protein, which is hypothesised to prevent premature termination of this process (**Tanner2014CrystalPhosphorylation**).

Introducion

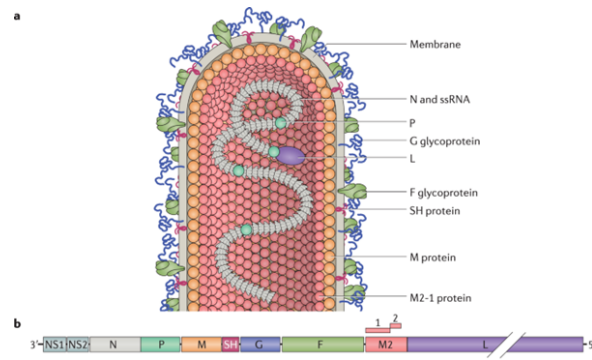
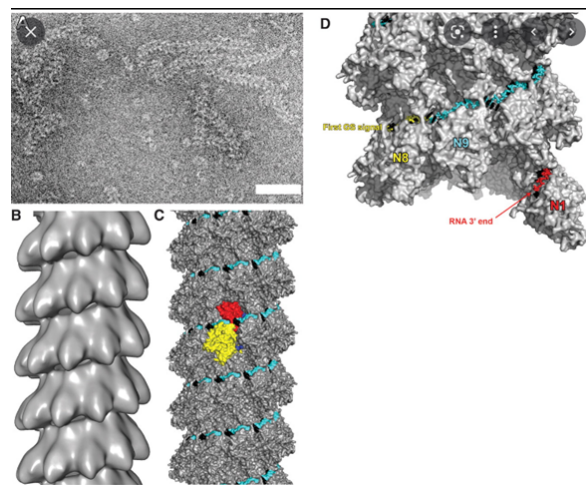


Figure 1.5: Enter Caption



RSV transcripts are modified with 5' cap structures prior to their translation. Both viral replication and transcription were previously believed to happen diffusely throughout the cytoplasm; however, recent studies suggest viral inclusion bodies (IBs) are the main site for RSV replication and transcription (**Rincheval2017FunctionalVirus**).

1.2.1 Disease

dfasdfasdf

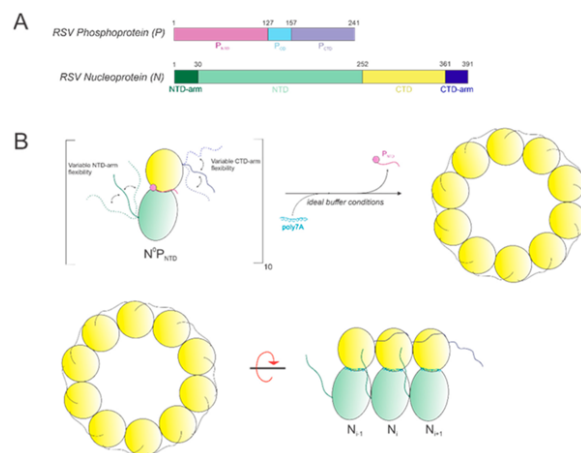
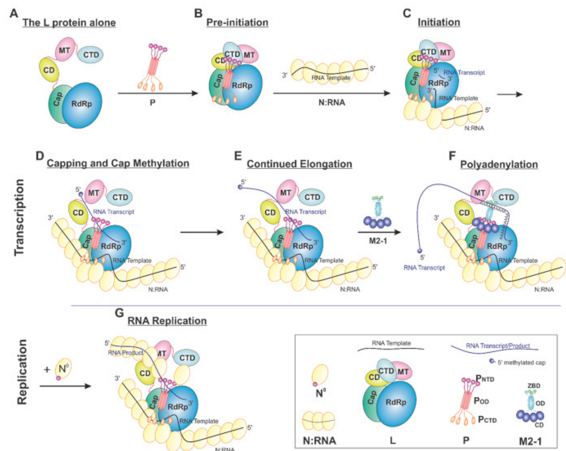
1.2.2 Composition

asdfasdf

1.2.3 Life Cycle

asdfasdf

1.2 Respiratory Syncytial Virus



Introducion

1.2.4 RSV Inclusion Bodies

IBs are amorphous membranelles aggregates, which have been observed to form as early as 6 hours post-infection and often localise in close proximity to the nucleus (**Bachi1973MorphogenesisVirus; Jobe2020RespiratorySignaling**). They have characteristics of biomolecular condensates (with a similar electron density under electron microscopy to the nucleoli) and resemble cytoplasmic inclusions associated with other viral infections e.g. Negri bodies forming during rabies virus infection (**Nikolic2017NegriOrganelles**). RSV N and P proteins are found on the edges of IBs, while L and M2-1 proteins are located inside the structure. (**Rincheval2017FunctionalVirus**), using super-resolution imaging, discovered internal IB compartments called IB-associated granules (IBAGs). These not only contained different viral proteins compared to the rest of the IB, but nascent RNA labelling also suggested IBAGs to be the sites where newly synthesized mRNA concentrates (**Jobe2020RespiratorySignaling; Richard2018RSVTranscription**). Taken together, data suggests that IBs are specialised sites which enable viral replication and transcription and that these processes may be compartmentalised.

It is currently unknown if IFIT proteins interact with these structures. Given the well-described roles of IFITs in sensing viral RNA, it is possible that different IFITs may localise into IBs and IBAG, potentially interacting with viral RNA before the capping process takes place or directly interfere with the translational machinery. It is also possible that IFITs are restricted from accessing IBs by an unknown mechanism. Understanding these processes may reveal novel routes of increasing viral sensitivity to the innate immune response.

1.2.4.1 Membrane-less Molecular Condensates and LLPS

ssdfasdfg

1.2.4.2 IBAGs

asdfasdf

1.2.4.3 Known Siphoning

asdfasdf

1.2.5 Bovine vs Human Comparison

asdfasdf

1.3 Aims of the Study

Here have a paragraph of the aims.

A detailed comparative study of human and bovine IFITs and their interaction with RSV. Looking at their induction, expression, and changes in localisation. Looking at interaction with RSV IBs. Assessing the involvement of IFIT2 in the RSV life cycle.

Chapter 2

Materials and Methods

2.1 Cell Culture

2.1.1 Cell Culture Conditions

All cell lines listed in Table ?? were cultured in cell culture flasks (Corning) at 37°C in a 5% CO₂ atmosphere. All cell lines with the exception of BEAS-2B were maintained in complete Dulbecco's Modified Eagle's Medium (DMEM; Sigma-Aldrich) supplemented with 10% Foetal Bovine Serum (FBS, Sigma-Aldrich), 1% L-Glutamine (Sigma-Aldrich) and 1% penicillin and streptomycin mixture (ThermoFisher). BEAS-2B cell line was cultured in LHC basal medium (ThermoFisher), supplemented with 10% FBS (Sigma-Aldrich), 1% L-Glutamine (Sigma-Aldrich) and 1% penicillin and streptomycin mixture (ThermoFisher).

Cell Line	Description	Source
VERO	monkey kidney epithelial cells	The Pirbright Institute's Central Services Unit (CSU)
A549	human alveolar epithelial cancer cells	
HEK293T	human embryonic kidney cells	
MDKB	Madin-Darby bovine kidney cells	
BT	bovine turbinate epithelial cells	
HeLa	human uterine epithelial cancer cells	
BEAS-2B	human bronchial epithelial cells	ATCC

Table 2.1: Cell lines used in this study.

Materials and Methods

Name	Provider	Product Number
Human IFN α	Sigma-Aldrich UK	SRP4596
Bovine IFN α	Bio-Techne Ltd.	RP0008B-025
Human IFN γ	PeproTech, Inc.	300-02
Bovine IFN γ	Cambridge Bioscience	2300-BG-025
LPS	Sigma-Aldrich UK	L4391-1MG
Poly I:C	Sigma-Aldrich UK	P1530-25MG

Table 2.2: Activators of the Innate Immune System.

2.1.2 Passaging and Seeding Cells

All cell lines were grown until 80% confluent, at which point the growth media was removed and cells were washed with sterile Phosphate Buffered Saline (PBS). Cells were detached from the flasks using Trypsin/EDTA solution (Life Technologies). After complete detachment, cells were diluted in complete media and 5% of the cells were transferred to a new flask for further passaging. The remaining cells were used for seeding for experiments.

2.1.3 Transfecting Cells

Plasmids were transfected to well-adhered cells (>6 hours post seeding) using TransIT-X2 (Geneflow). Plasmid DNA was diluted in Opti-MEM (ThermoFisher), TransIT-X2 was added in 1:2 ratio (μ g of DNA to μ L of TransIT-X2), vortexed and then incubated at room temperature for 40 minutes. The transfection mix was added dropwise to cells and incubated at 37°C and 5% CO₂ for the required times to allow protein expression.

2.1.4 Treatment with the Activators of Innate Immune System

Several known activators of the innate immune system were used for cellular treatment (see Table ??). These were human and bovine interferon-alpha and gamma (IFN), *E. Coli* lipopolysaccharide (LPS) and polyinosinic:polycytidylic acid (poly I:C). 2 μ g of poly I:C was transfected as described in Section ?? and incubated for 24 hours. Concentrations used for bovine IFN α were 0.5 and 5 ng/mL with an incubation of either 3, 6 or 24 hours. Human IFN α was used in the concentration of 1000 units per mL, with the incubation time of 6 or 24 hours. Human IFN γ was used in concentrations of 500, 1000, and 2000 units per mL for a duration of 6 hours. LPS was used in a concentration of 5 and 5000 μ g/mL for human cell lines and concentrations of 0.5, 1, 2.5, 5, and 10 for the bovine cell lines, for a duration of 6 hours.

2.2 Virus Work

2.2.1 Virus Propagation and Production

Viruses (outlined in Table ??) were propagated in the VERO cell line. 70% confluent T175 cell culture flask was incubated with 0.01 multiplicity of infection (MOI) concentration of virus of choice diluted in serum-free cell culture medium for 2 hours. Afterwards, the virus-containing media was washed away with PBS and cells were incubated in 2% serum-containing growth media for 72 hours. After, cells were scraped into the media and the viral particles were liberated from cytoplasm by sonication. This was done at 70% amplitude and 1 second long on and off pulses. Cell debris was separated by centrifugation at 2900 g for 30 minutes at 4°C. The supernatant was either snap-frozen in a dry ice ethanol mixture and stored at -80°C as crude extracted virus or was further purified. Further ultracentrifugation purification was conducted to ensure that all cytokines, chemokines, and other stimulants are removed from the viral stock. Crude extracted supernatants were mixed with MgSO₄ (Sigma), 50% (w/v) polyethylene glycol (PEG) 6000 (Sigma) in NT buffer (100mM MgSO₄, 150 mM NaCl (Sigma), 1mM EDTA (Invitrogen), 50 mM Tris-HCl (Sigma), pH 7.5) and serum-free DMEM to a final concentration of 100 mM, 10% and 2.3% (v/v) respectively. The solution was thoroughly mixed with a magnetic stirrer at 4°C for 90 minutes to precipitate the viral particles. Afterwards, the particles were pelleted by centrifugation at 2900 g for 20 minutes at 4°C and resuspended in 700 μL 4°C NT buffer. Finally, viral particles were separated and concentrated by ultracentrifugation at 32,000 rpm at 4°C for 1.5 hours in the SW-32 rotor on a discontinuous sucrose gradient. The gradient was prepared by sequential layering and freezing at -80°C 60%, 45%, and 30% sucrose (Sigma) in NT buffer, placed in Ultra-Clear 14x95 mm centrifuge tubes (Beckman Coulter UK Ltd). The outcome was two viral bands (at 30-45% and 45-60% interface) which were both collected and snap-frozen in a dry ice ethanol mixture and stored at -80°C.

2.2.2 Virus Quantification by TCID₅₀ Assay

Crude or ultra-purified samples from Section ref{Virus Propagation and Production} were thawed at room temperature and serially diluted in 0% FBS DMEM in 1:10 ratios in quadruplicates with final volume of 50 μL. A TC75 cell culture flask with 100% confluent permissive cell line of choice (preferably one that will be used for subsequent experiments) was trypsinised and diluted in 100 mL of 2% FBS DMEM and 100 μL of it was dispensed per titration well. Plates were left to incubate at 37°C in a 5% CO₂ atmosphere for 4 days,

Materials and Methods

Virus name	Species	Strain	Modification	Source
hRSV	Human	A2	WT	
hRSV-GFP	Human	A2	GFP	
bRSV	Bovine	A51908	WT	
BRSV-GFP	Bovine	A51908	GFP	
bRSV ΔSH	Bovine	A51908	ΔSH	The Pirbright Institute
bRSV ΔNS1	Bovine	A51908	ΔNS1	
bRSV ΔNS2	Bovine	A51908	ΔNS2	
bRSV ΔNS1/2	Bovine	A51908	ΔNS1 & ΔNS2	

Table 2.3: Outline of Viruses Used.

after which they were analysed for the presence of cytopathic effects. This data was used to calculate the multiplicity of infection.

2.2.3 Viral Infections, UV-Inactivation and Ruxolitinib Treatment

Crude or ultra-purified samples from Section ref{Virus Propagation and Production} were thawed at room temperature. If the experimental procedure required UV-inactivation, the viral extract was placed in circular plastic dish, transferred to the UV cross-linker (COMPANY), and irradiated without the lid for 60 seconds at the power of WHATEVER. Cells at the confluence of 80% had their media removed and were washed with PBS. Afterwards, the virus diluted at the desired MOI in serum-free cell culture media was added and samples were incubated at 37°C in a 5% CO₂ atmosphere for 2 hours. Afterwards, the inoculum was removed and replaced with 2% serum cell culture medium and left to incubate at 37°C in a 5% CO₂ atmosphere. If the experimental procedure required the presence of ruxolitinib, it was mixed-in with the culture medium at 5 nM and cells were left to incubate at 37°C in a 5% CO₂ atmosphere until the end point of the experiment.

2.2.4 Viral Growth Curves

Cells infected as described in Section ?? were collected as a supernatant and cellular fraction at time intervals of 24, 48, 72, 96, 120, 144, and 168 hours post-infection, snap frozen in dry ice ethanol mixture, and later tittered as described in Section ??.

2.3 Quantitative Real Time/Reverse Transcription PCR

2.3 Quantitative Real Time/Reverse Transcription PCR

2.3.1 RNA Extraction and cDNA Synthesis

Initially, cells were washed using phosphate-buffered saline (PBS; 137 mM NaCl, 10 mM phosphate, 2.7 mM KCl, pH 7.4) after which RNA was extracted using an RNeasy Mini Kit (Qiagen). The concentration and purity of samples were assessed using the NanoDrop One spectrophotometer (Thermo Fisher). Complementary DNA (cDNA) was synthesised using Moloney Murine Leukaemia Virus Reverse Transcriptase (MMLV RT; Promega). Firstly, RNA was mixed with oligo dT primers (Sigma-Aldrich) at a 2:1 ratio and the resulting mixture was topped up with nuclease-free H₂O to a final volume of 13 µL. Denaturation, which removes any secondary structures in the samples was done by incubation at 70°C for 5 minutes, followed by a step of rapid primer annealing by incubating the samples in icy water for 2 minutes. 12 µL of reaction master mix consisting of 5 µL 10 mM dNTPs, 5 µL MMLV RT Buffer, 1 µL of RNase inhibitor and 1 µL of MMLV reverse transcriptase (Promega) was then added. Samples were then incubated at 42°C for 1 hour, after which they were diluted 1:4 using nuclease-free H₂O. As a control for DNA contamination evaluation, there was always at least one sample in which the MMLV RT was substituted with H₂O.

2.3.2 Quantitative PCR

RNA transcripts of interest were quantified using quantitative polymerase chain reaction (qPCR). Luna Universal qPCR Master Mix and Luna Universal Probe qPCR Master Mix (New England Biolabs) were used for SYBR-based and TaqMan-based qPCR, respectively. For SYBR-based method, 10 µL of Master Mix was mixed with template cDNA, 1 µL of primer set, and topped up to 20 µL by nuclease-free water. Probe-based sample preparation only differs in using 2 µL of primer/probe mix instead of the above mentioned 1 µL. Samples were run on the QuantStudio 3 Real-Time PCR System (Thermo Fisher) on a MicroAmp Fast Optical 96-Well reaction plates (Fisher Scientific), sealed with MicroAmp Adhesive qPCR plate seal (Fisher Scientific). The temperature of the metal cover on the top was set to 105°C to prevent evaporation, and plates were run on a standard thermal cycling mode as depicted in Table ???. The temperature changes between different stages were set to 1.6°C/s. During the extension step of the PCR stage, signal acquisition took place. For TaqMan-based qPCR only hold and PCR stages were run, whereas for SYBR-based qPCR the quality control step of melt curves acquisition was also conducted. During the transition from the annealing step of melt curve stage to the final step, the temperature increase was 0.1°C/s, with a continual signal acquisition.

Materials and Methods

Stage	SYBR	TaqMan	Step	Temperature	Time	Cycle
Hold	Yes	Yes	Annealing	50°C	2'	1
Hold	Yes	Yes	Initial Denaturation	95°C	10'	1
PCR	Yes	Yes	Denaturation	95°C	15"	40
PCR	Yes	Yes	Extension	60°C	60'	40
Melt Curve	Yes	No	Denaturation	95°C	15"	1
Melt Curve	Yes	No	Annealing	60°C	60"	1
Melt Curve	Yes	No	Dissociation	95°C	15"	1

Table 2.4: qPCR Cycling Conditions.

2.3.3 Primer Design and Assay Setup

To amplify specific regions of genes of interest, commercial forward-reverse primer with fluorescent probe were bought where available (see Table ??). However, there were no available primers for amplification of bovine *IFIT* genes. For this reason, these primers were designed *in silico*. Using coding DNA sequences obtained from ENSEMBL database (**Cunningham2022Ensembl2022**) and the PrimerQuest software (Integrated DNA Technologies) with its default parameters (50 mM of monovalent salt, 3 mM of bivalent salt, 0.8 mM dNTP, and 200 nM of primer DNA), 3 forward-reverse primer sets were established per bovine *IFIT* gene. Minimal, optimal and maximal values for amplicon size, GC content, melting temperature and sizes of both probes and primers are depicted in ???. Three primer sets, optimized for TaqMan, were designed per the gene of interest. The sequences can be seen in Table ???. Although the probes were not used this approach presents itself with a possibility of changing the methodology to decrease protentional false positives if needed. The rest of the targets were commercially purchased with the exception of primers for quantification of *bRSV N* gene, which are based on publication of Boxus and colleagues (**Boxus2005RealVirus**). A summary of these can be found in Table ???. For establishing efficiencies of our designed primers and for quantitative transcript characterisation, standard curves were designed for each target gene on those plates. This was done using plasmid DNA containing the gene of interest, diluted in a series of 10-fold dilutions from 10² to 10⁸ copies per sample.

2.3.4 Data Processing

Data processing, statistical analysis and graph generation was conducted R programming language (**RCoreTeam2022R:Computing**) using RStudio environment (**RStudioTeam2022RStudio:RStudio**). Tidyverse and data.table R packages (**Wickham2019WelcomeTidyverse; Dowle2022Data.table:data.frame**)

2.3 Quantitative Real Time/Reverse Transcription PCR

Target	Provider	TaqMan / SYBR
Human IFIT1	Life Technologies	TaqMan
Human IFIT2	Life Technologies	TaqMan
Human IFIT3	Life Technologies	TaqMan
Human IFIT5	Life Technologies	TaqMan
Human GAPDH	Primer Design Ltd	TaqMan
Bovine GAPDH	Life Technologies	TaqMan
Bovine Mx1	Sigma-Aldrich	SYBR
hRSV N	Sigma-Aldrich	SYBR
bRSV N	Sigma-Aldrich	SYBR

Table 2.5: Commercial qPCR Primers.

		Minimal	Optimal	Maximal
Primer	Amplicon Size (nt)	75	100	150
	Tm (°C)	59	62	65
	GC (%)	35	50	65
Probe	Size (nt)	17	22	30
	Tm (°C)	64	68	72
	GC (%)	40	50	60
	Size (nt)	20	24	30

Table 2.6: Parameters for qPCR Primer Design.

Materials and Methods

Target	Primer Set	Sense	Sequence (5'-3')
bIFIT1	1	Forward	CAGGGTCTTGGAGGAGATTATG
bIFIT1	1	Reverse	CTCTTCAGGGCTTCTTCATTCT
bIFIT1	2	Forward	CAGGCAGAAGCCCAGATTAA
bIFIT1	2	Reverse	TCCTTCCTCACAGTCCATCT
bIFIT1	3	Forward	CTGAGAGGCCAGAACATGAAGAAG
bIFIT1	3	Reverse	GTAATGCAGCCAGGCATAGT
bIFIT2	1	Forward	CAGGGATCAAAGGAAGGAGAAA
bIFIT2	1	Reverse	TCCTGAAGAACGCCAAGAG
bIFIT2	2	Forward	TTCCGTATCGGCTCCTATCT
bIFIT2	2	Reverse	GGAAGCTCTTGCTGAATTCTTT
bIFIT2	3	Forward	TGAGAAGGCTCTGGAGAAGA
bIFIT2	3	Reverse	GCTTGCCTCAAAGGTTAATG
bIFIT3	1	Forward	ACTACGCCTGGGTCTACTATC
bIFIT3	1	Reverse	TCCAGCTCAGGACATTCAATAC
bIFIT3	2	Forward	CTTGGTCTCTCCAAGGCTTAAT
bIFIT3	2	Reverse	GCTGTTCTTAGGAGGTGATCC
bIFIT3	3	Forward	CTGGATCACCTCTAAAGAACAG
bIFIT3	3	Reverse	TCGGGAAGCTCTGAGTATAG
bIFIT5	1	Forward	CCACTCGAACAGACCTAAA
bIFIT5	1	Reverse	CGTGTAGGCAAATGCAAACATA
bIFIT5	2	Forward	GCTTGAAACAAGCGGAAGAAA
bIFIT5	2	Reverse	GTCATAGTAAACCCACGCATAGT
bIFIT5	3	Forward	GGAAGAAATCATACGGCGAGAG
bIFIT5	3	Reverse	AGCTGACCCATGTCATAGTAAAC

Table 2.7: Bovine IFIT qPCR Primers.

2.3 Quantitative Real Time/Reverse Transcription PCR

$$\text{Relative Quantification} = 2^{\Delta\Delta Ct}$$

$$\Delta\Delta Ct = \Delta Ct_{\text{Test Samples}} - \Delta Ct_{\text{Calibrator Samples}}$$

$$\Delta Ct_{\text{Test Samples}} = Ct_{\text{Target Gene in Tests}} - Ct_{\text{Reference Gene in Tests}}$$

$$\Delta Ct_{\text{Calibrator Samples}} = Ct_{\text{Target Gene in Calibrator}} - Ct_{\text{Reference Gene in Calibrator}}$$

Figure 2.1: Mathematical Bases of $\Delta\Delta Ct$ Relative Quantification Method.

$$\text{Amplification Efficiency} = 10^{-1/\text{slope}} - 1$$

Figure 2.2: Amplification Efficiency Equation.

were used for data manipulation, while `ggplot` and `scales` R packages were utilised for plotting (**Wickham2019WelcomeTidyverse**; **Wickham2022Scales:Visualization**). For human *IFIT* targets and bovine *Mx1*, relative differences in transcript abundance between conditions were established using $\Delta\Delta$ cycle threshold (Ct) methodologies using internal calibrators (human and bovine *GAPDH* respectively). The formulae can be seen in Equation ???. The final values were divided by the mean control values to standardise the data. For custom-created bovine *IFIT* primer pairs described in Section ?? the absolute amount of material detected was extrapolated from standard curves, which were calculated using Equation ???. The slope of the standard curves was also assessed for the evaluation of the best candidate primer pairs to be used in subsequent experiments and as the internal control for batch variation. The internal calibrator (bovine *GAPDH*) was run alongside the bovine *IFIT* samples and was used to factorise the extrapolated values in accordance with the differential abundance of the internal calibrator detected between conditions. In other words, the $2^{-\Delta\Delta Ct}$ values from bovine *GAPDH* of different conditions were divided by the value measured in control conditions. This vector of relative abundance between conditions was applied as a factor on measured bovine *IFIT* extrapolated values, which were prior modified into a vector of relative abundances standardised to control themselves. This was all done to control for differential amplification efficiencies observed between different bovine *IFIT* primer pairs. As each experiment was standardised to the control conditions it was possible to aggregate data points from different experiments into one large dataset. Because control conditions had always a relative value of one, they were emitted from the graphs. All the other conditions are shown as a relative abundance value to the control, and in term to each other.

Materials and Methods

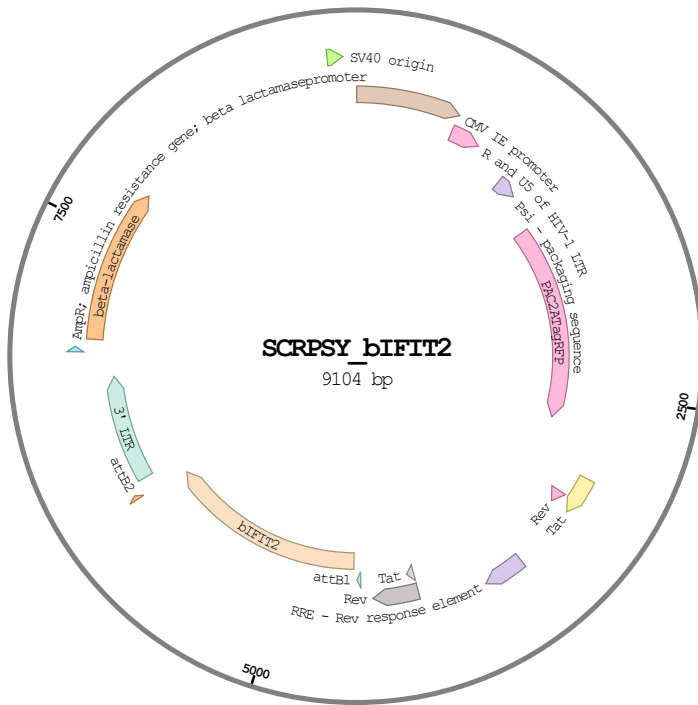


Figure 2.3: SCRPSY Representative Map.

2.4 DNA Work

2.4.1 DNA Plasmids

All plasmids used in this project had their backbone based either on SCRPSY or on pcDNA3.1. Their schematics can be seen in Figure ?? and Figure ??, respectively. SCRPSY backboned plasmids were provided by CRV Glasgow and were part of their interferon stimulated genes plasmid library. These included open reading frames (ORFs) of bovine *IFIT1*, *IFIT2*, *IFIT3*, and *IFIT5* as well as human *IFIT1B*, *IFIT2*, *IFIT3* and *IFIT5*. The ORFs in these constructs do not possess any tags. The benefit of SCRPSY backbone is the possibility of delivery inside the cells by direct transfection or by transduction. SCRPSY plasmids containing bovine *IFIT* ORFs were used as templates for generation of tagged bovine *IFITs* in pcDNA3.1 plasmid backbones. pcDNA3.1 backboned plasmids with ORFs for human *RSV P*, human *RSV N*, human *RSV N* conjugated to green fluorescent protein (GFP), bovine *RSV P*, bovine *RSV N*, bovine *RSV N* conjugated to GFP, and *GFP* conjugated to FLAG, human *IFIT1* conjugated to FLAG, human *IFIT2* conjugated to FLAG, and human *IFIT5* conjugated to FLAG were provided by the Viral Glycoproteins Group and Viral Gene Expression Group (both from the Pirbright Institute) respectively.

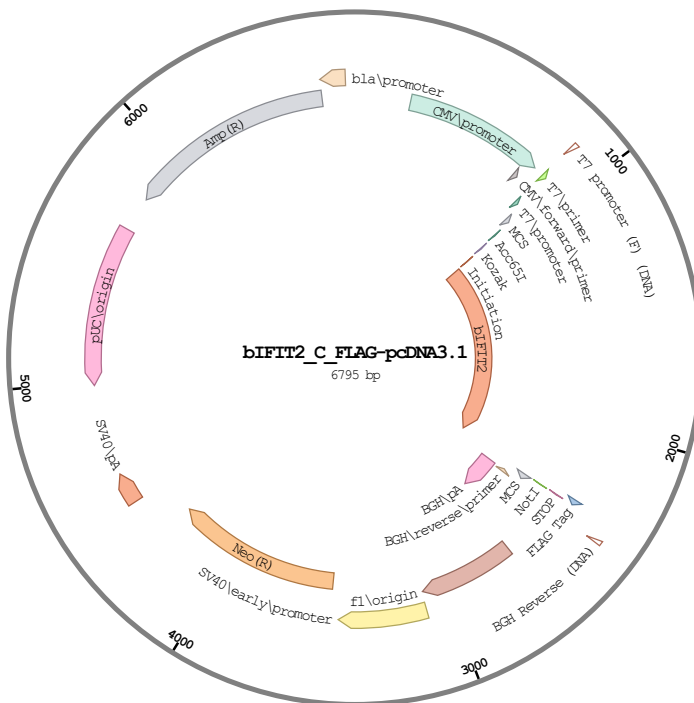


Figure 2.4: pcDNA3.1 Representative Map.

2.4.2 Common Subcloning Methodologies

2.4.2.1 Analysis of DNA by Agarose Gel Electrophoresis and Gel Extractions

Linearised DNA was resolved and potentially isolated on 0.8% agarose in Tris-Borate EDTA (TBE) buffer gel. 0.8% agarose mixture was used as it provides resolution power greater than 10kbp-0.1kbp. DNA visualisation was enabled by the addition of 15 μ L ethidium bromide into 50 mL agarose TBE solution at $\tilde{50}^{\circ}\text{C}$ prior to gel casting. DNA samples were mixed with 6X loading buffer (NEB) and loaded onto the gel. A DNA ladder was also electrophoresed in a separate well to allow size comparison. Samples were run at 80V for 90 minutes. After the run DNA bands were visualised using UV. Samples intended for gel purifications were excised from the gel using a clean scalpel and were placed into clean 1.5 mL tubes.

2.4.2.2 DNA Clean-Up After PCR or Gel Extraction

DNA clean-up was performed using QiaQuick Gel Extraction kit (Qiagen) with accordance to the manufacturers protocol. In short, 3 volumes of buffer QC were added to either post PCR DNA or to a gel slice (where 1 mg of gel was assumed to be equivalent to 1 μL). Samples were incubated at 50°C for 10 minutes, after which one sample volume of isopropanol was added to the samples. Samples were collected on a QIAquick spin column via centrifugation

Materials and Methods

and washed with buffer PE twice. DNA was eluted to 1.5 mL tube using centrifugation.

2.4.2.3 DNA Ligation

20 μ L total volume ligation reaction was prepared using DNA to be ligated, 2 μ L T4 DNA ligase buffer (NEB) and 1 μ L of T4 DNA ligase (NEB). Samples were incubated at 16°C for 72 hours.

2.4.2.4 Transformation of Chemically Competent *E.Coli* Cells and Bacterial Culture Amplification

2 μ L of ligated samples or 1 μ L of concentrated DNA were mixed with 25 μ L *E. coli* in 0.5 mL PCR tubes and were placed in a PCR cycler. Samples were initially incubated at 4°C for 15 minutes, following by heat shock performed by incubation at 42°C for 45 seconds followed by 2 minutes at 4°C. Afterwards, 75 μ L of SOC solution was added and samples were left to incubate at 37°C for 60 minutes. Finally, 100 μ L of transformed bacterial culture was streaked on room temperature agar plate containing ampicillin with a quadrant streaking method to ensure dilution gradient establishment on the plate allowing for single colony formation in the final quadrant. Plates were left to incubate for 24 hours at 37°C. Afterwards, single colonies were picked, annotated, and amplified in LB broth containing 1 μ L per mL of ampicillin for 24 hours at 37°C.

2.4.2.5 DNA Purification and Sequencing

Bacterial cultures from the final step of Section ?? were pelleted by centrifugation at 4°C for 30 minutes at 4000 g. Based on the size of the culture, the plasmid DNA was purified either by Miniprep or Midiprep kit (Quiagen; from 5 mL and 50 mL cultures respectively) based on the manufacturers protocol using the alkaline lysis method. Final purified DNA was quality assessed by restriction digestion followed by agarose gel electrophoresis (described in Section ??), which, if successful, was followed by sanger sequencing. Sequencing primers used to sequence ORFs of pcDNA3.1 plasmids were the forward T7 promoter primer and reverse BGH primer.

2.4.3 PCR for Cloning into pcDNA3.1

In order to create tagged bovine *IFIT* ORFs and subclone them from SCRPSY backbone into pcDNA3.1 backbone the following protocol was used. Primers were designed based on the

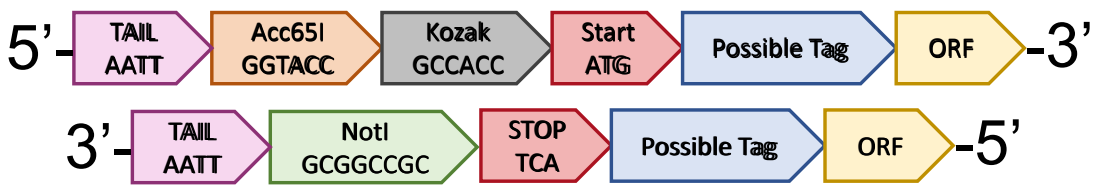


Figure 2.5: Schematic for PCR Primer Design.

schematic in ???. The primers were 27-60 nucleotides in length. Their melting temperatures were established and used in the PCR protocol. PCR reaction mixtures with final volume of 100 μ L were created by combining 10 μ L of 10X Pfu Buffer (Promega) with 100 ng of plasmid DNA, 4 μ L of 5 nM dNTPs (NEB), 2 μ L of Pfu DNA polymerase (Promega), 1 μ L of 100 μ M forward and reverse primer and nuclease-free water. Samples were placed in PCR thermocycler and incubated for 30 seconds at 98°C. Followed were 30 cycles of 10 seconds at 98°C, followed by 30 seconds at 58°C and 90 seconds at 72°C. Final step was incubation at 72°C for 2 minutes. To degrade the original plasmid material, samples were incubated with DpnI restriction enzyme for 1 hour at 37°C. Afterwards, samples were cleaned as described in Section ???. The ORF amplicons had their ends digested by a sequential restriction digest with Acc65I (NEB) and NotI (NEB) restriction enzymes. This was done by diluting samples with 10X 3.1 buffer into 1X, adding restriction enzyme, incubation for 1 hour at 37°C and heat inactivation of enzyme at 65°C for 15 minutes. Digested amplicons were cleaned-up as described in Section ???. Donor plasmid pcDNA3.1 was linearised using Acc65I and NotI restriction enzymes as described above, and gel extracted as detailed in Section ?? and ???. Linearised plasmid was dephosphorylated using Antarctic phosphatase (NEB). Amplicons and dephosphorylated plasmid were ligated in 5:1 molar ratio as described in Secton ??.

2.4.4 PCR for Point Mutant Generation

To create *IFIT2* RNA-binding mutants a following protocol was used. Based on the publication in Tran *et al.*, inverse PCR methodology was used with the primers for hIFIT mutations being taken from the study (**Tran2020InfluenzaMRNAs**). bIFIT2 primers were based on the human ones. A protein model of human IFIT2 complex, visualised in PyMol software (**SchrodingerTeam2023TheSystem**), had the amino acid residues 292 and 410 highlighted and compared to the residues on the corresponding place of predicted bovine IFIT2 structure. The effects of the mutations on the surfaces polarity assayed *in silico*. This established that the corresponding amino acid residues on the bovine IFIT2 needed to be mutated were 287

Materials and Methods

Primer Name	Sequence 5'-3'
hIFIT2 R292E forward	GTGCTGCTATgagGCAAAAGTCTTC
hIFIT2 R292E reverse	CCAATTGGCAATGCAGG
hIFIT2 K410E forward	GGAGAAAGAAGagATGAAAGACAAAC
hIFIT2 K410E reverse	CTTGATTCTGGTTATTTTACAC
bIFIT2 R287E forward	GTGCTGCTATgagGCCAAAGTCCT
bIFIT2 R287E reverse	CCAATATGGCAATGCAGG
bIFIT2 K401E forward	GAAGGGAGAAgaaATGAAAAACAAAC
bIFIT2 K401E reverse	CTTGATCCCTGGTTAT

Table 2.8: Primers for Inverse PCR Mutagenesis.

and 401. The final primers can be seen in table Table ??, where the mutating nucleotides are shown using lower case characters. PCR reaction mixtures with final volume of 100 μL were created by combining 10 μL of 10X Pfu Buffer (Promega) with 100 ng of plasmid DNA, 4 μL of 5 nM dNTPs (NEB), 2 μL of Pfu DNA polymerase (Promega), 1 μL of 100 μM forward and reverse primer and nuclease-free water. Samples were placed in PCR thermocycler and incubated for 30 seconds at 98°C. Followed were 30 cycles of 10 seconds at 98°C, followed by 30 seconds at 58°C and 200 seconds at 72°C. Final step was incubation at 72°C for 2 minutes. To degrade the original plasmid material, samples were incubated with DpnI restriction enzyme for 1 hour at 37°C. Afterwards, samples were cleaned as described in Section ?? and eluted in 20 μL of nuclease-free water. DNA was phosphorylated by adding 2 μL of 10X ligase buffer and 1 μL of T4 Polynucleotide Kinase (NEB) and incubating the samples for 30 minutes at 37°C. The enzyme was inactivated by incubation at 65°C for 20 minutes. Samples were then ligated by addition of 1 μL of T4 DNA ligase and incubation at 16°C for 72 hours.

2.5 Protein Work

2.5.1 Immunoprecipitation

Immunoprecipitation (IP) and co-immunoprecipitation (co-IP) was performed to isolate specific proteins or protein complexes, respectively. 2,000,000 HEK293T cells were seeded in a 10 cm dish. For transfection experiments 7.7 μg of DNA was transfected as described in Section ?? . 24 hours post transfection cells, or at the terminal point of experiment cells were scraped and transferred into a 50 mL conical tube. Cells were repeatedly spun down and washed with PBS until there was no residual contamination from culture media. Final

cell pellet was resuspended in 1 mL of cold lysis buffer (10 mM Tris/HCl pH 7.5; 150 mM NaCl; 0.5 mM EDTA; 0.5% NP-40; 1:100 protease inhibitors (Sigma)) and incubated for 30 minutes on ice. Afterwards samples were spun down at 20,000 g for 10 min at 4°C and the supernatant was transferred into pre-cooled tube. Dynabead protein-G beads (ThermoFisher) were bind to a target antibody by combining 50 μ L of magnetic beads with 5 μ g of target antibody in 200 μ L of PBS with Tween 20 for 10 minutes at room temperature. Afterwards, using a magnet, the supernatant was removed without removing the bead-antibody complexes. After the beads were resuspended in lysis buffer. After centrifuging the lysates were added to the beads and incubated using a rotor for 30 minutes at 4°C. Afterwards the samples were washed twice using magnetic rack and a wash buffer (10 mM Tris/HCl pH 7.5; 150 mM NaCl; 0.5 mM EDTA). After the final wash was removed the bead-sample complexes were resuspended in 45 μ L 2x SDS loading buffer, incubated at 95°C for 5 minutes. Afterwards the samples were centrifuged at top speed for 2 minutes and the pellet was discarded. This was the **bound** sample, which contained the immunoprecipitated target, along with the antibody which was used to precipitate it. During the experiment two additional samples were aliquoted, each 50 μ L in volume. First was after centrifugation of the lysates (**input** sample) and the second after incubation of lysates with the beads on rotor (**unbound** sample). Both of these samples were mixed 1:1 with 2x SDS loading buffer and boiled at 95°C for 5 minutes.

2.5.2 SDS-PAGE and Western Blotting

At the end point of experiments with cells, the growth medium was removed, and the cells were washed with PBS. Cells were lysed in 1X Laemmli SDS sample buffer (Bio-Rad) supplemented with β -mercaptoethanol (Sigma) and denatured by boiling at 95°C for 5 minutes. Samples were run on 10% SDS polyacrylamide gels. The running gel was prepared using 10-% v/v polyacrylamide (Protogel), 0.39 M Tris pH 8.8, 0.1% w/v SDS, 0.1% w/v ammonium persulphate (APS) and 0.04% w/v tetramethylethylenediamine (TEMED; Bio-Rad). The stacking gel consisted of 5% v/v polyacrylamide, 0.13 M Tris pH 6.8, 0.1% w/v SDS, 0.1% w/v APS and 0.1% w/v TEMED. PageRuler Plus prestained protein ladder (Thermo Scientific) was used as a molecular weight marker. Samples were run in a Mini-PROTEAN Tetra Vertical Electrophoresis Cell (BioRad) at 110 V for 120 minutes. Afterwards the proteins were transferred into polyvinylidene difluoride (PVDF) membranes (Bio-Rad) using the Trans-blot Turbo blotting system (Bio-Rad) with 1X transfer buffer (25 mM Tris, 192 mM glycine, pH 8.3; Bio-Rad) following the manufacturer's

Materials and Methods

instructions (30 min at 25 V). Afterwards the membranes were blocked by incubation with 5% (w/v) skimmed milk in PBS with 0.1% Tween 20 (PBST) for an hour. Afterwards the membranes were washed several times with in PBS with 0.1% Tween 20. During this step it is possible to reversible visualise proteins on the membrane using Ponceau S (ThermoFisher). After washing steps the membranes were incubated with milk-PBST-primary antibody mixtures overnight at 4°C, washed three times with PBS-T and probed with either horseradish peroxidase-conjugated secondary antibodies or fluorophore-conjugated secondary antibodies, diluted in 5% milk in PBST. Protein bands were detected either directly or using Clarity Western ECL substrate (Bio-Rad) and imaged with Bio-Rad ChemiDoc MP Imaging System.

2.6 Confocal Microscopy

Cells grown on a glass coverslip with 13 mm diameter (Agar Scientific) were washed with PBS and fixed by incubating for 15 minutes with room temperature 4% paraformaldehyde (Sigma-Aldrich) at the end point of the experiments. Samples were subsequently permeabilised by being incubated in 0.2% Triton X-100/PBS solution for 5 minutes. Residual Triton was removed by PBS washes, after which the coverslips were blocked using 1% bovine serum albumin (BSA; Sigma-Aldrich) in PBS for at least 30 minutes. Samples were then incubated overnight with the primary antibody 1% BSA in PBS solution, diluted as specified in Table ???. Afterwards, they were washed again with PBS and incubated for an hour at room temperature with secondary antibodies diluted in 1% BSA in PBS solution, as specified in Table ???. Nuclei of the cells were stained by 4,6-diamidino-2-phenylindole (DAPI; Abcam), diluted 1:20,000 in water. After 10-minute incubation, residual DAPI was washed away by water, following by an additional wash with PBS. Stained slides were mounted on glass slides using Vectashield (Vector Labs). Confocal images were acquired on Leica TCS SP5 and Zeiss LMS700 confocal microscopes using 405 nm, 488 nm, and 568 nm laser lines with 63X oil immersion objective. Laser lines were operated in sequential manner to prevent bleed-through and the image quality was enhanced by frame averaging. The pinhole was set to 1 airy unit. Maximal laser line gains were established per experiment using secondary antibody only controls, while minimal gains were established using the maximum intensity of sample slides, allowing for maximum range of signal acquisition. Image analysis was conducted in Fiji ([Schindelin2012Fiji:Analysis](#)) and final figures were constructed using QuickFigures Fiji plugin ([Mazo2021QuickFigures:Figures](#)).

2.7 RNAseq Differential Expression Analysis

Antibody Target	Host Species	Provider	Working Dilution
RSV N	Mouse	Abcam	1:400
RSV P	Mouse	FILL	1:400
RSV M2/1	Mouse	FILL	1:400
IFIT1	Rabbit	Invitrogen	1:200
IFIT2 (A)	Rabbit	Proteintech	1:200
IFIT2 (B)	Rabbit	Novus Biologicals	1:200
IFIT3	Rabbit	Proteintech	1:200
IFIT5	Rabbit	Invitrogen	1:200
FLAG	Rabbit	Invitrogen	1:200
Rabbit Igg	FILL	Invitrogen	1:10000
Mouse Igg	FILL	Invitrogen	1:10000

Table 2.9: Antibodies for Confocal Microscopy.

2.7 RNAseq Differential Expression Analysis

RNAseq experiments comparing the transcript levels between control cells and cells infected with either wild-type bovine RSV or bovine RSV with a deleted SH gene, either 16 and 40 hours post infection were previously performed by Dr. Fouthemata Jobe from the Viral Glycoproteins Group at the Pirbright Institute. The initial data analysis was performed by the bioinformatics team of the Pirbright Institute. They included the viral genes as a part of the analysis and therefore these were the only differentially expressed genes from the study. I have reanalysed the counts dataset, which had viral genes omitted. Data processing, statistical analysis and graph generation was conducted R programming language (**RCoreTeam2022R:Computing**) using RStudio environment (**RStudioTeam2022RStudio:RStudio**). Initial exploratory data analysis and differential expression analysis was done using the DESeq2 R package (**Love2014ModeratedDESeq2**). Viral genes were filtered from the dataset pre analysis. After creation of DESeq2 object, genes with no counts were filtered. To perform initial exploratory data analysis and visualization data was transformed using regularized logarithm (rlog) and the variance stabilizing transformation (VST) methods. This was done to stabilize the variance across the mean. The transformed data was visualised using the principal component analysis (PCA) plot and sample distance matrix. Following this the differential expression analysis was performed on non-transformed filtered data. Following the recommendation of Schurch *et al.*, the fold-change threshold was set to 0.5 and the minimum adjusted p value was set to 1% to optimise the true positive rate and false positive rates (**Schurch2016HowUse**). The data was visualised by volcano plots, MA plots and heatmaps (using pheatmap R package

Materials and Methods

(**Kolde2019Pheatmap:Heatmaps**). The final dataset was annotated with the appropriate gene names and gene symbols from latest available bovine genomic dataset using org.Bt.eg.db R package (**Carlson2022Org.Bt.eg.db:Bovine**).

2.8 Statistical Analysis

Statistical analysis was performed using R programming language (**RCoreTeam2022R:Computing**) using the RStudio environment (**RStudioTeam2022RStudio:RStudio**). The pipeline can be viewed in the following URL: <http://rpubs.com/ogosimiso/995988>. Initially, data was assessed visually using boxplots and Q-Q plots. Boxplots were used to roughly assess the normality, whereas Q-Q plots were used for rough equality of variance assumptions. A mathematical test of the normality of distribution was done using the Shapiro-Wilk normality test. This was performed on each individual condition as well as the whole dataset in its entirety. Mathematical assessment of equality of variance was done by Bartlett test of homogeneity of variances for normally distributed samples and by Levene's Test for Homogeneity of Variance (car package for R (**Fox2019AnRegression**)) for non-normally distributed samples. To obtain the final significance values various mathematical tests were used based on the number of comparisons and the previously established type of distribution and equality of variance. For a pair of samples with normal distribution and equal variance a two-sample t-test was conducted. For multiple comparisons of normally distributed data with equal variance analysis of variance (ANOVA) combined with Tukey multiple comparison of means was performed. For a pair of samples with non-normal distribution but equal variance, a two-sample t-test was conducted. For multiple comparisons of non-normally distributed data with equal variance a Kruskal-Wallis rank sum test was performed (dunn.test R package (**Dinno2017Dunn.test:Sums**)). For a single comparison of data which has normal distribution but non-equal variance a Welch Two Sample t-test was performed. For multiple comparisons of data with normal distribution but non-equal variance one-way analysis of means (not assuming equal variances) combined with Games-Howell test was performed (rstatix R package (**Kassambara2022Rstatix:Tests**))).

Chapter 3

Assesment of Transcriptional Induction and Subcellular Localisation of Human IFITs in the Context of RSV

3.1 Introduction and Aims

Half page intro: Ifit gene regulation (promoters and such)

Ifit paths of induction

interferons

Lps tlr4

Poly IC

Ifit induction by other viruses and inducers

Half page aims: We hypothesised both human IFITs to be induced by human RSV infection. We aimed to systematically test this by initially confirming that our model cell lines are capable of IFIT induction following the treatment of known innate immune system activators such as interferons, LPS, and poly I:C. These would also allow us to assess the We would then assess the IFIT induction during human and bovine RSV infection using a range of viral concentrations and end assay time points. Lastly, we would validate this data in more physiologically relevant cell lines as well as using omics approaches.

3.2 Results

Assesment of Transcriptional Induction and Subcellular Localisation of Human IFITs in the Context of RSV

3.2.1 Transcriptional Changes of Human *IFITs*

To unravel the impact of cellular stimulation with activators of the innate immune response and human RSV, on the expression of human *IFIT* genes, quantitative real-time reverse transcription PCR (qPCR) analysis was executed in accordance with the methodology outlined in Section ???. Briefly, cells were cultivated in 12-well plates and subsequently subjected to the respective stimulants. At the endpoint of the experiments, the RNA was extracted, followed by cDNA synthesis and the transcript quantification by qPCR. All transcript levels were standardized to human *GAPDH* expression, employing the $\Delta\Delta Ct$ method. Subsequently, all values were normalized against mock-treated samples, enabling data aggregation and inter-experimental induction value comparison. The statistical analysis was conducted as outlined in Section ???. Notably, the choice of the appropriate statistical test hinged on the normality of data distribution and equality of variance, aspects that will be underscored in the ensuing text.

3.2.1.1 Human *IFITs* Responses of to Known Activators of Innate Immune Response

In order to establish the expression competency of human *IFITs* of the A549 cell line, along with elucidating how different innate immune pathways contribute to the overall expression profile, I treated the cells with differing activators of the innate immune response. As described in Section ???, and depicted in Figure ??, interferon-stimulated genes (ISGs) can have their induction activated either via the interferon receptor signalling, intracellular foreign nucleic acid detection or via extracellular PAMP sensing. The latter, in the context of RSV, includes stimulation of TLR4 with either LPS or RSV particles. After surveying the literature I ended up using 1,000 international units (IU) per mL of human interferon alpha (**Terenzi2006DistinctISG56; Santhakumar2018ChickenViruses**). For interferon-gamma stimulation, which stimulates predominantly immune cells *in vivo* concentrations of 500, 1,000 and 2,000 IU/mL were used. LPS was administered in concentrations of 5 ng/mL and 5 μ g/mL for the duration of 6 hours. (**Mears2019Ifit1Cells; Zhang2019GrouperResponse**). To stimulate intracellular foreign nucleic acid recognition 2 μ g of poly I:C were transfected into A549 cells and incubated for 24 hours (**Mears2019Ifit1Cells; Palchetti2015TransfectedCells**).

The A549 cell line, derived from lung carcinomatous tissue from a 58-year-old Caucasian male in 1972 is a well-established model of alveolar epithelial cells, routinely used for cancer to viral research alike (**Lieber1976ACells**). We observe that after the stimulation of the A549 cell line with 1,000 IU/mL of hIFN α for either 6 or 24 hours human *IFIT1*, *IFIT2*, and *IFIT3* were induced drastically, especially *IFIT1*, which was induced around 200-fold (Figure ??).

3.2 Results

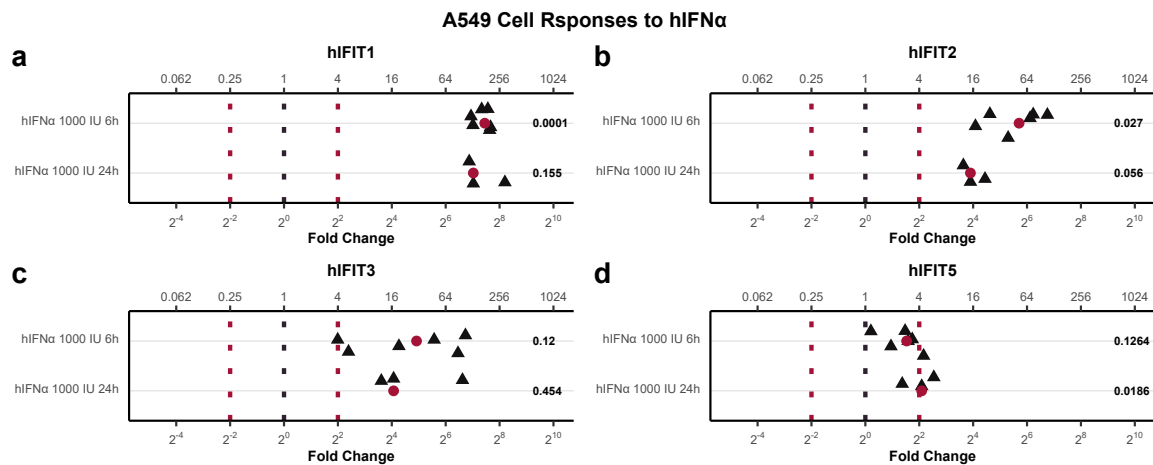


Figure 3.1: qPCR Analysis of A549 hIFIT to hIFN α . The relative abundance of (a) hIFIT1, (b) hIFIT2, (c) hIFIT3, and (d) hIFIT5 genes, extracted from the A549 cell line, with response to human interferon alpha (IFN α) at a concentration of 1000 IU per mL for a treatment duration of 6 or 24 hours. The shown values are relative to standardised mock values. The red circles signify median values. The black dotted line indicates mock expression, while the red dotted lines indicate biologically significant levels of induction. Numeric values signify the p-values compared to mock.

The relative induction levels were identical between IFIT2 and IFIT3. For all of these 3 genes, we can observe a decreased expression with longer incubation of IFN α , i.e. approximately half of the induction levels caused by 6-hour long incubation. Human IFIT5 shows minimal induction compared to the other IFITs (3 and 4-fold for 6 and 24-hour long incubation respectively), which hovers around the mark of what is considered biologically significant induction, especially for ISGs, which are supposed not to be highly basally expressed. We can also observe a reverse trend of the time dependency of hIFN α -induced expression. This suggests differential induction sensitivities between hIFIT1 (highly induced), hIFIT2 and hIFIT3 (medium induced) and hIFIT5 (low induced). All hIFIT values had normal distributions and unequal variance other than hIFIT5, which had normal distribution and normal variance.

The response of human IFIT genes to human IFN gamma can be seen in Figure ???. We can observe all IFITs other than hIFIT5 responding equally to all concentrations tested i.e. 500, 1,000 and 2,000 IU/mL. Their response was concentration independent of a magnitude of around 15-fold. hIFIT5 response to very low concentration and very high concentrations was around 10-fold, while its transcript abundance increased only 4 times when treated with 1,000 IU/mL concentration. This suggests that the interferon-gamma component of the human IFIT response is relatively equal for all of the IFIT genes. This data, along with the data from hIFN α induction also confirms that the A549 cell line is hIFIT induction capable,

Assesment of Transcriptional Induction and Subcellular Localisation of Human IFITs in the Context of RSV

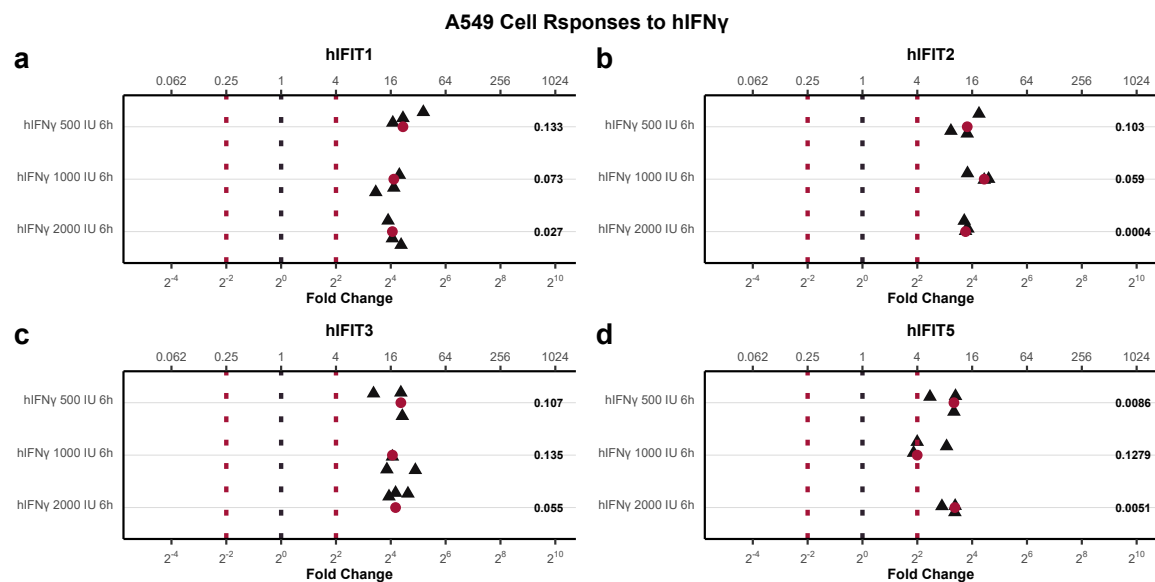


Figure 3.2: qPCR Analysis of A549 hIFIT Response to hIFN γ . The relative abundance of (a) hIFIT1, (b) hIFIT2, (c) hIFIT3, and (d) hIFIT5 genes, extracted from the A549 cell line, with response to human interferon-gamma (IFN γ) at concentrations of 500, 1000, and 2000 IU per mL for a treatment duration of 6 hours. The shown values are relative to standardised mock values. The red circles signify median values. The black dotted line indicates mock expression, while the red dotted lines indicate biologically significant levels of induction. Numeric values signify the p-values compared to mock.

which is great. All hIFIT values had normal distributions and unequal variance other than hIFIT5, which had normal distribution and normal variance.

In order to assess the involvement of TLR4, a receptor also responsible for detecting RSV particles, A549 cells were incubated for 6 hours with low (5 ng/mL) and high (5,000 ng/mL) concentrations of bacterial LPS, its known activator. We can see that all IFITs respond in a concentration-dependent manner but the response is the lowest out of the different stimulants used. Low-concentration LPS incubation causes biologically insignificant induction of all hIFITs of 2-fold for hIFIT5 and 3-fold for the other IFITs. The high concentration on the other hand yields biologically significant induction levels of 4-8 fold induction. All hIFIT values had normal distributions and unequal variance other than hIFIT3, which had normal distribution and normal variance.

When A549 cells were transfected with 2 μ g of poly I:C for 24 hours we were able to observe the biggest induction compared to the other inducers previously used (Figure ??). As with the other inducers, hIFIT1 induction is the greatest (circa 500-fold), followed by hIFIT2 and hIFIT3 with 300-fold and 200-fold responses respectively, with hIFIT5 trailing behind with the lowest response of only 10-fold. This again suggests that hIFIT5 seems to have differential transcriptomic regulation compared to the other genes of the IFIT family.

3.2 Results

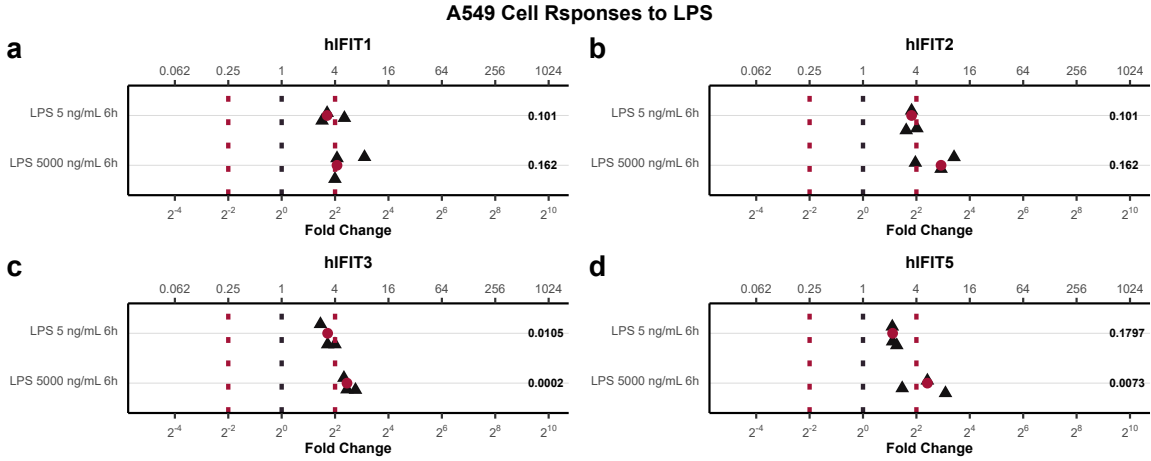


Figure 3.3: qPCR Analysis of A549 hIFIT Response to LPS. The relative abundance of (a) *hIFIT1*, (b) *hIFIT2*, (c) *hIFIT3*, and (d) *hIFIT5* genes, extracted from the A549 cell line, with response to lipopolysaccharide (LPS) at concentrations of 5 and 5000 ng/mL for a treatment duration of 6 hours. The shown values are relative to standardised mock values. The red circles signify median values. The black dotted line indicates mock expression, while the red dotted lines indicate biologically significant levels of induction. Numeric values signify the p-values compared to mock.

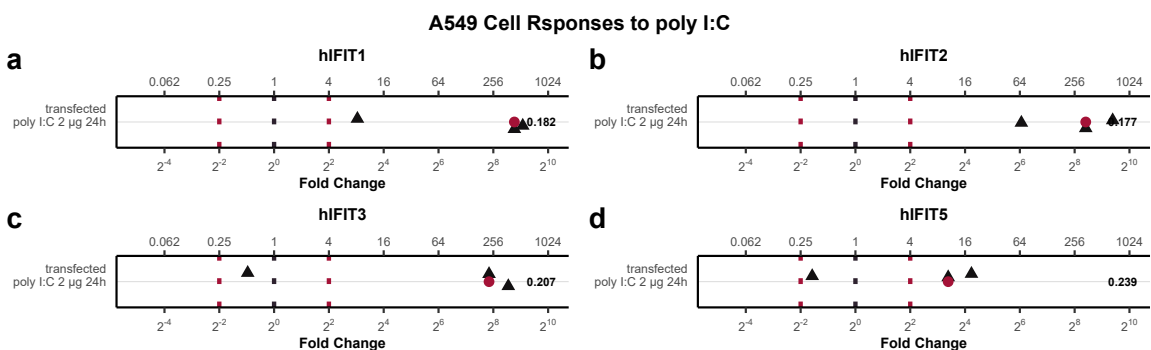


Figure 3.4: qPCR Analysis of A549 hIFIT Response to Transfected poly I:C. The relative abundance of (a) *hIFIT1*, (b) *hIFIT2*, (c) *hIFIT3*, and (d) *hIFIT5* genes, extracted from the A549 cell line. The cells were transfected with 2 µg of poly I:C for 24 hours. The shown values are relative to standardised mock values. The red circles signify median values. The black dotted line indicates mock expression, while the red dotted lines indicate biologically significant levels of induction. Numeric values signify the p-values compared to mock.

Assesment of Transcriptional Induction and Subcellular Localisation of Human IFITs in the Context of RSV

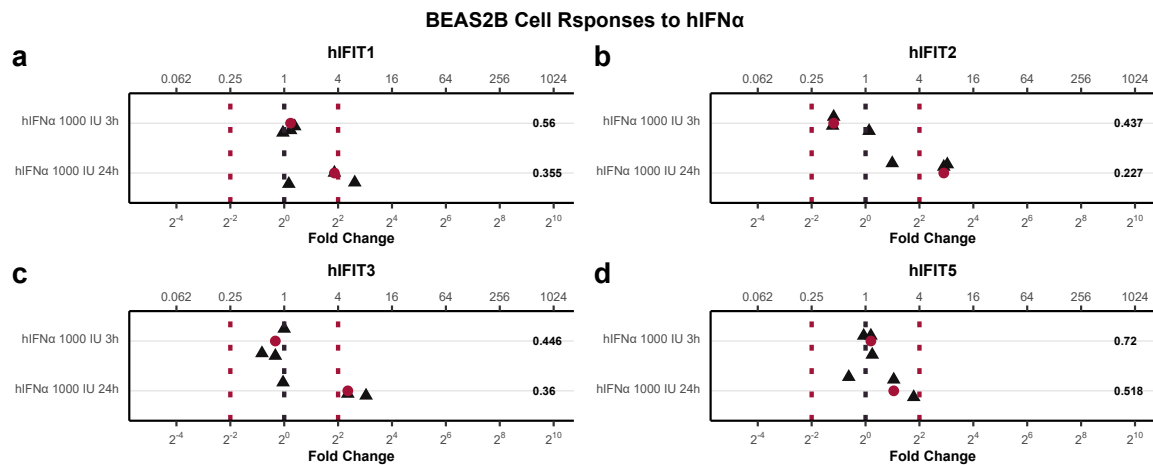


Figure 3.5: qPCR Analysis of BEAS-2B hIFIT Response to hIFN α . The relative abundance of (a) hIFIT1, (b) hIFIT2, (c) hIFIT3, and (d) hIFIT5 genes, extracted from the BEAS-2B cell line, with response to human interferon alpha (IFN α) at a concentration of 1000 IU per mL for a treatment duration of 3 or 24 hours. The shown values are relative to standardised mock values. The red circles signify median values. The black dotted line indicates mock expression, while the red dotted lines indicate biologically significant levels of induction. Numeric values signify the p-values compared to mock.

All hIFIT values had normal distributions and unequal variance.

Lastly, we validated the human interferon alpha induction data in a more biologically relevant cell line, BEAS-2B. Established from bronchial epithelial biopsies from healthy samples, and later immortalised using the transfection of cyclin-dependent kinase 4 and human telomerase reverse transcriptase, these cells are an invaluable tool in the field of bronchial development and pathogenesis (**Ramirez2004ImmortalizationOncoproteins**). After the treatment with human interferon alpha at concentrations of 1,000 IU/mL for 3 hours, we can see that this stimulation was not sufficient to induce the expression of any human IFIT (Figure ??). However, when the cells were stimulated for 24 hours we can observe induction above biological significance for hIFIT1, hIFIT2, and hIFIT3, with 4-fold, 8-fold, and 5-fold increase respectively. hIFIT5 shows only 2-fold median induction, which could be caused by the intrinsic variability of the assay. So as we observed with the A549 cell line, hIFIT5 behaves in discord with the other human IFITs. All hIFIT values had normal distributions and unequal variance.

3.2.1.2 Human IFITs Responses to Human RSV Infection

After successfully confirming the IFIT induction competency of our workhorse cell line A549 as well as in the more physiologically relevant cell line BEAS-2B, we turn our attention

3.2 Results

to assessing the effect of human RSV infection on *hIFIT* induction. To date, no studies have ever investigated this. Initially, we wanted to assess the effect of low, medium and high (0.1, 1, and 2 MOI respectively) infections as well as short and long-term infections (24 and 48 HPI respectively) on *hIFIT* induction. My colleagues in the Viral Glycoproteins from the Pirbright Institute routinely perform hRSV infections of both A549 and BEAS-2B cell lines and thus the knowledge of what constitutes low and high MOI infection, as well as what short and long infection periods are widely known and available (I GUESS SOME CITATION HERE). The virus was prepared and quantified as described in Section ?? and Section ???. Briefly, infected cells were sonicated, cell debris was separated by centrifugation and virus-containing supernatant was gathered and titred. A549 cells were infected with the hRSV-containing supernatant at multiplicities of infection (MOI) of 0.1, 1, and 2. Total mRNA was collected from the samples either 24 or 48 hours post-infection (HPI) and converted to complementary DNA, as described in Section ???. This was subsequently quantified by qPCR as described in Section ?? and the data analysed as described in Section ???. The responses of *hIFITs* as a function of HPI and MOI can be seen in Figure ??, along with a plot quantifying human RSV *N* mRNA as a control for viral replication. The relative quantification values of RSV *N* have to be taken with a grain of salt as it is being compared to mock-infected samples that should have no RSV *N* mRNA present. As a result, the actual relative values are dependent on the Ct values detected in the mock.

First of all, we can observe low MOI infection, although causing a productive infection as seen by *hRSV N* mRNA relative quantification, did not yield any relative change of *hIFIT* levels, suggesting that their induction is dependant not solely on the viral replication, but on the underlying magnitude of infection. In general, MOI 2 infection yields higher induction for all *hIFITs*, although the magnitude is comparable with MOI 1 infections. *hIFIT1* is induced the highest out of the other genes at 24 HPI, with both MOI 1 and 2 reaching 120-fold induction levels, while the induction magnitude diminishes slightly at 48 HPI, where infections at MOI 1 and 2 yield 50-fold and 80-fold median induction values. As seen previously in Section ??, *hIFIT2* and *hIFIT3* display very similar trends of induction (with the only difference being *hIFIT2* responses being 2 times the ones of *hIFIT3*) for all the conditions tested here. In more detail, 24 HPI *hIFIT2* gets induced 60-fold and 90-fold to the MOI of 1 and 2 respectively, while at 48 HPI the median induction magnitude increases to 100-fold and 120-fold respectively. This makes *hIFIT2* the highest induced *hIFIT* at 48 HPI. This also suggests that the induction dynamics of *hIFIT1* differ from those of *hIFIT2* and *hIFIT3*. With regards to *hIFIT5*, it displays the lowest, albeit still biologically significant induction for MOIs 1 and 2 for both time-points tested at median induction levels of 4 and

Assesment of Transcriptional Induction and Subcellular Localisation of Human IFITs in the Context of RSV

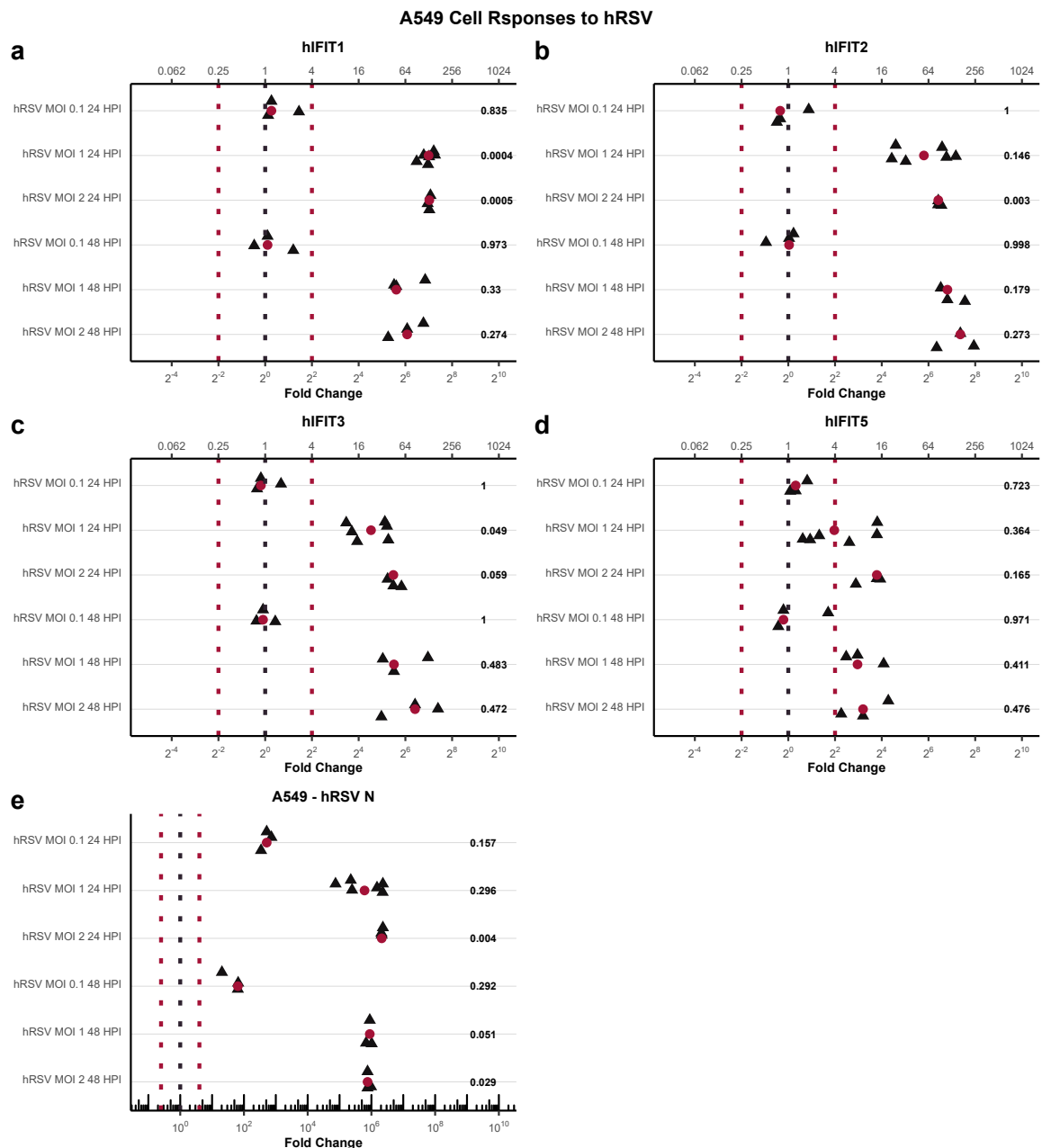


Figure 3.6: A549 hIFIT Response to hRSV as a Function of Time and MOI. The relative abundance of (a) *hIFIT1*, (b) *hIFIT2*, (c) *hIFIT3*, (d) *hIFIT5*, and (e) *hRSV N* genes, extracted from A549 cell line following infection with human RSV at MOI of either 0.1, 1, or 2 for either 24 or 48 hours post-infection. The shown values are relative to standardised mock values. The red circles signify median values. The black dotted line indicates mock expression, while the red dotted lines indicate biologically significant levels of induction. Numeric values signify the p-values compared to mock.

3.2 Results

12 for 24 HPI MOIs 1 and 2 respectively, and 9 and 10 for 48 HPI MOIs 1 and 2 respectively. All datasets were of normal distribution and non-equal variance.

After confirming and concluding that human RSV infection indeed induces *hIFIT* mRNA expression, we wanted to investigate the underlying induction principles. We wanted to investigate if the induction observed is indeed caused by human RSV detection and not by any other contaminants present in the virus prep such as cytokines, chemokines, and other stimulants. To do this, we created ultra-purified hRSV preps by ultra-centrifugation on a discontinuous sucrose cushion, as described in Section ???. We also wanted to test if it is predominately the infected cells that have the *hIFIT* expression increased as a defence mechanism to acute infection, or if the infected cells stimulate the *hIFIT* expression in neighbouring cells as a prophylactic against the infection, or both. To test this, after the infection procedure, we incubated the cells with 5 nM of ruxolitinib, a well-established small molecule JAK/STAT inhibitor, as is described in Section ???. Based on the observations from Figure ?? we used MOI of 1, 24 HPI to ensure sufficient *hIFIT* induction while decreasing the stress of the cells. Lastly, we also hypothesised that viral replication is required for *hIFIT* expression. To test this, some ultra-purified hRSV samples were UV-inactivated by a UV-cross-linker, as described in Section ???.

The results of the experiment can be seen in Figure ???. *hRSV N* dataset was of normal distribution with equal variance, while all the others were of normal distribution and non-equal variance. We can see that although purified hRSV infection yielded lower induction compared to what was observed in Figure ?? with regards to hRSV MOI 1 24 HPI infection (10^6 -fold to $10^{4.5}$ -fold), it induced all *hIFITs*, even to higher mounts than what was seen with crude-extracted virus. In more detail, *hIFIT1* was induced the highest at 180-fold (compared to 120-fold observed previously), closely followed by *hIFIT2*, whose median induction was at 180-fold (compared to 80-fold observed previously). *hIFIT3* induction was 75-fold, double what was seen previously with crude extracted hRSV, while *hIFIT5* median induction was 6-fold, a very comparable level to 4-fold that was observed previously. Regardless of the absolute magnitude of the relative values, this data suggests that the main driving force in hRSV presence and not contaminants in the viral prep. With regards to the effect of JAK/STAT inhibitor ruxolitinib, its presence diminished induction of all *hIFITs*. *hIFIT1*, *hIFIT2*, and *hIFIT3* maintained median induction values above the biologically significant threshold at 8, 10, and 5-fold respectively, while *hIFIT5* showed only minimal median induction value of only 1.5-fold. We can also observe an order of magnitude more *hRSV N* mRNA detection, suggesting that inhibiting interferon signalling is beneficial for the virus, which makes sense. Lastly, we assessed how the detection of non-replicative

Assesment of Transcriptional Induction and Subcellular Localisation of Human IFITs in the Context of RSV

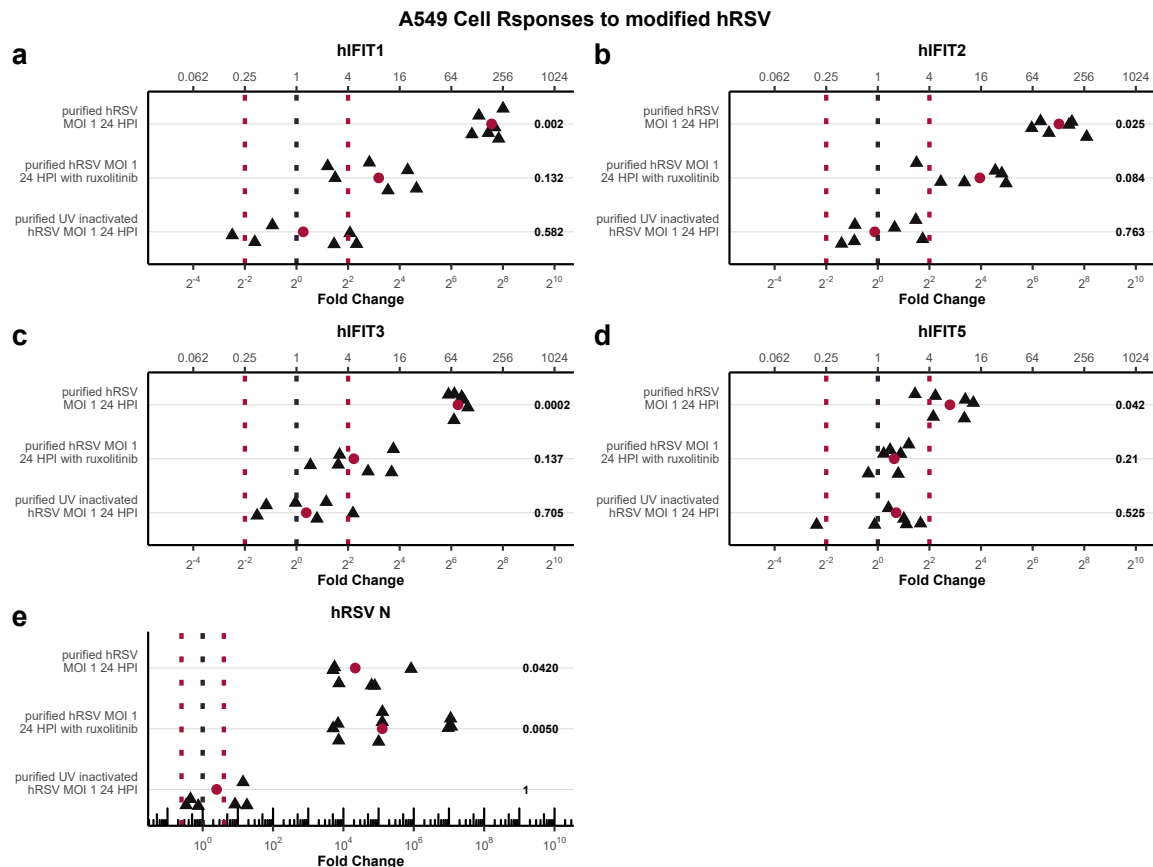


Figure 3.7: The Effect of Ultra-Purification, UV-Inactivation and INFR Inhibition on *hIFIT* Induction Following hRSV Infection in A549. The relative abundance of (a) *hIFIT1*, (b) *hIFIT2*, (c) *hIFIT3*, (d) *hIFIT5*, and (e) *hRSV N* genes, extracted from A549 cell line following infection with ultra-purified hRSV at MOI 1 for 24 hours. The cells were either treated with the virus alone (first row), with the virus and 5 nM of ruxolitinib (interferon receptor inhibitor) during the whole infection period (second row), or with UV-inactivated hRSV (last row). The shown values are relative to standardised mock values. The red circles signify median values. The black dotted line indicates mock expression, while the red dotted lines indicate biologically significant levels of induction. Numeric values signify the p-values compared to mock.

3.2 Results

hRSV particles contributes to *hIFIT* induction. UV-cross-linking of hRSV inhibited viral replication, as can be seen by the hRSV N mRNA quantification. This in fact prevented induction of all the *hIFITs*, suggesting that TLR4 sensing of RSV particle is not sufficient to initiate signalling cascades that would lead to *hIFIT* induction. Altogether, this data suggests that hRSV particles indeed drive the *hIFIT* induction, however, they have to be replication-competent. The additional essential aspect is the presence of functional interferon signalling cascades and the underlying paracrine interferon signalling initiated by infected cells in order to protect their neighbours.

Next, we validated the findings using the BEAS-2B cell line. We recreated the experiment from Figure ?? and the results can be seen in Figure ???. All datasets were of normal distribution and non-equal variance. All *hIFITs* are induced to biologically significant levels by the infection of ultra-purified hRSV infection by 40, 15, 32, and 7-fold for *hIFIT1*, *hIFIT2*, *hIFIT3*, and *hIFIT5* respectively. These responses are also significantly higher than what was observed with human interferon alpha treatment (Figure ??). In line with what we have seen in the A549 cell line, *hIFIT1* is the highest induced, while *hIFIT5* responds the worst to the infection. Interestingly, *hIFIT3* median induction is higher than the one of *hIFIT2*. When looking at the effect of ruxolitinib we can see that it prevented the induction of *hIFIT2* and actually significantly decreased the relative levels of *hIFIT1*, *hIFIT3*, and *hIFIT5* to the levels of 2^{-3} , $2^{-3.5}$, and 2^{-2} respectively. This suggests that not only is the interferon signalling required for *hIFIT2* induction, it is vital for the maintenance of basal *hIFIT1*, *hIFIT3*, and *hIFIT5* levels in this cell line. Lastly, when the cells were infected with UV irradiated ultra-purified hRSV, none of the *hIFITs* relative expression changed to biologically significant levels. This is in line with what we observed with the A549 cell line. Taken together, we validate that replication-competent viral particles are required for *hIFIT* induction and while functional interferon receptor signalling cascades as also required, as we have seen in A549, in BEAS-2B they are necessary for maintaining the basal expression levels of *hIFIT1*, *hIFIT3*, and *hIFIT5* mRNA levels.

To conclude the assessment of human IFIT responses to human RSV, I was kindly provided with a quantitative mass spectrometry dataset of human IFITs detected in either cytosolic or membrane fraction of either mock-infected or cells infected with human RSV at MOI 1, processed 24 or 48 HPI. This dataset was provided by Dr Kelly and Dr Jobe from the Pirbright Institute and its findings have now been published (**Jobe2023ViralCondensates**). Quintuplicates of cytosolic and membrane fractions were isolated by in-gel digestion and analysed by label-free quantitative mass spectrometry. Normalised and log-transformed ion abundance data for *hIFIT1*, *hIFIT2*, and *hIFIT3* can be seen in Figure ???. *hIFIT1* cytoplasmic

Assesment of Transcriptional Induction and Subcellular Localisation of Human IFITs in the Context of RSV

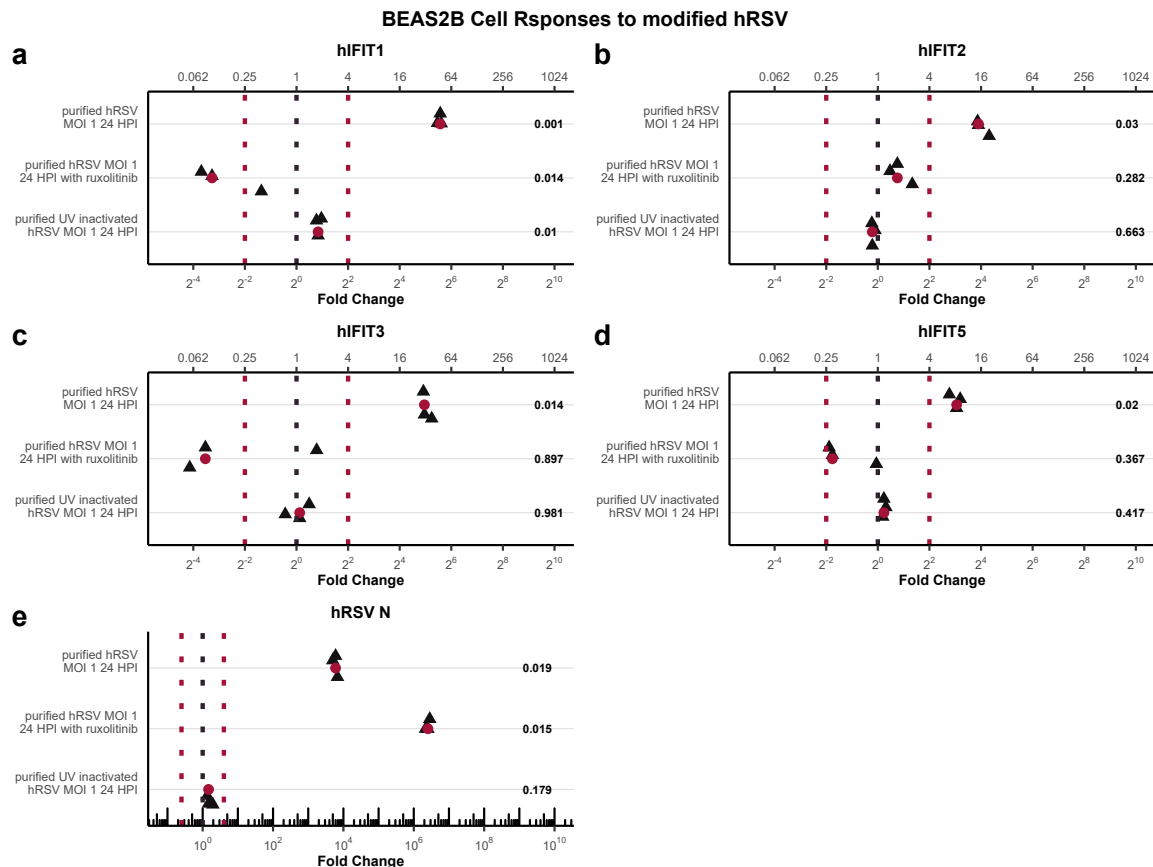


Figure 3.8: The Effect of Ultra-Purification, UV-Inactivation and INFR Inhibition on *hIFIT* Induction Following hRSV Infection in BEAS-2B. The relative abundance of (a) *hIFIT1*, (b) *hIFIT2*, (c) *hIFIT3*, (d) *hIFIT5* and (e) *hRSV N* genes, extracted from BEAS-2B cell line following infection with ultra-purified hRSV at MOI 1 for 24 hours. The cells were either treated with the virus alone (first row), with the virus and 5 nM of ruxolitinib (interferon receptor inhibitor) during the whole infection period (second row), or with UV-inactivated hRSV (last row). The shown values are relative to standardised mock values. The red circles signify median values. The black dotted line indicates mock expression, while the red dotted lines indicate biologically significant levels of induction. Numeric values signify the p-values compared to mock.

3.2 Results

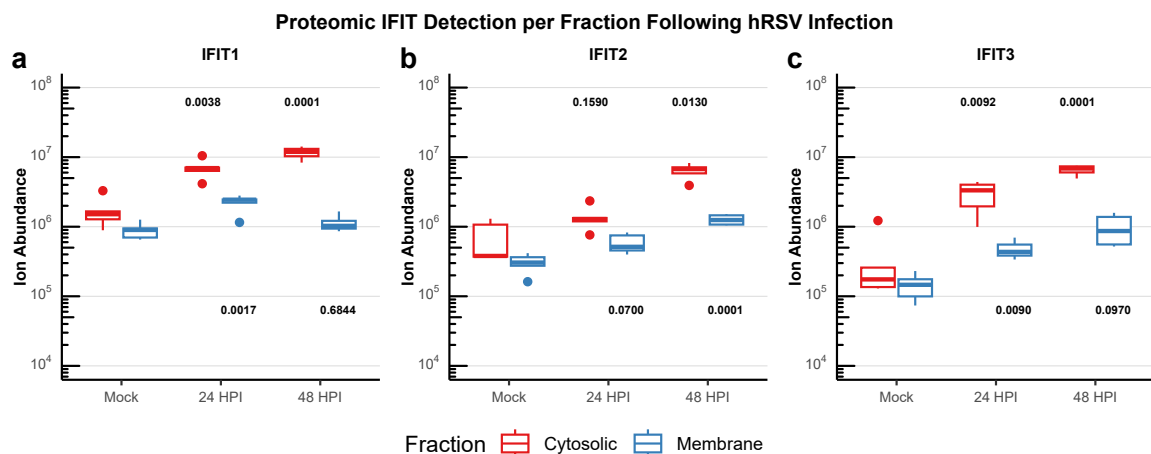


Figure 3.9: Human IFIT proteins detected per fraction. Analysis of summed peptide intensities of (a) hIFIT1, (b) hIFIT2, and (c) hIFIT3 detected per either cytosolic or membrane fractions of A549 cells which were either mock-infected or infected with hRSV MOI 1 for either 24 or 48 hours. There were no hits for IFIT5. This data is from a proteomic study, published in **Jobe2023ViralCondensates**. Samples are composed of biological quintuplicates. Numeric values signify the p-values compared to the respective mock, i.e. top numbers for cytosolic fraction, bottom for membrane fraction.

and hIFIT2 membrane datasets had normal distributions and equal variances, while all the others displayed normal distributions with non-equal variances. Human IFIT5 did not yield any hits and thus was excluded from the analysis and we can conclude that its proteome is not drastically changed by hRSV infection, which is in line with our qPCR data. hIFIT1 is the most basally abundant, followed by hIFIT2 and hIFIT3. The basal abundance of hIFITs is around equal between the fractions. The infection at 24 HPI causes increased abundance of all hIFITs in all fractions, more specifically hIFIT1 increased 5x in the cytosolic fraction and 1.3x in membrane fraction; hIFIT2 increased 4x in cytosolic and 2x in membrane fractions; and hIFIT3 increased relatively the most by 13.5x in the cytosolic fraction and 3x in the membrane fraction. The highest total abundance at 24 HPI was still hIFIT1. At 48 HPI we can observe a further increase in abundance for all other than hIFIT1 in membrane fraction which decreased to mock levels. In more detail, hIFIT1 in cytosolic fraction increased further 2x; hIFIT2 increased further 5x in cytosolic and 4x in membrane fraction; and hIFIT3 further increased 3x in cytosolic fraction and 2.5x in membrane fraction. These data together validate our qPCR results seen in Figure ?? and Figure ?? and highlight the differential spatio-temporal expression dynamics of human IFITs.

Assesment of Transcriptional Induction and Subcellular Localisation of Human IFITs in the Context of RSV

3.2.1.3 Human *IFITs* Responses to bRSV Infection

We were interested in knowing if there is cross-species protection between hRSV and bRSV, with regards to cell infectivity and *hIFIT* induction. We had an arsenal of several bRSV viruses including the wild-type (WT) along with a panel of mutant viruses with deletions of small-hydrophobic (SH) protein, non-structural (NS) protein 1 or 2 or both (see Table ??). As described in INTRODUCTION these proteins are responsible for STUFF FROM INTRODUCTION. The viruses were prepared and quantified as described in Section ?? and Section ?. Briefly, infected cells were sonicated, cell debris was separated by centrifugation and virus-containing supernatant was gathered and titred. It is to be noted that due to the lack of anti-antiviral proteins meant the virus preparation of *DeltaNS* viruses had orders of magnitude lower titre than the other viruses. Regardless, A549 cells were initially infected with the WT and *DeltaSH* bRSV-containing supernatant at MOI of 1. Total mRNA was collected from the samples 24 HPI and converted to complementary DNA, as described in Section ?. This was subsequently quantified by qPCR as described in Section ?? and the data analysed as described in Section ?. The responses of *hIFITs* as a function of HPI and MOI can be seen in Figure ??, along with a plot quantifying bovine *RSV N* mRNA as a control for viral replication.

We can see that both bRSV WT and bRSV Δ SH were successfully replicating in the A549 cell line and this in fact both induced all *hIFITs* to biologically significant levels. Interestingly, although bRSV Δ SH *N* relative mRNA levels were two orders of magnitude higher than the ones of WT bRSV, the detected induction magnitudes of *hIFITs* were, in general, lower compared to the ones caused by bRSV WT infection. This is counterintuitive as the lack of SH protein should make the virus less infectious and thus show worse replication competency, while it should allow higher *ISG* induction as there is less antagonism of the activation cascades present. Regardless, looking at the *hIFITs* in more detail, *hIFIT1* median induction by bRSV WT and Δ SH infection was 400-fold and 150-fold respectively, which were again the highest induction magnitudes detected out of all *hIFIT* response. On the other side of the spectrum is *hIFIT5* with the median induction of 6-fold for both viruses, which are the lowest induction values and are consistent with what we observed so far throughout the study. *hIFIT2* was induced 180-fold and 80-fold by the WT and Δ SH, while *hIFIT3* was induced 128 and 70 fold respectively. Intriguingly, when compared to crude-extracted hRSV MOI 1 24 HPI from Figure ?? we can see that although *bRSV N* median relative abundances were two and one orders of magnitude lower for bRSV WT and Δ SH respectively compared to *hRSV N* but regardless, they caused greater induction of all *hIFITs*. This suggests that bRSV is potentiated in human cells, probably due to the lack of species-specific inhibition,

3.2 Results

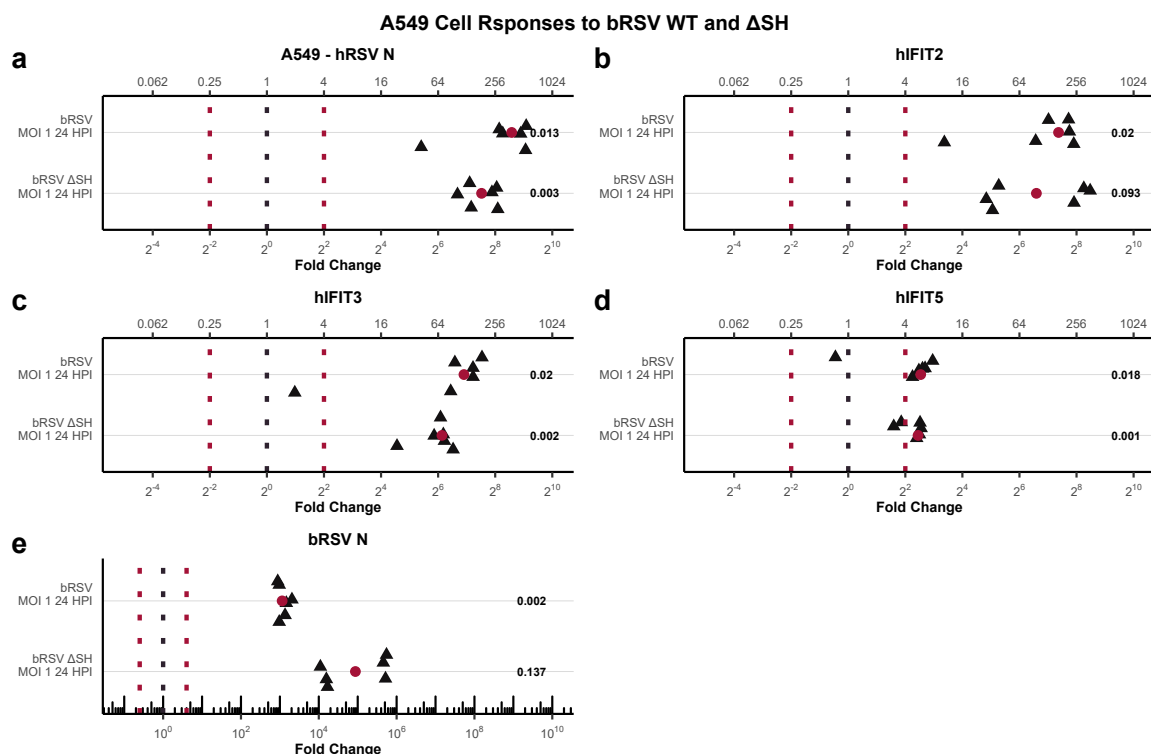


Figure 3.10: A549 hIFIT Response to WT and ΔSH bRSV Infection. The relative abundance of (a) *hIFIT1*, (b) *hIFIT2*, (c) *hIFIT3*, (d) *hIFIT5* and (e) *bRSV N* genes, extracted from A549 cell line following infection with WT or ΔSH bRSV at MOI 1, 24 HPI. The shown values are relative to standardised mock values. The red circles signify median values. The black dotted line indicates mock expression, while the red dotted lines indicate biologically significant levels of induction. Numeric values signify the p-values compared to mock.

Assesment of Transcriptional Induction and Subcellular Localisation of Human IFITs in the Context of RSV

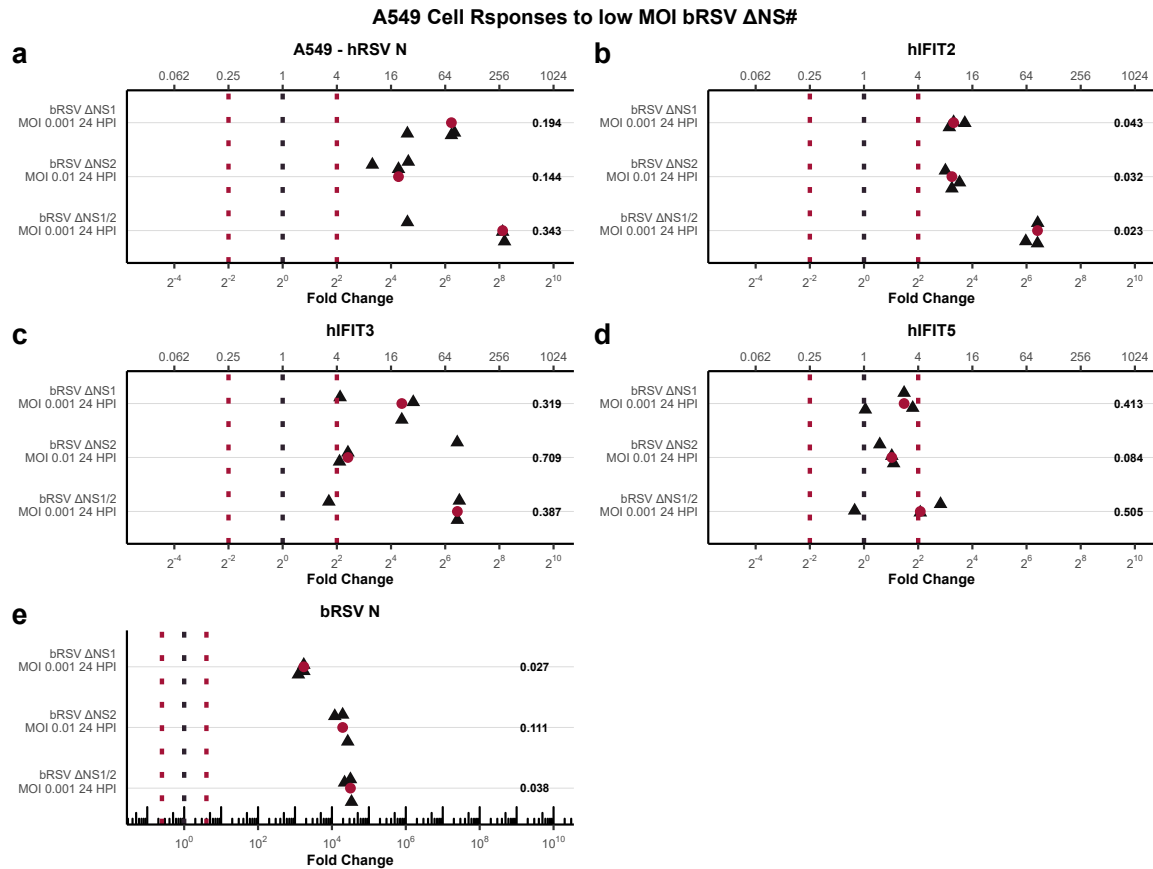


Figure 3.11: A549 hIFIT Response to Low MOI ΔNSs bRSV Infection. The relative abundance of (a) *hIFIT1*, (b) *hIFIT2*, (c) *hIFIT3*, (d) *hIFIT5* and (e) *bRSV N* genes, extracted 24 HPI from A549 cell line following infection with bRSV ΔNS1, ΔNS2, and ΔNS1/2 at MOIs of 0.001, 0.01, and 0.001 respectively. The shown values are relative to standardised mock values. The red circles signify median values. The black dotted line indicates mock expression, while the red dotted lines indicate biologically significant levels of induction. Numeric values signify the p-values compared to mock.

and this potentiation in turn causes higher *hIFIT* induction as a response.

Next, we investigated the effect of the rest of the mutant bRSV viruses, namely ΔNS1, ΔNS2, and a double knock-out ΔNS1/2. As mentioned above, we had trouble achieving high titres using the crude-extraction methodology and thus the MOIs used are lower than what was conducted with WT and ΔSH bRSV, more precisely 0.001 for ΔNS1 and ΔNS1/2, and 0.01 for ΔNS2 bRSV. Total mRNA was extracted 24 hours post-infection. In Figure ?? we can see that all 3 viruses were able to successfully replicate, despite the low MOI. The replication magnitude mimics what was seen in Figure ?? where ΔNS1 *bRSV N* mRNA levels were comparable to the wild-type infection and ΔNS2 and ΔNS1/2 levels were comparable to ΔSH bRSV infection, although slightly lower. We can also observe mixed responses of *hIFITs*, albeit all of them upregulation. *hIFIT1* again was upregulated the highest, 70-fold,

3.2 Results

20-fold and 300-fold to Δ NS1, Δ NS2, and Δ NS1/2 respectively. *hIFIT2* induction levels were almost identical for Δ NS1 and Δ NS2 viruses at around 8-fold despite the difference in MOI. Δ NS1/2 bRSV infection induced it the highest, 70-fold. For *hIFIT3* we can observe different induction dynamics. While Δ NS1 infection induced it to higher levels than what we observed in *hIFIT2* (20-fold), Δ NS2 yielded barely biologically significant induction (4-fold), while virus lacking both non-structural proteins induced *hIFIT3* to equal levels as was observed with *hIFIT2* (70-fold). Although we can see similar upregulation trends with *hIFIT5* to what was observed with other *hIFITs*, meaning Δ NS1 causes medium induction, Δ NS2 causes low induction, and Δ NS1/2 causing high induction, only the latter can be considered biologically significant (4-fold). Yet again, compared to the results with low MOI infection with hRSV (Figure ??), bRSV seems to be more replication-competent, as seen by the relative *bRSV N* mRNA levels, and a more potent *hIFIT* inducer, as low MOI hRSV infection did not yield any induction what so ever. This data also highlights that NS1 negatively regulates *hIFIT* induction more compared NS2, and a lack of both proteins seems to have a synergistic effect on *hIFIT* induction.

Lastly, we wanted to validate these results in the BEAS-2B cell line. The experimental setup was identical to what was described above during the investigation of A549 *hIFIT* responses to bRSV infection. Figure ?? shows the induction levels caused by infection at MOI 1, 24 HPI with WT and Δ SH bSRV. We can see, based on the median relative *bRSV N* mRNA levels, that the viruses are capable of infecting BEAS-2B and are replicating approximately to the levels of what we observed in the A549 cell line. We can also observe that the general trend from A549 one experiment is present, meaning *hIFITs* are being positively induced, and more by the WT bRSV infection than the Δ SH one, with the difference being the magnitude of these inductions. In more detail, the induction of all *hIFITs* seems to be similar, barely biologically significant by WT infection (4-fold), and very weak by Δ SH infection (>2-fold). *hIFIT5* is induced just below biological significance by WT bRSV and at the same level as the other *hIFITs* by the mutant virus. So interestingly the *hIFIT* induction seems to be cell line and stimulus-specific.

Furthermore, we validated the Δ NSs infection data from A549 (Figure ??) using the same experimental setup as was described previously. As we can see in Figure ??, the induction behaviour again differs from what we observed with the A549 cell line. Based on *bRSV N* mRNA levels, we can see that the mutant viruses were able to replicate, although the absolute relative values are one order of magnitude lower than what was observed with the A549 cell line. *hIFIT5* does not respond to the infection with Δ NS1 and Δ NS2 bRSV and positively but biologically significantly responds to Δ NS1/2 virus. *hIFIT1*, *hIFIT2*, and *hIFIT3* display very

Assesment of Transcriptional Induction and Subcellular Localisation of Human IFITs in the Context of RSV

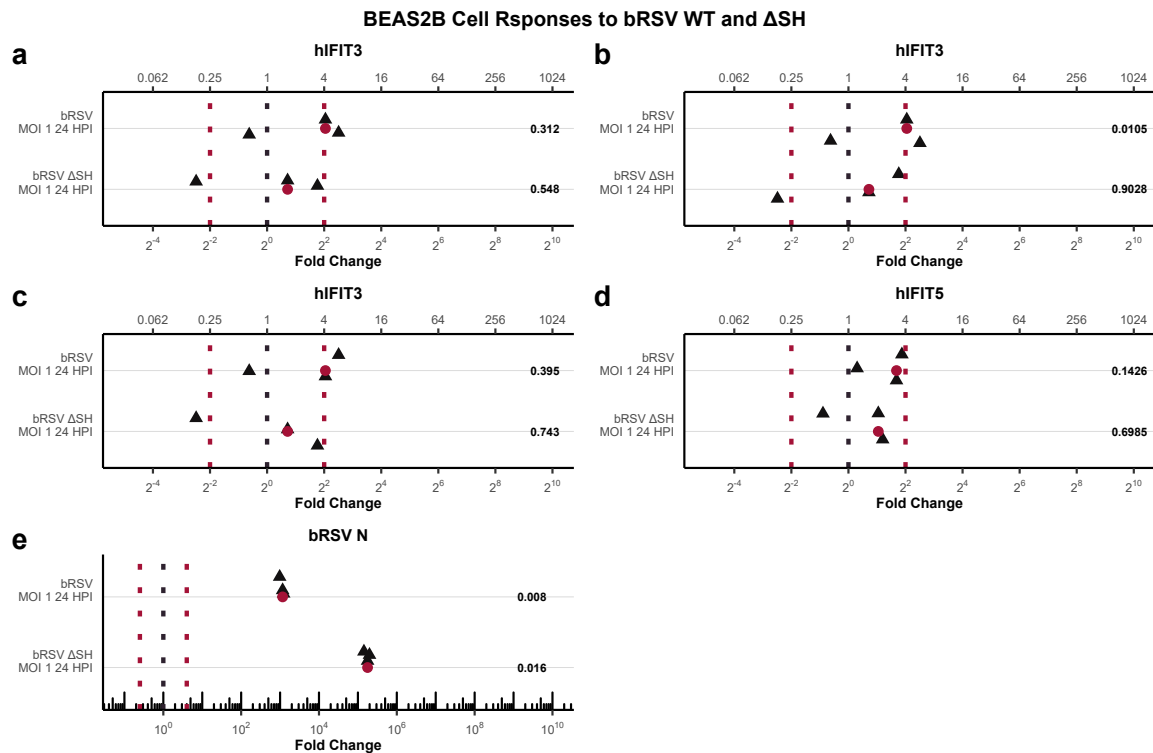


Figure 3.12: BEAS-2B *hIFIT* Response to WT and ΔSH bRSV Infection. The relative abundance of (a) *hIFIT1*, (b) *hIFIT2*, (c) *hIFIT3*, (d) *hIFIT5* and (e) *bRSV N* genes, extracted from BEAS-2B cell line following infection with WT or ΔSH bRSV at MOI 1, 24 HPI. The shown values are relative to standardised mock values. The red circles signify median values. The black dotted line indicates mock expression, while the red dotted lines indicate biologically significant levels of induction. Numeric values signify the p-values compared to mock.

3.2 Results

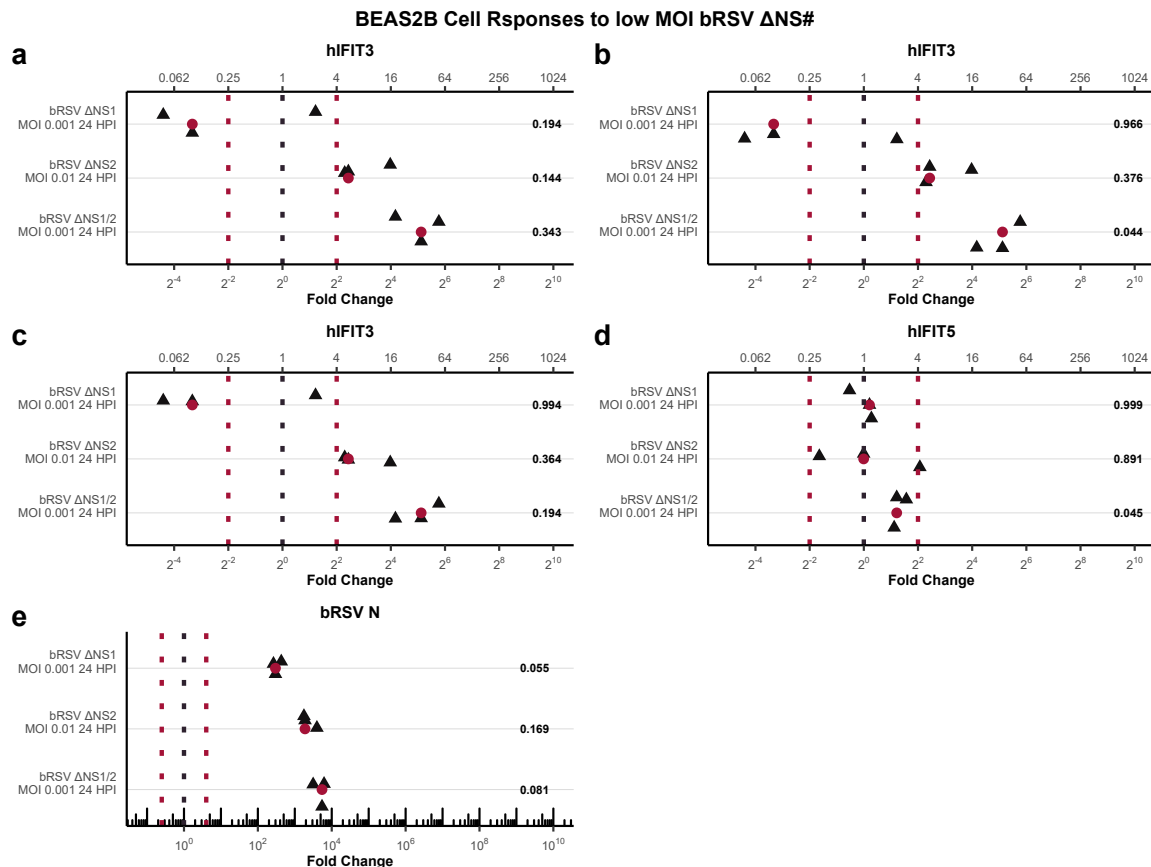


Figure 3.13: BEAS-2B *hIFIT* Response to Low MOI ΔNSs bRSV Infection. The relative abundance of (a) *hIFIT1*, (b) *hIFIT2*, (c) *hIFIT3*, (d) *hIFIT5* and (e) *bRSV N* genes, extracted 24 HPI from BEAS-2B cell line following infection with bRSV ΔNS1, ΔNS2, and ΔNS1/2 at MOIs of 0.001, 0.01, and 0.001 respectively. The shown values are relative to standardised mock values. The red circles signify median values. The black dotted line indicates mock expression, while the red dotted lines indicate biologically significant levels of induction. Numeric values signify the p-values compared to mock.

Assesment of Transcriptional Induction and Subcellular Localisation of Human IFITs in the Context of RSV

similar induction profile to the stimulant. More specifically, Δ NS1 infection downregulated all by 2^{-3} -fold, while Δ NS2 infection caused just biologically significant induction (4-fold), and the double mutant Δ NS1/2 caused median induction of 32-fold. This data suggests NS1 protein being *hIFIT* inductive, while the presence of NS2 negatively influences *hIFIT* expression. This is in reverse to what we observed with A549. A lack of both non-structural proteins seems to have a synergistically positive effect on *hIFIT* induction, like we observed with the A549 cell line.

Summary

Interestingly, the maximal induction of *hIFIT5* observed in this study seems to be 10-16 fold, an order of magnitude lower than what is observed for the other *hIFIT*.

3.2.2 Localisation Changes of Human IFITs

Asdfasfsdfasdf

IF Mock | INF | Infection

A549 BEAS2B

Merge pictures of clusters of cells looking at changes between subcellular localisation and a clear increase in mean intensity. Graphs show mean intensity changes from all cells imaged.

Summary

i guess tie it all together

3.3 Discussion

Recap human induction

Recap human localisation

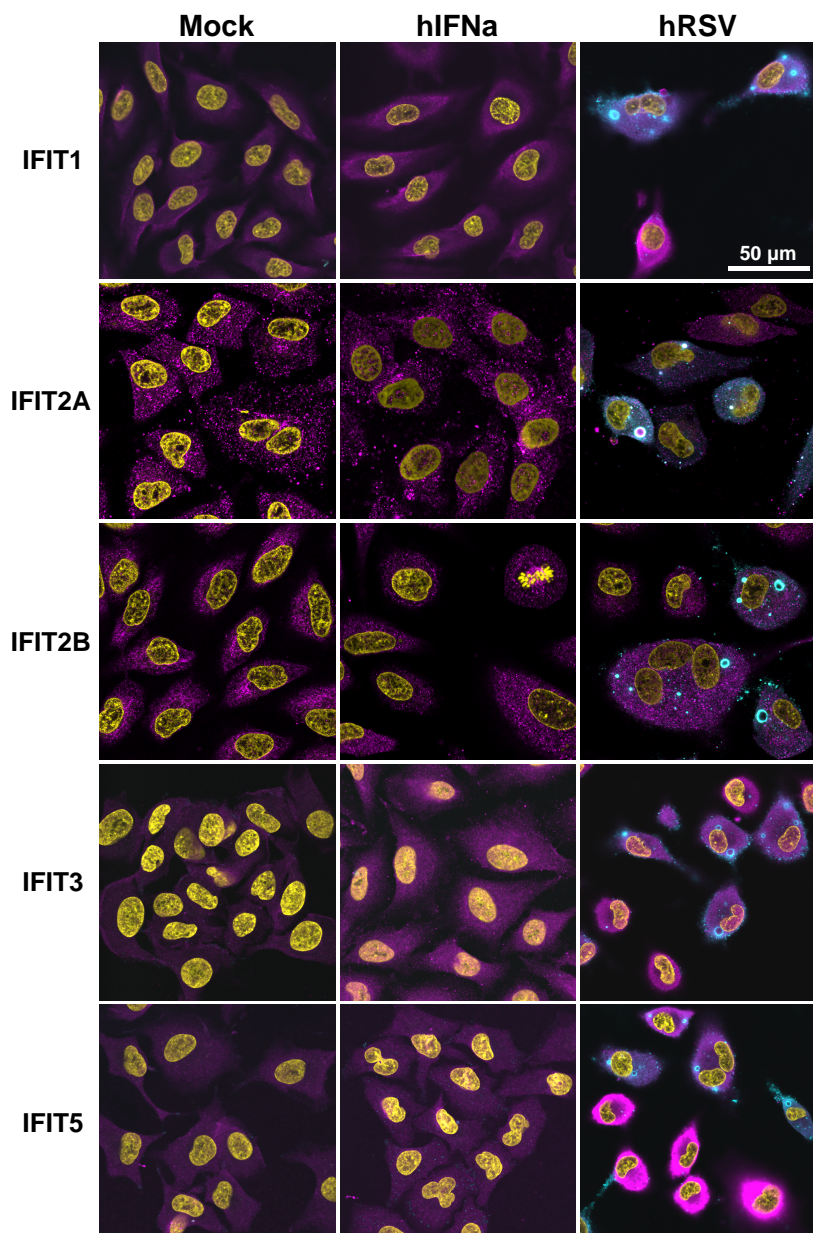


Figure 3.14: A549 localisation mergers.

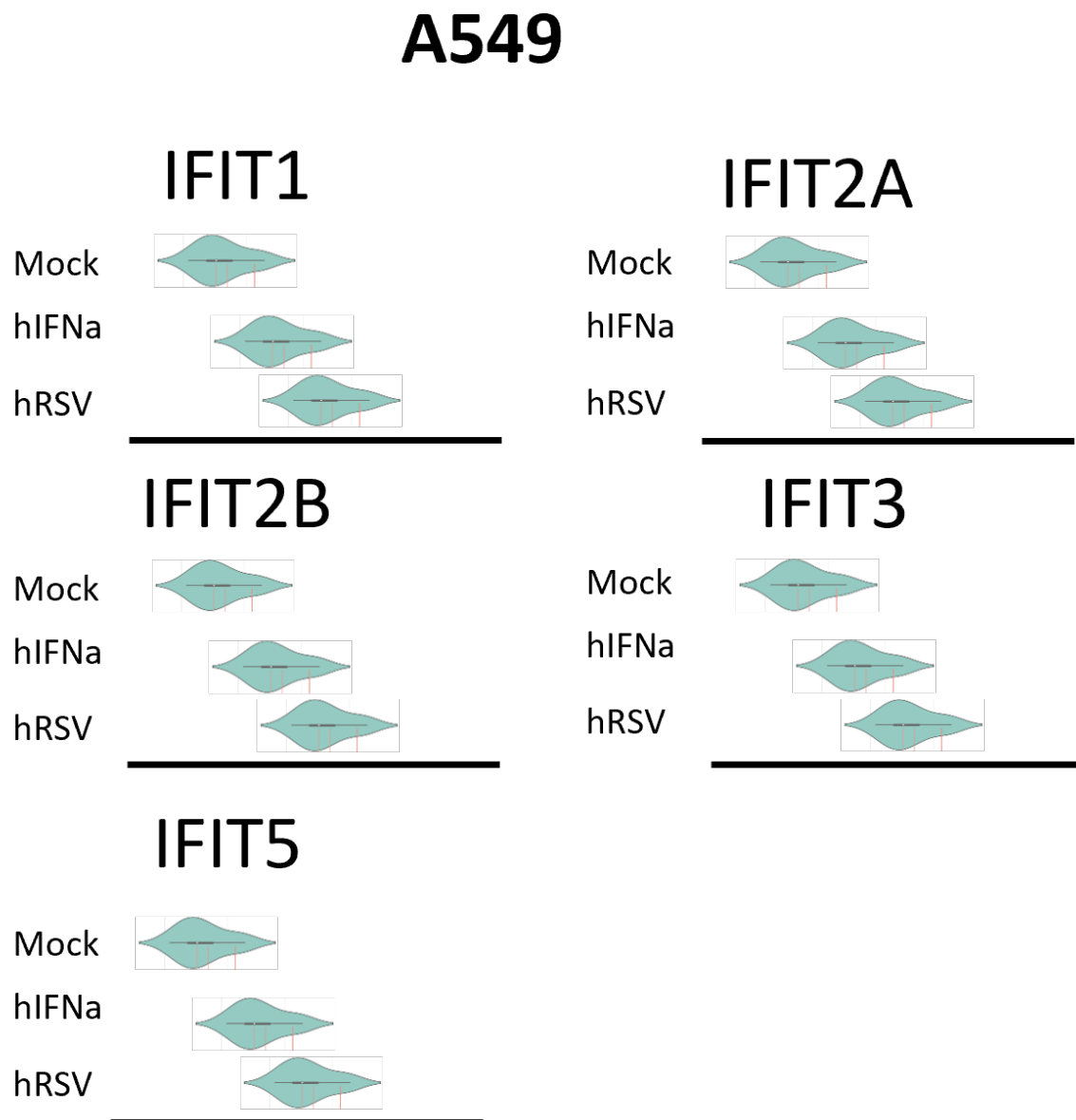


Figure 3.15: A549 localisation plots.

Chapter 4

Assesment of Transcriptional Induction and Subcellular Localisation of Bovine IFITs in the Context of RSV

4.1 Introduction and Aims

Half page intro: Ifit gene regulation (promoters and such)

Ifit paths of induction

interferons

Lps tlr4

about cross species interaction + question about lab attenuated or not the brsv stuff

Half page aims: We hypothesised bovine IFITs to be induced by human and bovine RSV infection. We aimed to systematically test this by initially confirming that our model cell lines are capable of IFIT induction following the treatment of known innate immune system activators such as interferon alpha, and LPS. We would then assess the IFIT induction during human and bovine RSV infection using a range of viral concentration and end assay time points. Lastly, we would validate this data in more physiologically relevant cell lines as well as using omics approaches.

4.2 Results

Assesment of Transcriptional Induction and Subcellular Localisation of Bovine IFITs in the Context of RSV

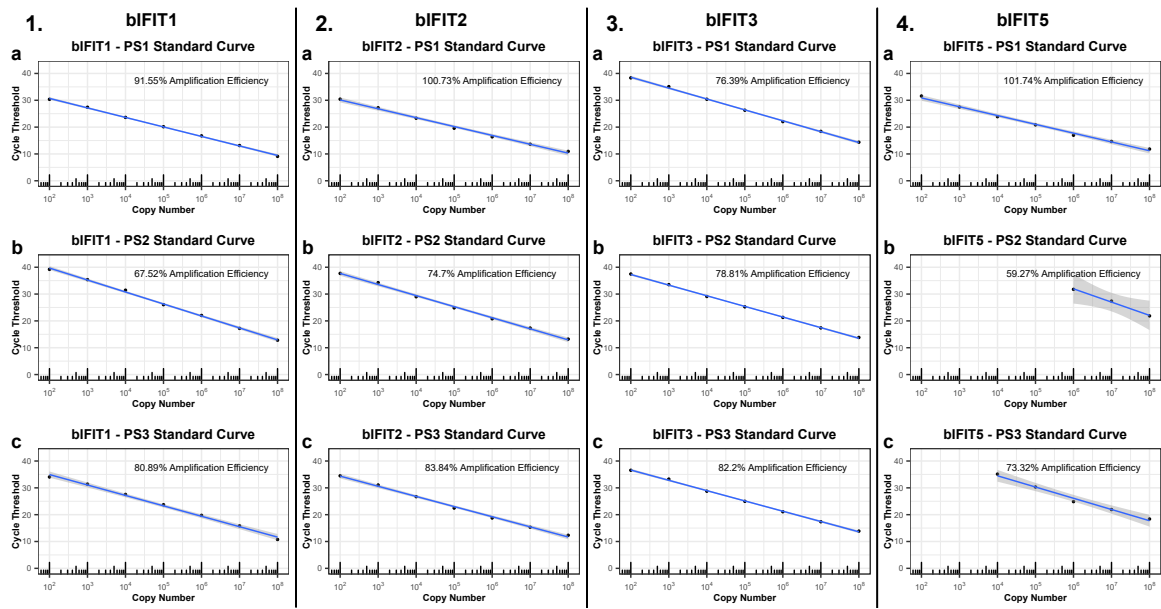


Figure 4.1: Validation of Custom-Made *bIFIT* qPCR Primers. The custom-designed primers were evaluated by creating a serial dilution of bovine *IFIT*-containing plasmids, provided by the CVR Glasgow. The resulting standard curves are shown here. Primer set (PS) 1 (a), 2 (b), and 3 (c) are depicted for bovine *IFIT1* (1.), *IFIT2* (2.), *IFIT3* (3.), and *IFIT5* (4.), along with their calculated amplification efficiencies.

4.2.1 Technologies

4.2.1.1 Bovine *IFIT* qPCR Primer Validation

Due to the initial lack of commercially available primers for the detection of bovine *IFIT* transcripts at the outset of the project, I devised a panel comprising three primer sets (PS) for each bovine *IFIT* gene. Detailed information about this process is outlined in Section ???. In a nutshell, I inputted the coding sequences into the PrimerQuest software (Integrated DNA Technologies) to identify the most suitable oligonucleotides. To evaluate the amplification efficiencies of each primer set, I employed *IFIT* DNA clones from a bovine ISG library as standards (accessible through a collaboration with CVR Glasgow). The outcomes are depicted in Figure ???. The graph demonstrates that primer sets 1 exhibited the most favourable amplification efficiencies. All primer sets, except for *bIFIT3*, yielded nearly impeccable amplification efficiencies of around 100%. Consequently, they were chosen for subsequent experiments. While *bIFIT3* primer sets demonstrated similar outcomes in terms of standard curve slopes and amplification efficiencies, PS1 consistently outperformed the others in repeated testing rounds (data not presented). As a result, it was singled out for further experimentation.

4.2 Results

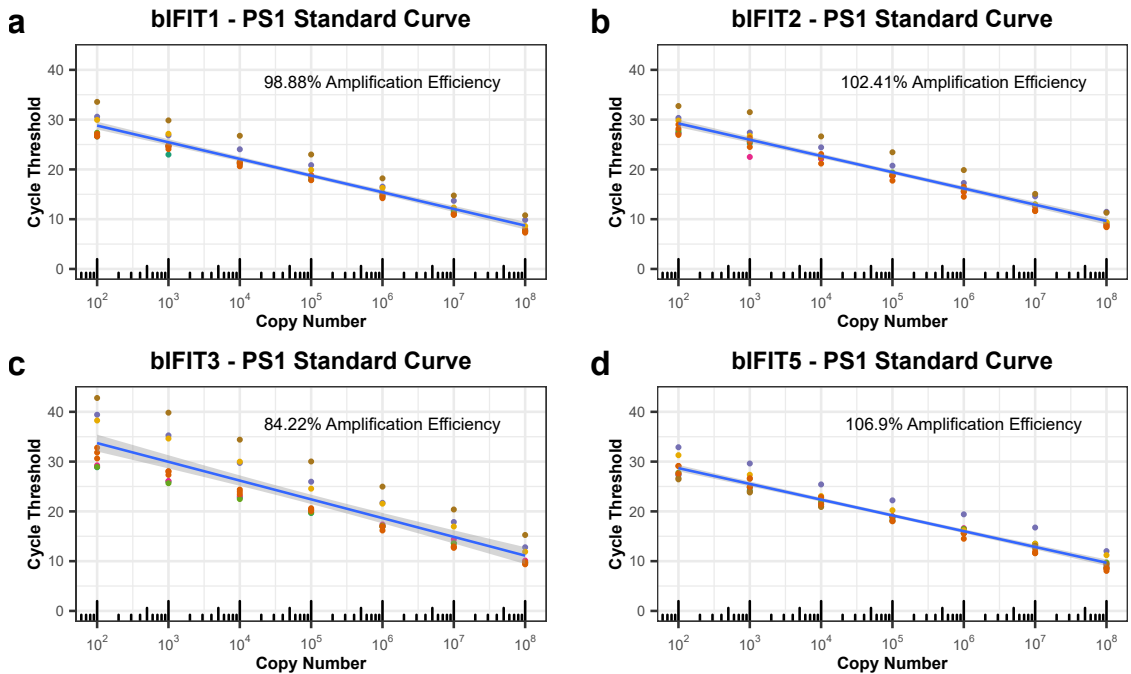


Figure 4.2: The Performance of Custom-Made Primer-Sets Over Time. During the experiments with custom-made *bIFIT* qPCR primers, standard curves had to be always constructed. Here, the underlying average amplification efficiencies and standard curves, along with the individual data, from all the experiments and coloured by the experiment are displayed.

The PSs behaviour was monitored throughout the project, as fresh standard curves were created per experiment. Figure ?? shows that the average data is consistent with what was observed in initial testing (Figure ??), however, there were per experiment deviations in slope angles for each of the selected primer pairs. The underlying amplification efficiencies stayed consistent, as is highlighted by the averaged efficiencies displayed. The initial *bIFIT3* PSs differential amplification slopes compared to the other *bIFIT* PSs, as well as the variable nature of PSs performance throughout the project prohibits the usage of $\Delta\Delta Ct$ methodologies for transcript quantification as the increase in cycle threshold would not be proportional to the decrease of transcript abundance between the *bIFITs*, and thus a different methodology had to be adopted. This is described in detail in Section ?? . In short, the copy numbers were deducted from standard curves and factorised by the relative abundance of bovine *GAPDH*. This ensured the slope-independent establishment of relative expression values, mirroring and complementing data from $\Delta\Delta Ct$ methodologies.

Assesment of Transcriptional Induction and Subcellular Localisation of Bovine IFITs in the Context of RSV

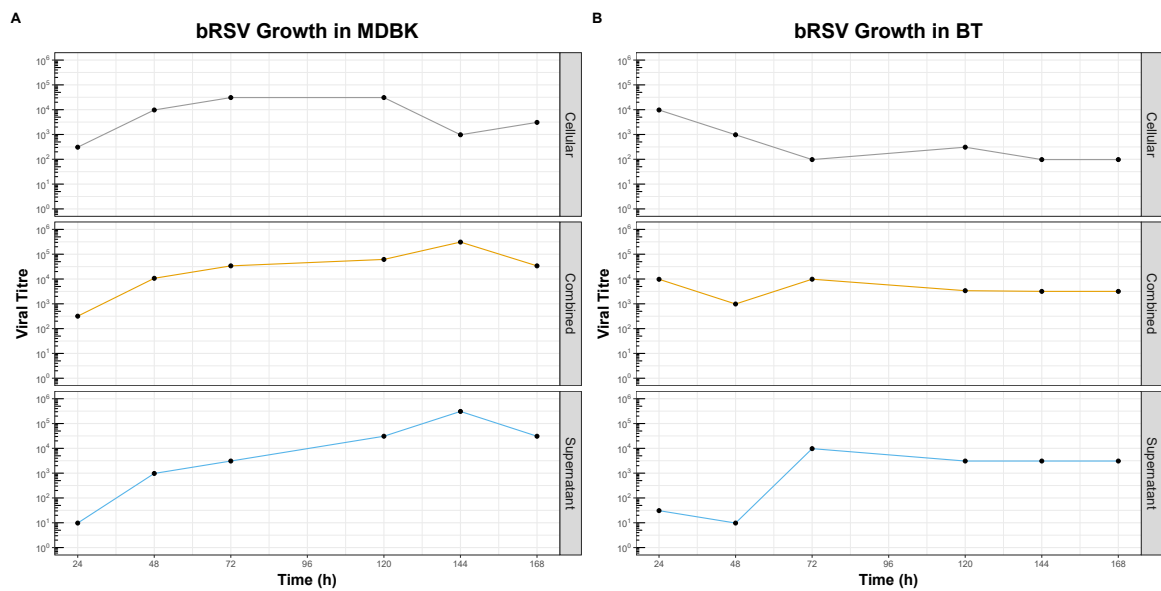


Figure 4.3: bRSV Growth Curves in MDBK and BT Cell Lines. MDBK and BT cell lines were infected with 0.1 MOI wild-type bRSV and the cellular (top panel) and supernatant (bottom panel) fractions were extracted at time intervals of 24, 48, 72, 96, 120, 144, and 168 hours post-infection. These were subsequently quantified by TCID₅₀ methodology.

4.2.1.2 Growth curves of bovine RSV in bovine cell lines

Although my colleagues in the Viral Glycoproteins from the Pirbright Institute routinely perform hRSV infections of MDBK cell line, the data in BT cell line is currently lacking. Therefore I set up bRSV growth curves in both cell lines side by side to investigate which time points would be relevant for further infection experiments. Crude-extracted bRSV, isolated as described in Section ?? and quantified as described in Section ?? was used for the establishment of growth curves as described in Section ???. In brief, MDBK and BT cell line was seeded in 96-well plates and infected with WT bRSV at MOI 0.1. The supernatant and cellular fractions were collected at time intervals of 24, 48, 72, 96, 120, 144, and 168 hours post-infection, snap frozen in dry ice ethanol mixture, and later tittered as described in Section ???. As can be observed in Figure ??,

4.2.2 Transcriptional Changes to Bovine *IFITs*

4.2.2.1 Responses of Bovine Cell Lines to Known Activators of Innate Immune Response

some text here about what wrote previously

some text about bifn stimulation

4.2 Results

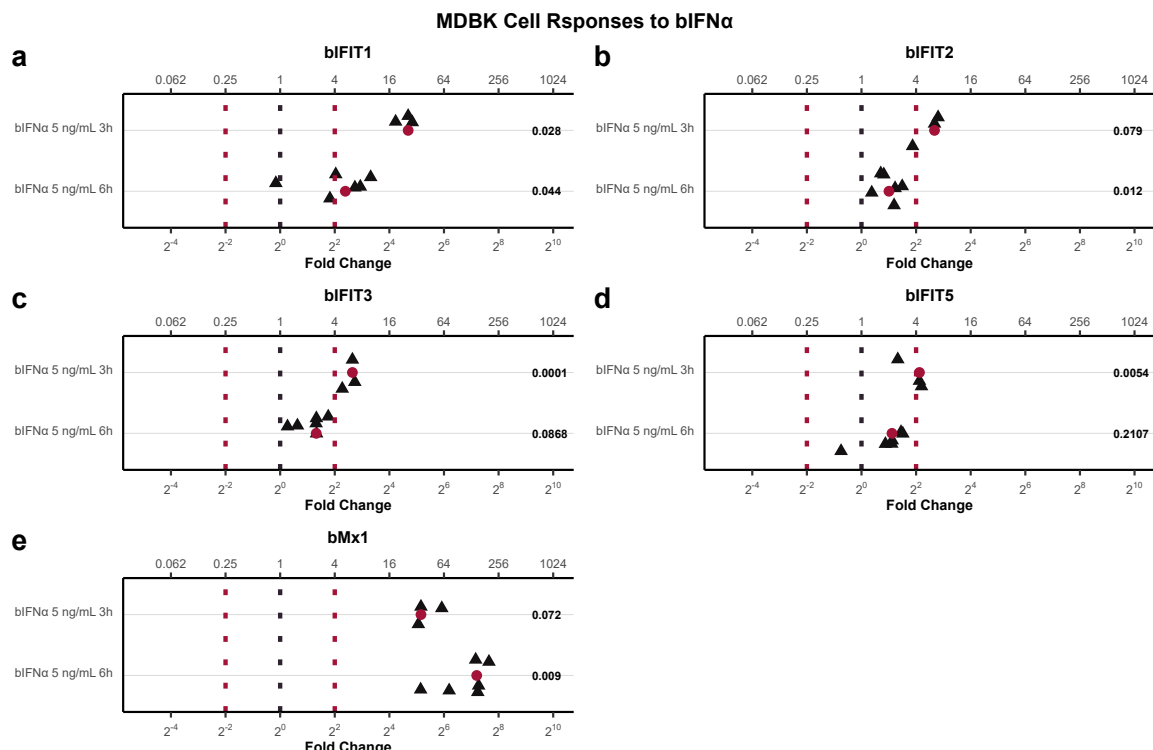


Figure 4.4: qPCR Analysis of MDBK *bIFIT* Response to bIFN α . The relative abundance of (a) *bIFIT1*, (b) *bIFIT2*, (c) *bIFIT3*, (d) *bIFIT5*, and (e) *bMx1* genes, extracted from the MDBK cell line, with response to bovine interferon alpha (IFN α) at a concentration of 5 ng/mL for a treatment duration of 3 or 6 hours. The shown values are relative to standardised mock values. The red circles signify median values. The black dotted line indicates mock expression, while the red dotted lines indicate biologically significant levels of induction. Numeric values signify the p-values compared to mock.

Assesment of Transcriptional Induction and Subcellular Localisation of Bovine IFITs in the Context of RSV

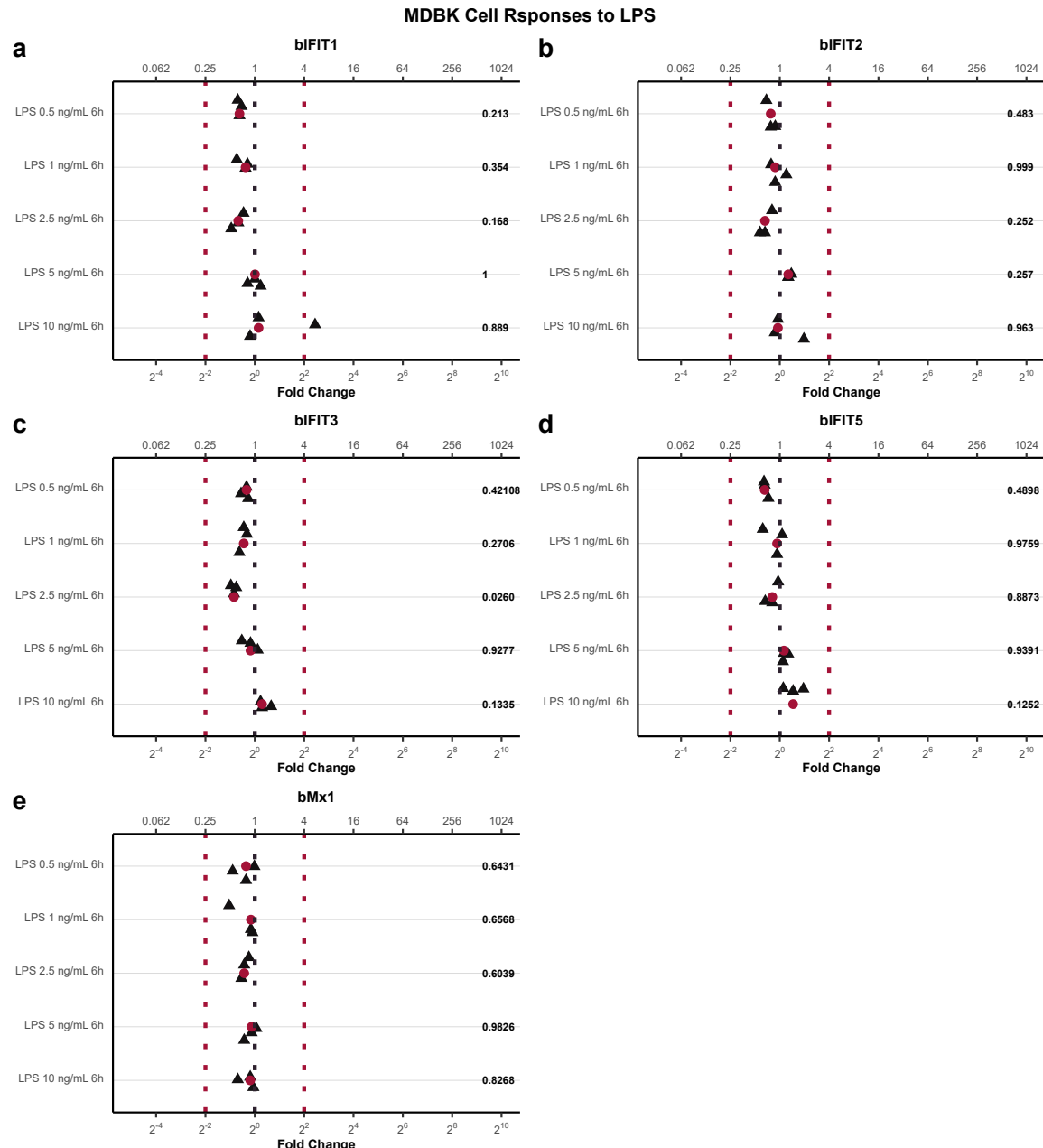


Figure 4.5: qPCR Analysis of MDBK *bIFIT* Response to LPS. The relative abundance of (a) *bIFIT1*, (b) *bIFIT2*, (c) *bIFIT3*, (d) *bIFIT5*, and (e) *bMx1* genes, extracted from the MDBK cell line, with response to bacterial LPS at a concentration of 0.5, 1, 2.5, 5, and 10 ng/mL for a treatment duration of 6 hours. The shown values are relative to standardised mock values. The red circles signify median values. The black dotted line indicates mock expression, while the red dotted lines indicate biologically significant levels of induction. Numeric values signify the p-values compared to mock.

4.2 Results

Bovine Mx1 is included in all experiments with bovine cells as it is an ISG that is induced by range of infections and the activators of innate immune response. It is also a control for bIFN alpha (if it works properly and is not degraded).

Neither bMx1 nor bIFITs are induced by LPS in the concentration range tested. bMx1 was induced by all bIFN alpha at different concentrations and timepoints, but at 5 ng/mL for 24h. This means that either that treatment failed or 24h post adding the bIFN treatment is too late to capture the ISG induction. All targets are induced by bIFN alpha treatment at 5 ng/mL for 3 hours. bIFIT1 also responds to low concentration (0.5 ng/mL) for 6h treatment, but not the other IFITs. No other concentration/time combination induced bIFITs.

This all suggests that MDBK are responsive to bIFN alpha and capable of bIFIT induction, but the responses are weak, especially compared to human cells.

I have a hypothesis that in bovine cells the IFITs are basally expressed to higher levels (that would explain why we can detect them by IF in mock and infected cell although the qPCR data suggest there is no induction).

4.2.2.2 Bovine *IFITs* Responses to bRSV

The Madin-Darby bovine kidney (MDBK) cell line, derived from bovine renal epithelium in 1958 (**Madin1958EstablishedOrigin**), is an established model system used in bovine virology studies. We assayed them for the induction potential of bovine *IFITs*, alongside bovine *Mx1* using bovine interferon alpha and LPS (bovine interferon-gamma was not available commercially). Bovine *Mx1* was included in the analyses as it is a ISG, widely reported in immunology and virology studies (ADD SOME REFERENCES HERE FOR CRYING OUT LOUD), and because we saw minimal bovine *IFIT* responses throughout the study and wanted to ensure the cell lines used had the internal pathways for ISG induction correctly functioning. Figure ?? shows the *bIFIT* and *bMx1* responses to the stimulation with bIFN α at a concentration of 5 ng/mL (equivalent to 1,000 UI/mL of hIFN α) for either 3 or 6 hours. Interestingly, we see a similar effect in induction amplitude but an opposing effect in time of stimulation to amplitude compared to hIFN α induction in BEAS-2B cells (Figure ??). DESCRIBE THE DATA ITSELF

Old text: Alongside confirming the induction potential of bIFITs in MDBK cells, we assessed the effect of bovine respiratory syncytial virus (bRSV) on IFIT induction. As bRSV is a known inducer of the interferon response we expect bovine IFIT genes to be upregulated following infection. MDBK cells were infected with purified bRSV at MOI of 1 for 24 and 48 hours. As a positive control human IFNa was used. This was due to the unavailability of a bovine counterpart at that point, however, Gresser and his colleagues (1974), reported that

Assesment of Transcriptional Induction and Subcellular Localisation of Bovine IFITs in the Context of RSV

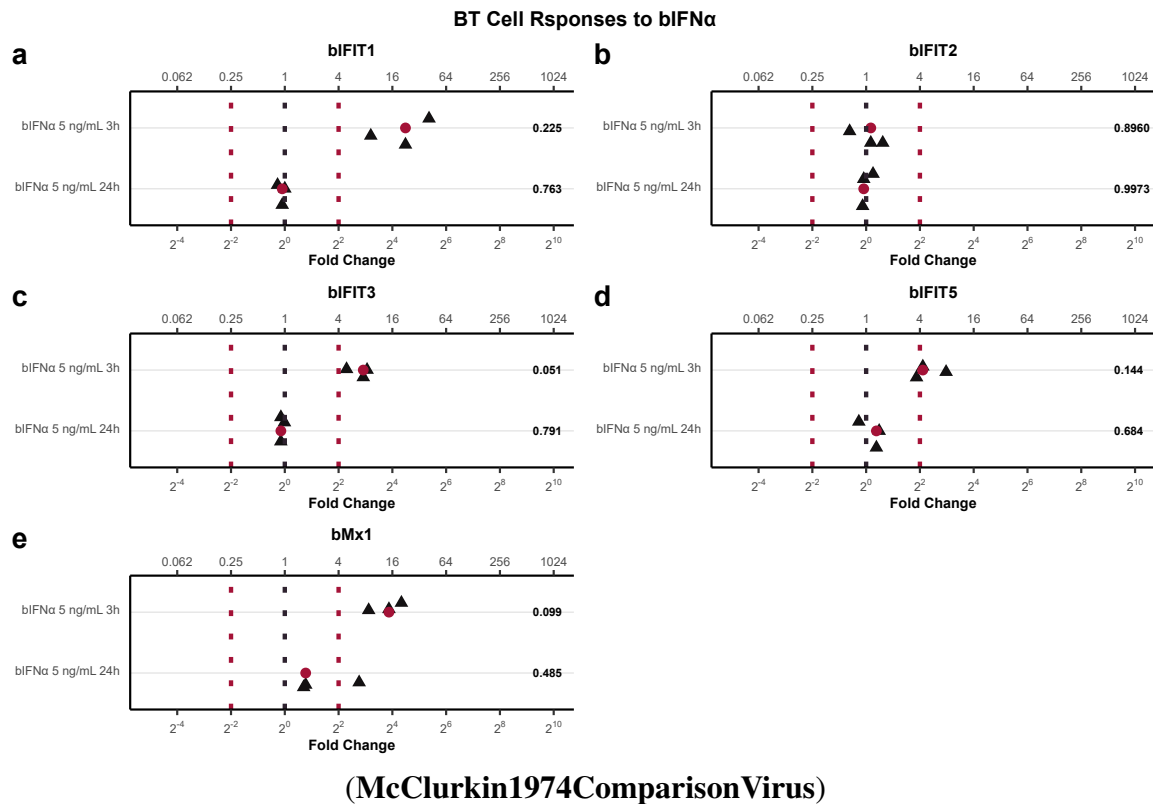


Figure 4.6: qPCR Analysis of MDBK *bIFIT* Response to bIFN α . The relative abundance of (a) *bIFIT1*, (b) *bIFIT2*, (c) *bIFIT3*, (d) *bIFIT5*, and (e) *bMx1* genes, extracted from the MDBK cell line, with response to bIFN α at a concentration of 0.5, 1, 2.5, 5, and 10 ng/mL for a treatment duration of 6 hours. The shown values are relative to standardised mock values. The red circles signify median values. The black dotted line indicates mock expression, while the red dotted lines indicate biologically significant levels of induction. Numeric values signify the p-values compared to mock.

4.2 Results

hIFNa does indeed affect bovine cells as well. Cellular RNA was extracted and converted to complementary DNA, as described in section 7.3. Bovine IFIT transcripts were quantified relative to mock-infected cells. qPCR results (Figure 7A) were normalised to bovine GAPDH levels. We observed large variation in the transcriptional response, even in mock-infected cells. bIFITs 2, 3 and 5 mRNA levels did not change in response at any time point post bRSV infection. bIFIT1 was induced at 48 hours post-infection, but the variation is too high to make firm conclusions at this point. However, consistent with Gresser et al's previous findings, bIFITs were responsive to 1000 units of hIFNa; all genes were highly induced (Figure 7B), although the fold expression increases varied greatly. bIFIT1 increased 10000-fold, followed by bIFIT2 and bIFIT3 with both having c. 700-fold increase. bIFIT5 mRNA expression was induced by c. 25-fold after treatment with hIFNa. This experiment was performed once and will be repeated. As a control for infection, quantification of viral RNA using qPCR will provide us with a clearer picture about the observed changes.

UV inactivated bRSV causes no change for bMx1 and bIFIT2 and seems to downregulate bIFIT1,3,5. Low, mid, and high MOI (0.1, 1, 2) and two different time points (24 and 48 HPI) do not seem to influence the levels of any genes tested other than for bMx1 for wt ultracentrifugation purified bRSV 24 HPI MOI 1. I have one experiment where bRSV MOI 1 24 HPI downregulates all genes tested but it might be a technical error. Very low MOI (0.001) wt bRSV along with MOI 1 dSH and very low MOI dNS1, dSN2 and dNS1/2 bRSV do not up or downregulate any genes tested in a biologically significant way.

some text some text some text some text some text
some text some text some text some text some text
some text some text some text some text some text
some text some text some text some text some text
some text some text some text some text some text

4.2.2.2.1 Validation by analysing bRSV RNAseq dataset

Describe data:

asdasdas

Data showing that bIFITs are not differentially expressed in cells infected with dSH bRSV.

This is a dataset that was present in Dalan's group. Comparing responses at 16 and 40 HPI between WT bRSV vs Mock and dSH bRSV vs Mock. The dataset was previously analysed by a bioinformatician in Pirbright which yield 0 differentially expressed host genes. He however included viral genes in the analysis, which I assume affected the adjusted p values of the host genes due to the relative viral genes abundance. We tried to get in touch

Assesment of Transcriptional Induction and Subcellular Localisation of Bovine IFITs in the Context of RSV

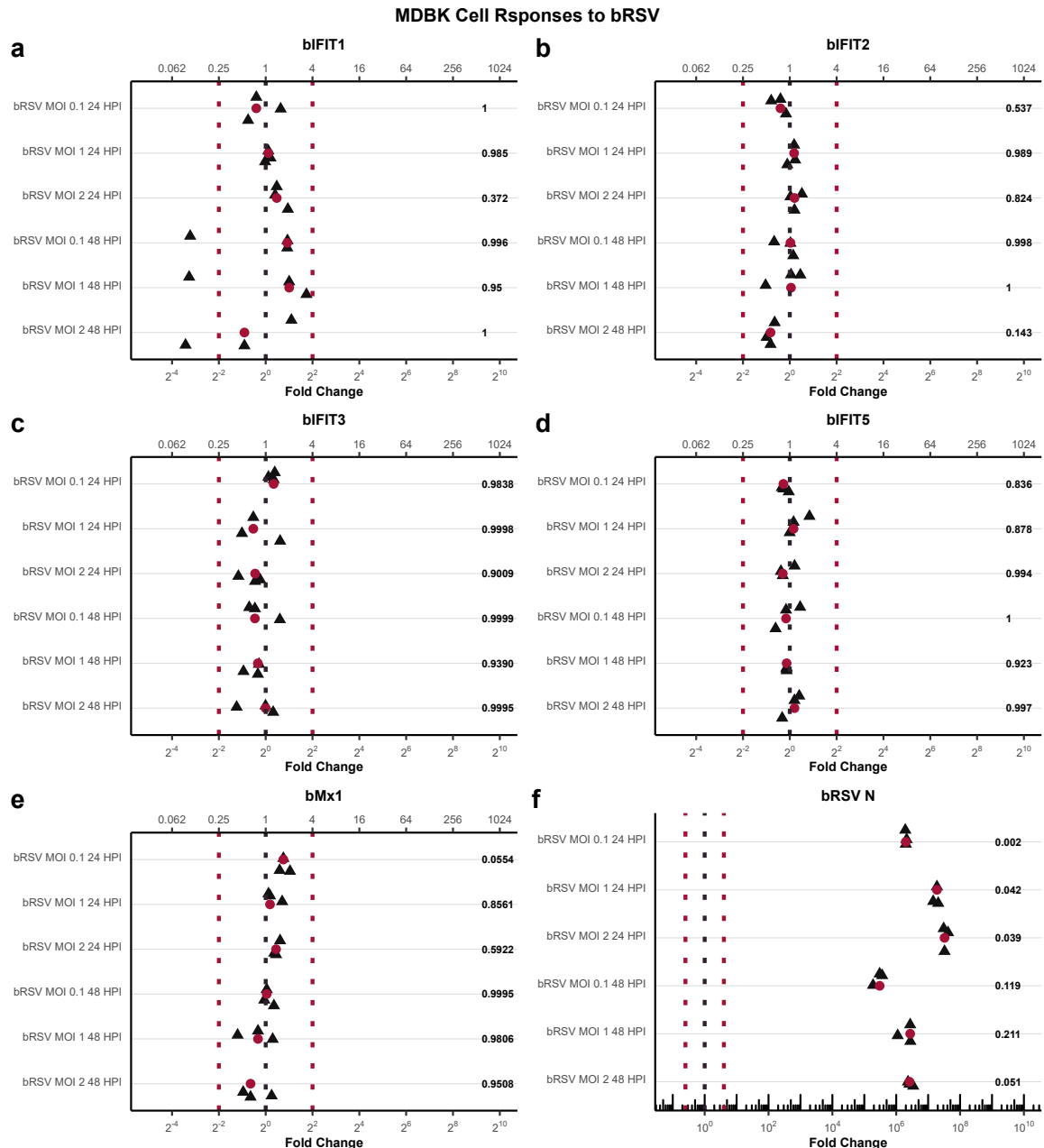


Figure 4.7: MDBK *bIFIT* Response to bRSV as a Function of Time and MOI. The relative abundance of (a) *bIFIT1*, (b) *bIFIT2*, (c) *bIFIT3*, (d) *bIFIT5*, (e) *bMx1* and (f) *bRSV N* genes, extracted from MDBK cell line following infection with bovine RSV at MOI of either 0.1, 1, or 2 for either 24 or 48 hours post-infection. The shown values are relative to standardised mock values. The red circles signify median values. The black dotted line indicates mock expression, while the red dotted lines indicate biologically significant levels of induction. Numeric values signify the p-values compared to mock.

4.2 Results

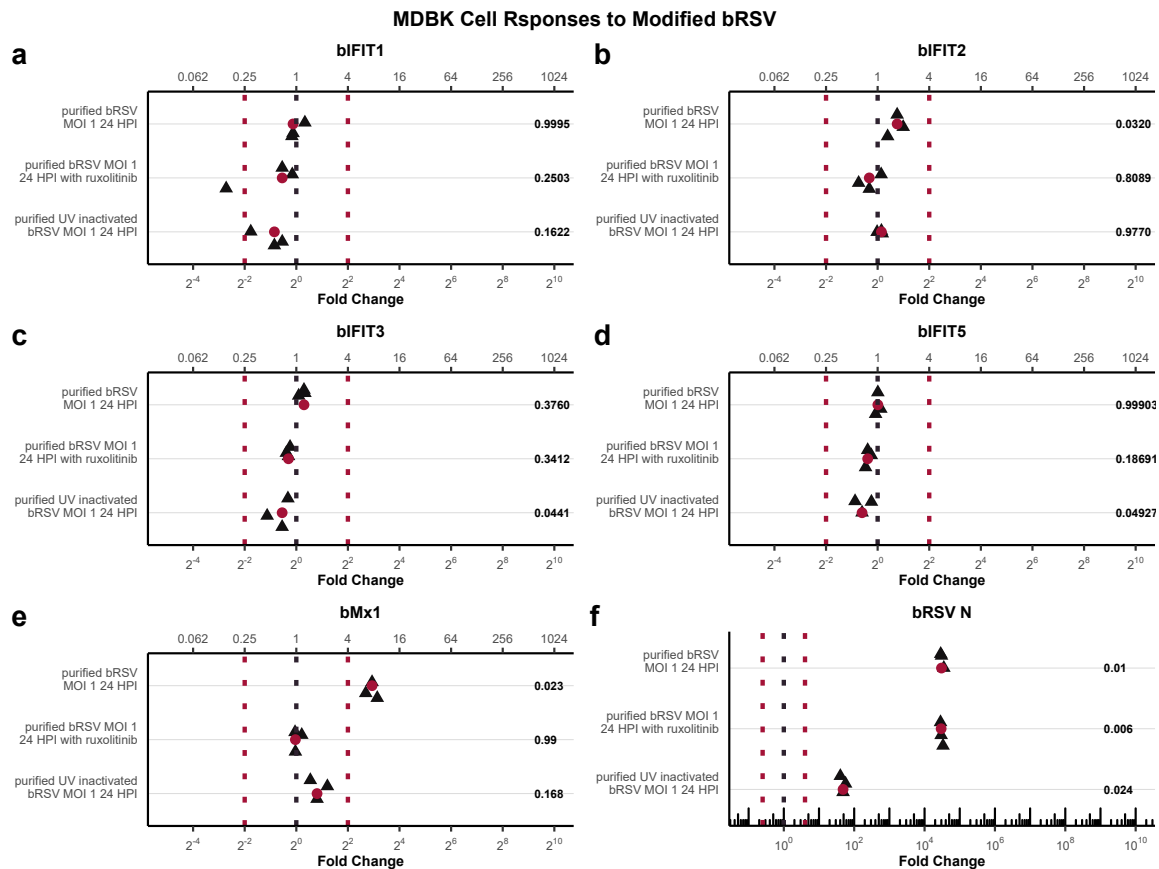


Figure 4.8: The Effect of Ultra-Purification, UV-Inactivation and INFR Inhibition on *bIFIT* Induction Following hRSV Infection in MDBK. The relative abundance of (a) *bIFIT1*, (b) *bIFIT2*, (c) *bIFIT3*, (d) *bIFIT5*, (e) *bMx1*, and (f) *bRSV N* genes, extracted from MDBK cell line following infection with ultra-purified bRSV at MOI 1 for 24 hours. The cells were either treated with the virus alone (first row), or with the virus and 5 nM of ruxolitinib (interferon receptor inhibitor) during the whole infection period (second row), or with UV-inactivated bRSV (last row). The shown values are relative to standardised mock values. The red circles signify median values. The black dotted line indicates mock expression, while the red dotted lines indicate biologically significant levels of induction. Numeric values signify the p-values compared to mock.

Assesment of Transcriptional Induction and Subcellular Localisation of Bovine IFITs in the Context of RSV

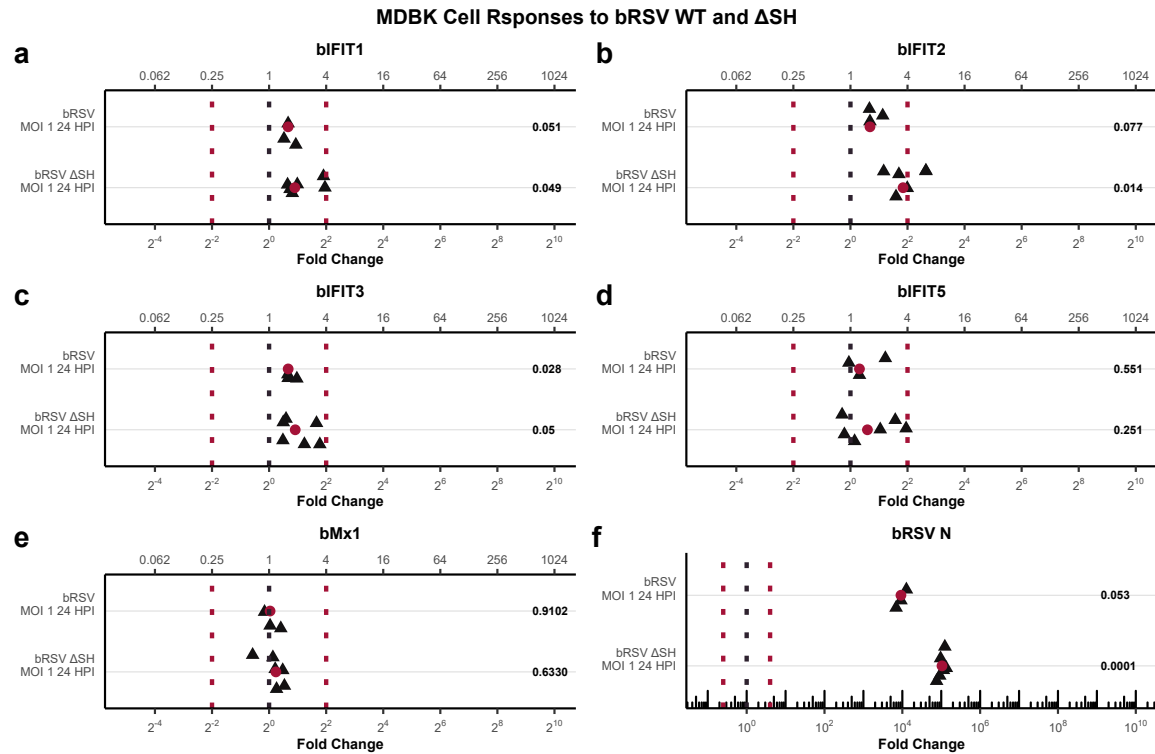


Figure 4.9: MDBK responses to dSH. timepoints infection

with him to discuss this but after several emails got no response. The re-analysis was done on raw annotated count data which had viral transcripts removed. Original analysis was done using EdgeR package, my re-analysis was with DESeq2 (both are valid way of doing DE analysis, EdgeR is more modular and harder to use).

All 4 volcano plots, showing bi1-5 and bm1, regardless where they are afterwards i would do a paragraph of the analysis as I did it so why not

4.2.2.3 Bovine IFITs Responses to hRSV

Data show that ultracentrifugation purified hRSV causes no response in terms of bIFIT induction. Infection with normally purified virus does not cause induction either but hints at downregulation actually.

Describe data:

asdasdas

Validation in more physiologically relevant cell line. All genes but bIFIT2 respond to bIFN alpha 5 ng/mL for 3h; treatment for 24h cause no change in any of the genes; treatment for 6h downregulates IFITs but not bMx1. This shows that BT cells are responsive to IFN

4.2 Results

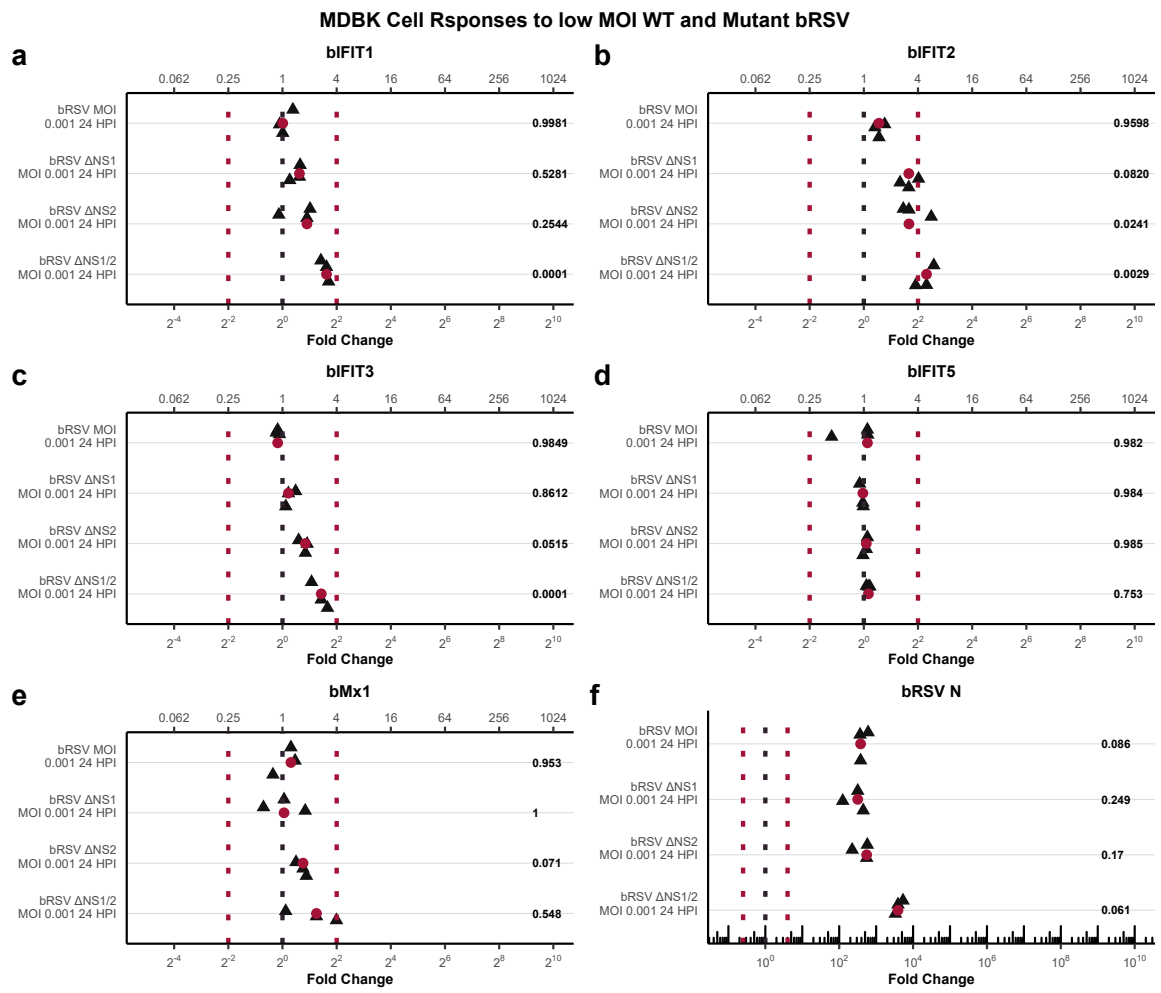


Figure 4.10: MDBK responses to low MOI mutant bRSV. asdf as asdf asdf asdf asdf asdf assd

Assesment of Transcriptional Induction and Subcellular Localisation of Bovine IFITs in the Context of RSV

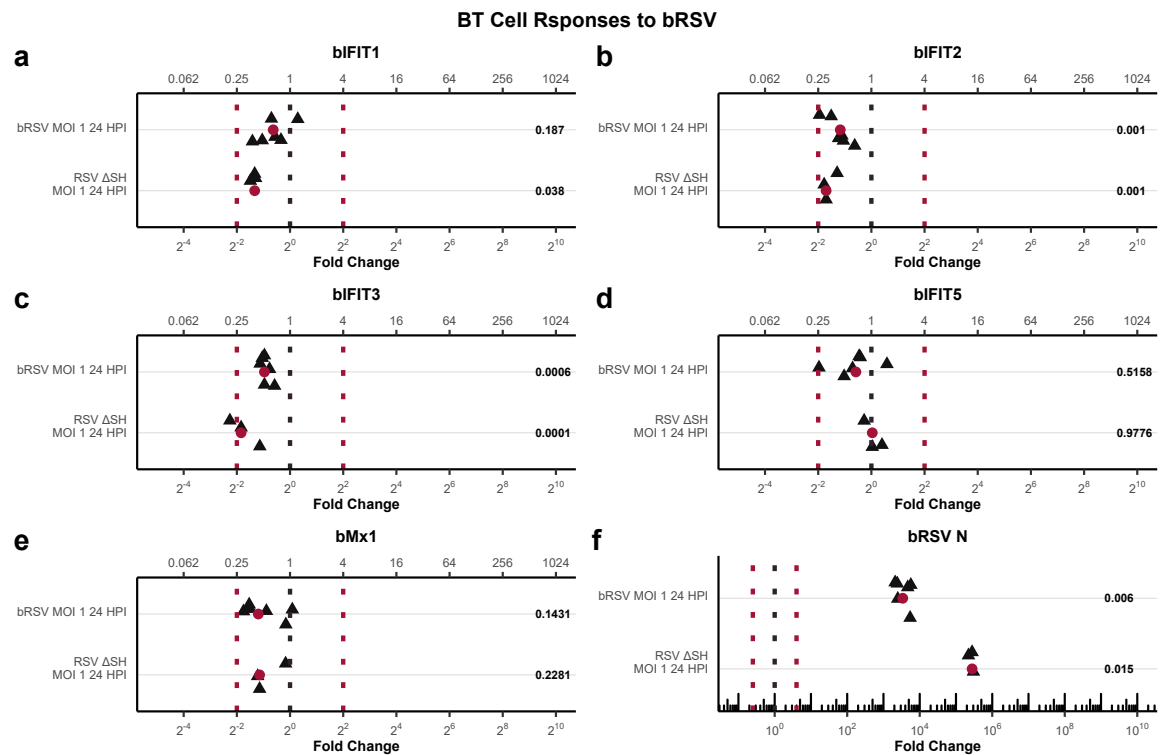


Figure 4.11: BT responses to bRSV. asdf as asdf asdf asdf as asdf asdf assd

and have the capability to express bIFITs and bMx1.

Ultracentrifugation purified hRSV causes downregulation in IFITs but not bMx1 (where it causes no change), while infection with normally extracted hRSV cause no change in none of the genes tested. Infections with wt bRSV and dSH bRSV at the same MOI and HPI (1 and 24) cause slight downregulation in all genes tested.

The trends seen with MDBK are kind of recapitulated.

Summary

i guess tie it all togeher

4.2.3 Localisation Changes of Bovine IFITs

Asdfasfsdfasdf

IF Mock | INF | Infection

MDBK BT

Merge pictures of clusters of cells looking at changes between subcellular localisation and a clear increase in mean intensity. Graphs show mean intensity changes from all cells

4.2 Results

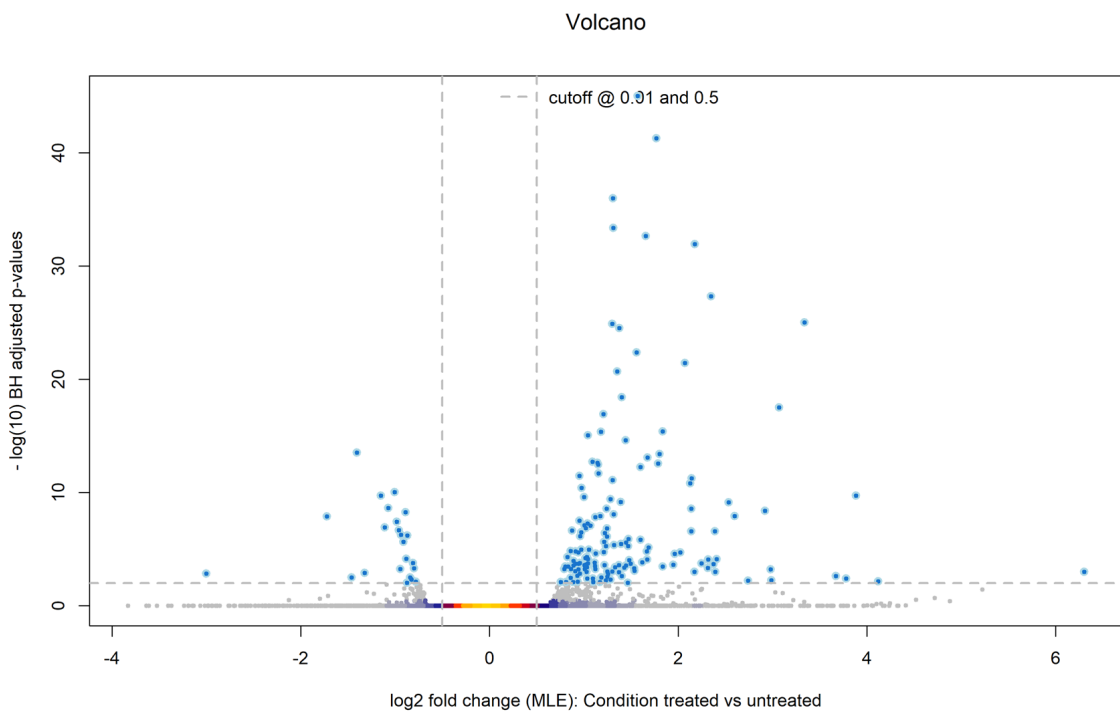


Figure 4.12: Volcano plot of DE genes in WT vs Mock 40 HPI. asdf asdf

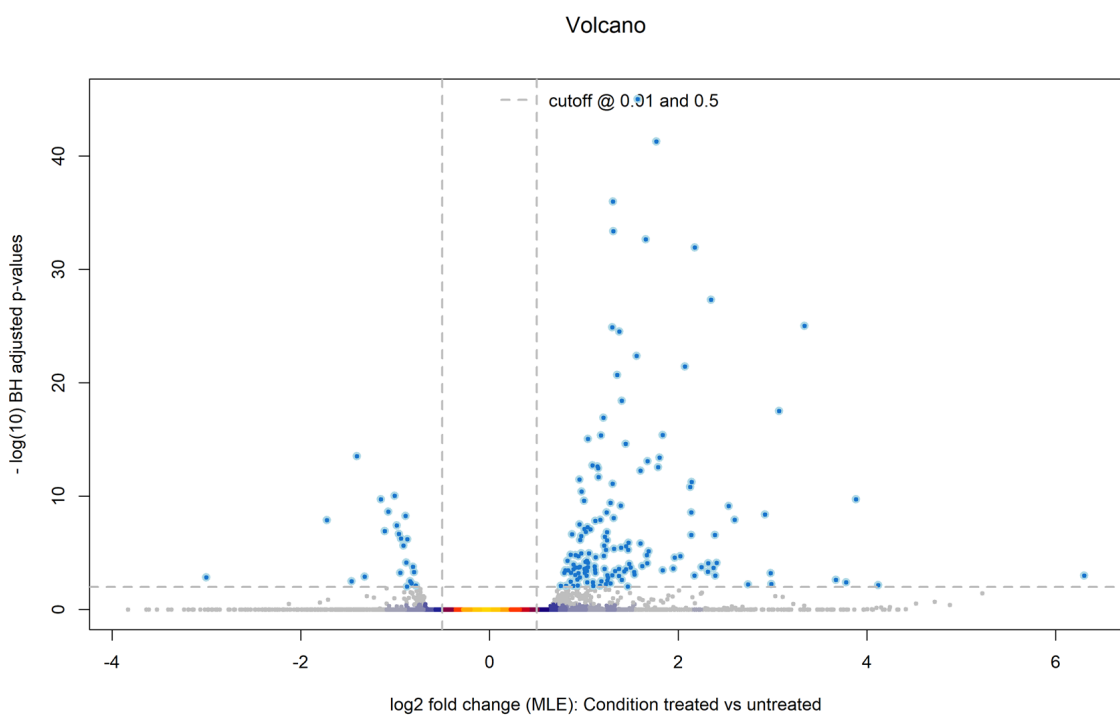


Figure 4.13: Enter Caption

Assesment of Transcriptional Induction and Subcellular Localisation of Bovine IFITs in the Context of RSV

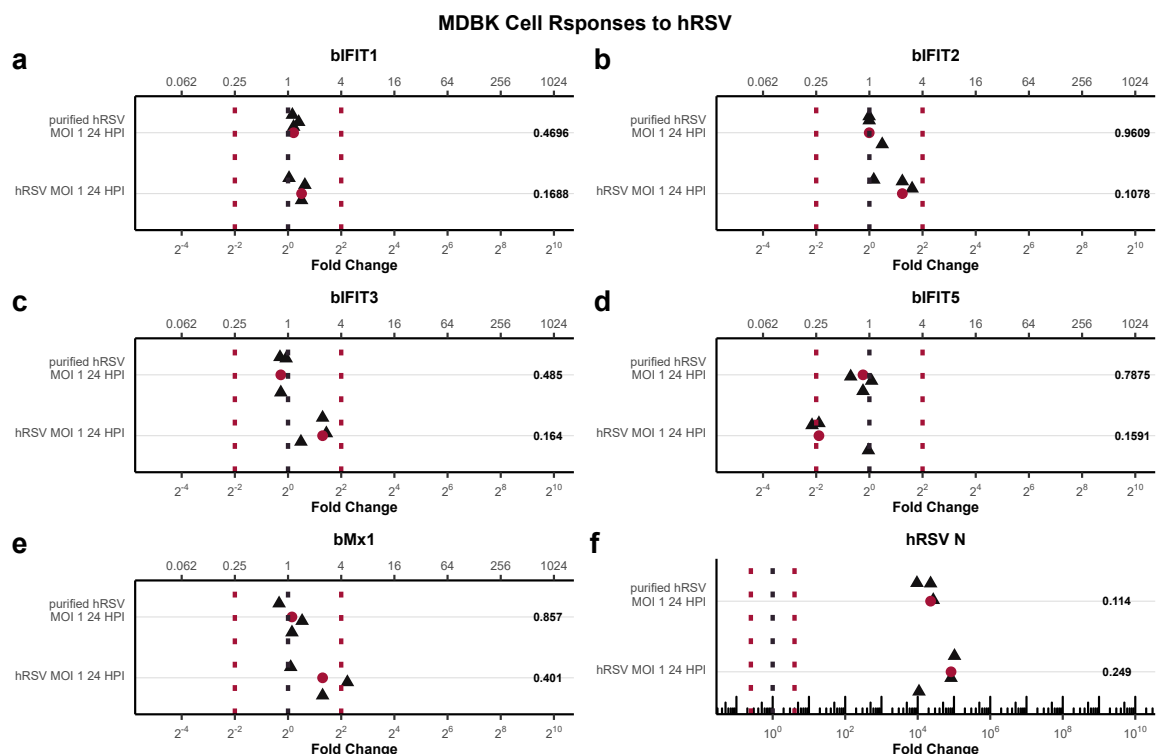


Figure 4.14: bIFIT responses to hRSV infection in MDBK. asdf asdf asdf asdf asdf asdf asdf asdf asdf asdf

4.3 Discussion

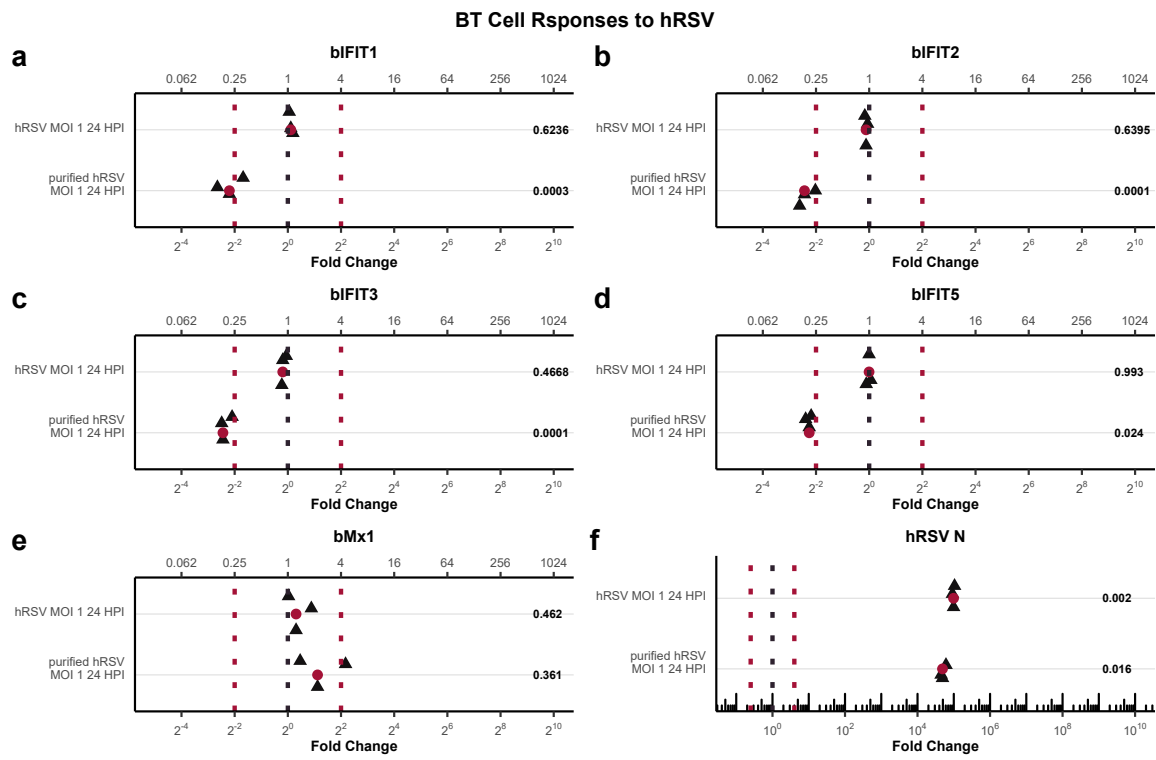


Figure 4.15: Bt responses to hRSV. asdf asdf asdf asds fasdf asdf a sdf asdf asdf asdf as dfas ddf asdf asd

imaged.

Summary

i guess tie it all togeher

4.3 Discussion

Recap human

Recap bovine

Bovine rna seq studies

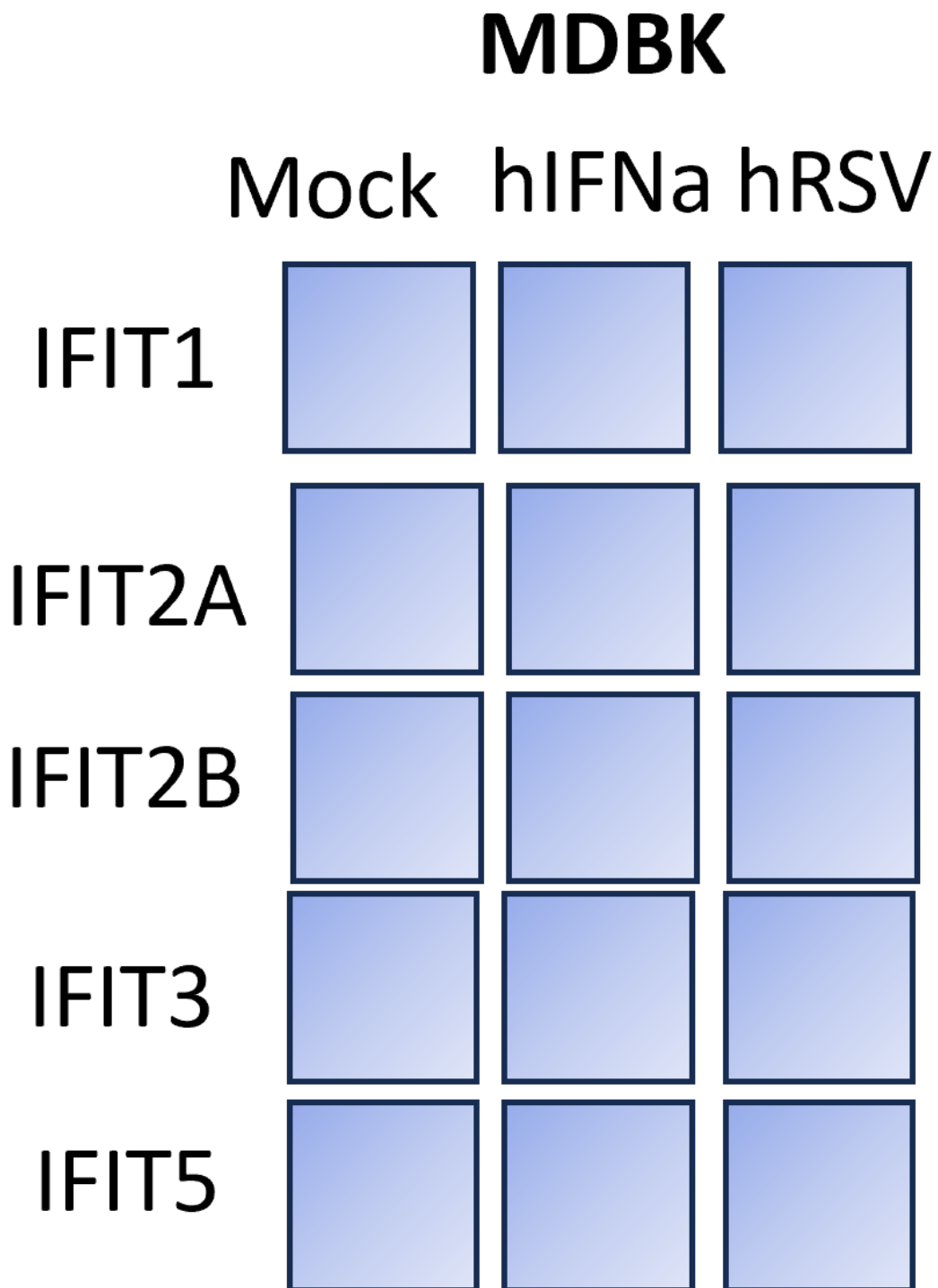


Figure 4.16: MDBK localisation mergers.

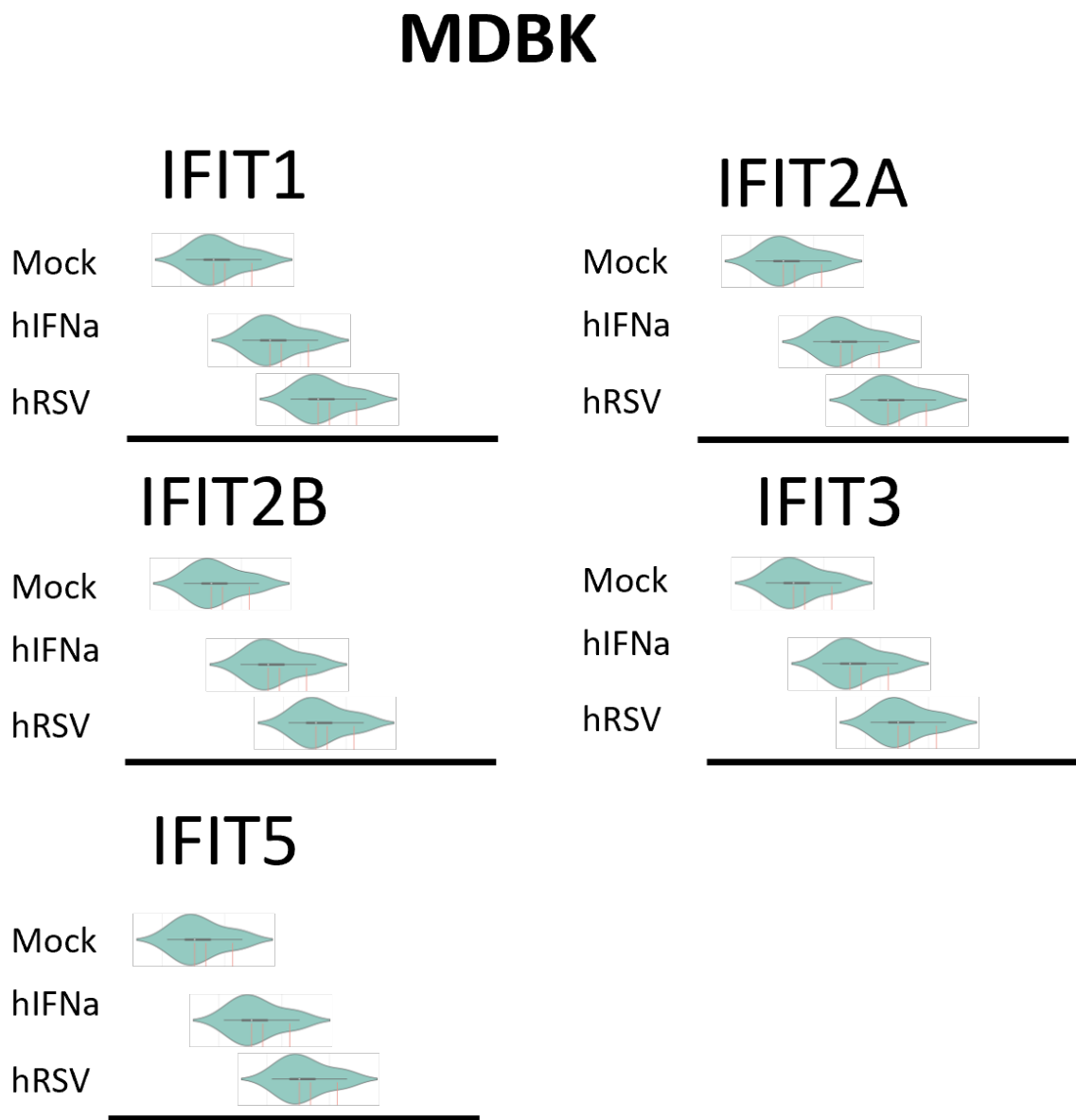


Figure 4.17: MDBK localisation plots.

Chapter 5

Detailed Analysis of Subcellular Localisation of Human and Bovine IFIT Proteins in the Context of RSV Inclusion Bodies

5.1 Introduction and Aims

Add intro about what we think it's happening with IBs and pIBs

Using pIBs as simpler model (only N+P+ cellular components) -> h/bRSV infections -> overexpression during infection

5.2 Results

5.2.1 IFIT1

5.2.1.1 Nascent Human and Monkey IFIT1 in a Simplified System of pseudo-IBs

5.2.1.1.1 293T hnhp

Detecting magenta: endogenous human IFIT1

Detecting cyan: human pIB

Cell Line: 293T

Detailed Analysis of Subcellular Localisation of Human and Bovine IFIT Proteins in the Context of RSV Inclusion Bodies

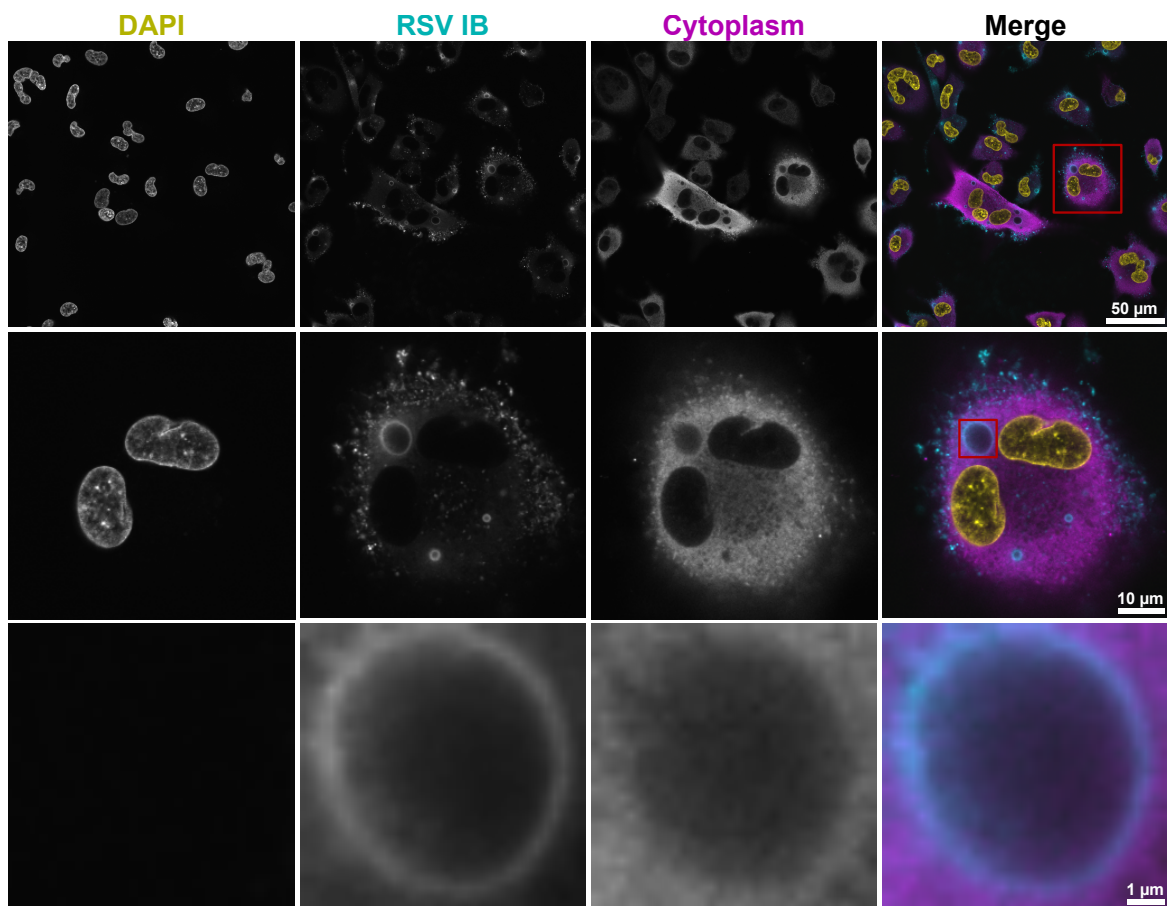


Figure 5.1: Representative Infection Zoom. asdf asdf asdf asdf asdf asdf sdfgsdfg

5.2 Results

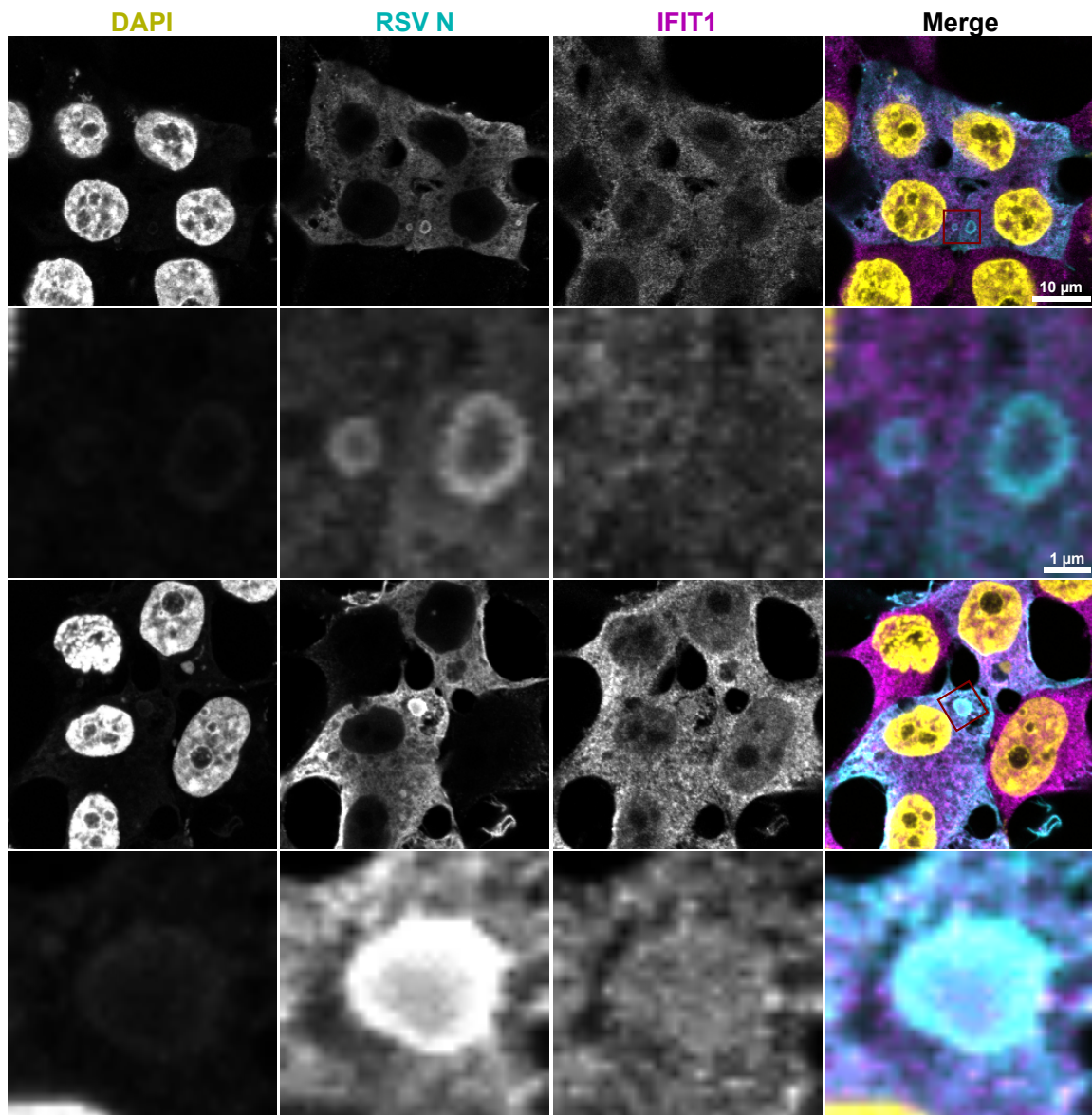


Figure 5.2: i1 293t hnhp

Detailed Analysis of Subcellular Localisation of Human and Bovine IFIT Proteins in the Context of RSV Inclusion Bodies

Treatment: hNhP

Nascent human IFIT1 seems to be diffused through the pIB structure i.e., the signal intensity and distribution between cytoplasmic and pIB staining is identical.

5.2.1.1.2 vero hnhp

Detecting magenta: endogenous monkey IFIT1

Detecting cyan: human pIB

Cell Line: VERO

Treatment: hNhP

Endogenous monkey IFIT1 displays colocalization with human pIB structures (top panel), or inclusion within the structures (bottom panel). Monkey IFIT1 signal is also excluded from the pIB filamentous network (top panel; shown by arrows). This suggests that the colocalization is not caused by mere interaction with N or P but its dependant on the integrity of pIBs. These data are supported by z stack measurements.

5.2.1.1.3 vero bnbp

Cell Line: VERO

Treatment: bNbP

Detecting magenta: endogenous monkey IFIT1

Detecting cyan: bovine pIB

In the context of bovine pIB structures, nascent monkey IFIT1 seems to colocalise with the edges of the structures (highlighted by the arrows). Consistent to human pIB data, nascent monkey IFIT1 is excluded from filamentous pIB network.

5.2.1.2 Nascent Human and Bovine IFIT1 Localisation During h/bRSV Infection

5.2.1.2.1 hIFIT1 Localisation During hRSV Infection

5.2.1.2.1.1 a549 hrsv

Detecting magenta: endogenous human IFIT1

Detecting cyan: human IB

Cell Line: A549

5.2 Results

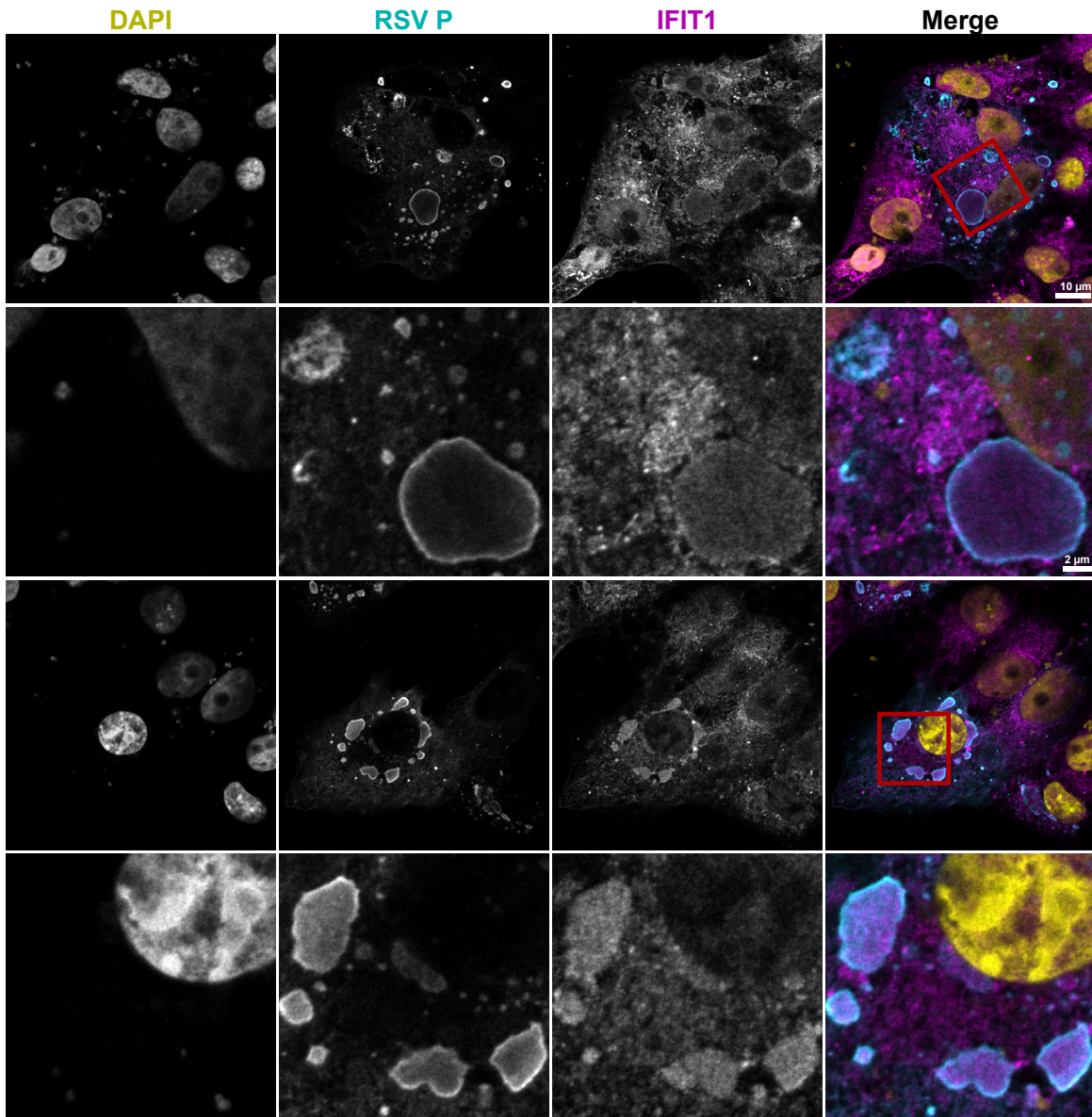


Figure 5.3: i1 vero hnhp

Detailed Analysis of Subcellular Localisation of Human and Bovine IFIT Proteins in the Context of RSV Inclusion Bodies

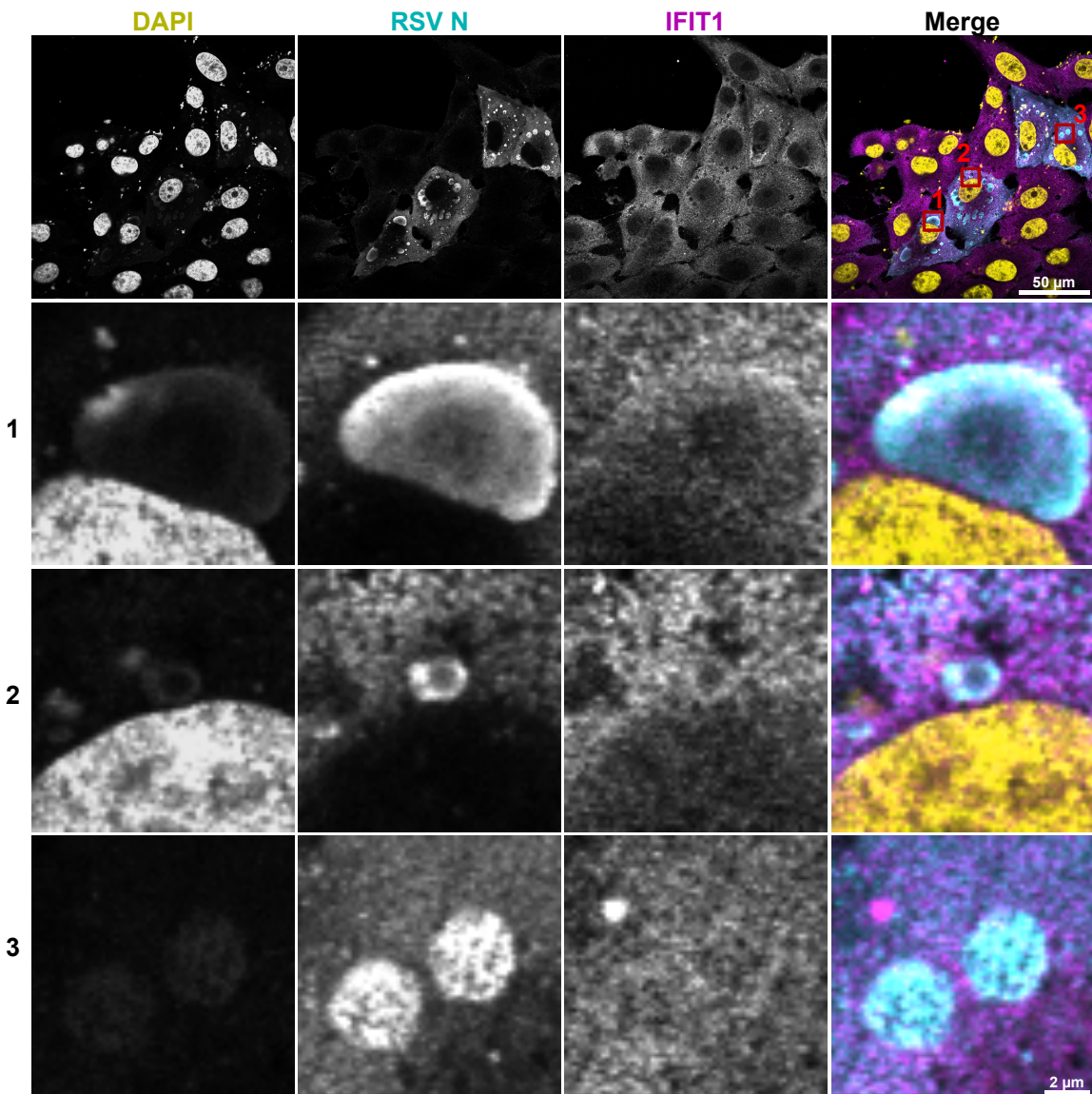


Figure 5.4: i1 vero bnbp

5.2 Results

Treatment: hRSV

Nascent human IFIT1 shows several distinct phenotypes with respect to the hRSV IB interaction. IFIT1 is either concentrated inside the structure (top panel), concentrated on the edge of IB ring (2nd and 3rd panels) , excluded from the IB structure (4th panel), or is diffused evenly between the cytoplasm and IB structure (bottom panel).

5.2.1.2.1.2 beas2b hrsv

Detecting magenta: endogenous human IFIT1

Detecting cyan: human IB

Cell Line: BEAS2B

Treatment: hRSV

5.2.1.2.2 bIFIT1 Localisation During h/bRSV Infection

5.2.1.2.2.1 mdbk hrsv

some text

5.2.1.2.2.2 mdbk brsv

Detecting magenta: endogenous bovine IFIT1

Detecting cyan: bovine IB

Cell Line: MDBK

Treatment: bRSV dSH + bIFNa

Nascent bovine IFIT1 in the context of bRSV infection has been observed to localise with the respect of IB in three distinct spaces. We observed it either concentrated inside the central point of the IB structure, while having reduced signal on the inner IB edge, compared to the cytoplasm (top and bottom panels), being excluded from the IB structure (3rd panel), or colocalising on the inner edge of the IB structure while having reduced signal in the middle of the structure compared to cytoplasm, or the edge staining (2nd panel).

5.2.1.3 Exogenously Expressed hIFIT1-FLAG During RSV Infection

Detailed Analysis of Subcellular Localisation of Human and Bovine IFIT Proteins in the Context of RSV Inclusion Bodies

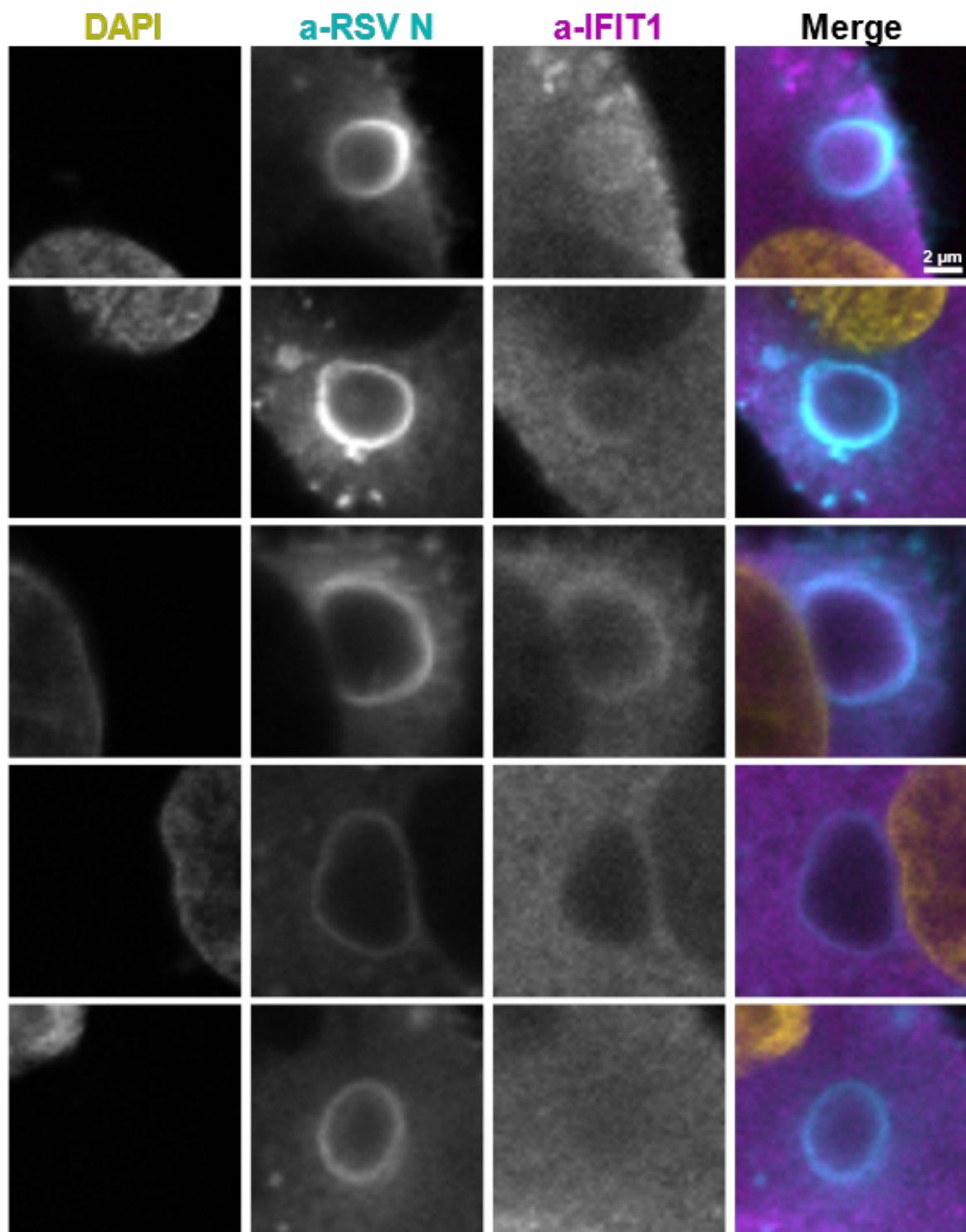


Figure 5.5: i1 a549 hrsv

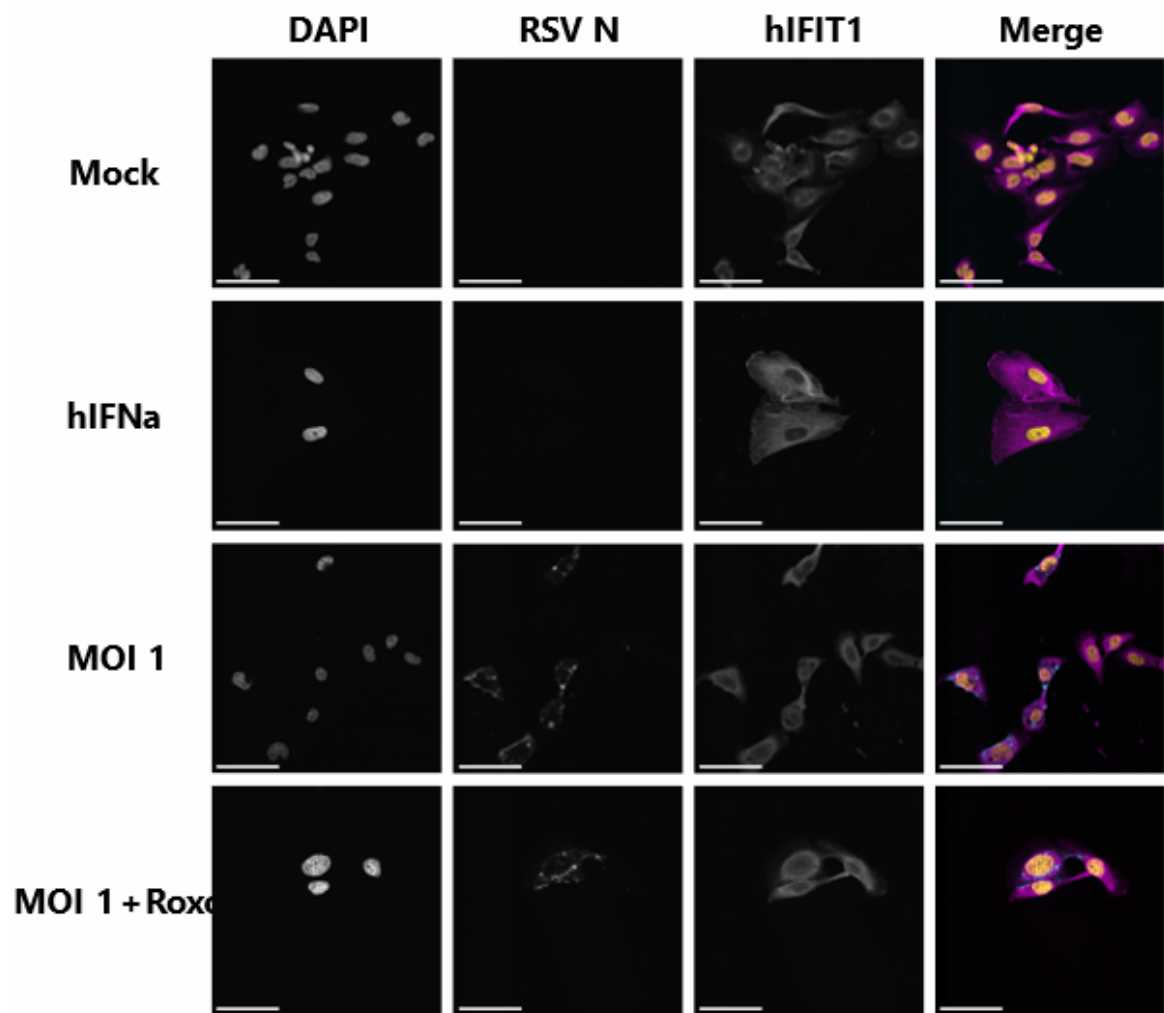


Figure 5.6: i1 beas2b hrsv

Detailed Analysis of Subcellular Localisation of Human and Bovine IFIT Proteins in the Context of RSV Inclusion Bodies

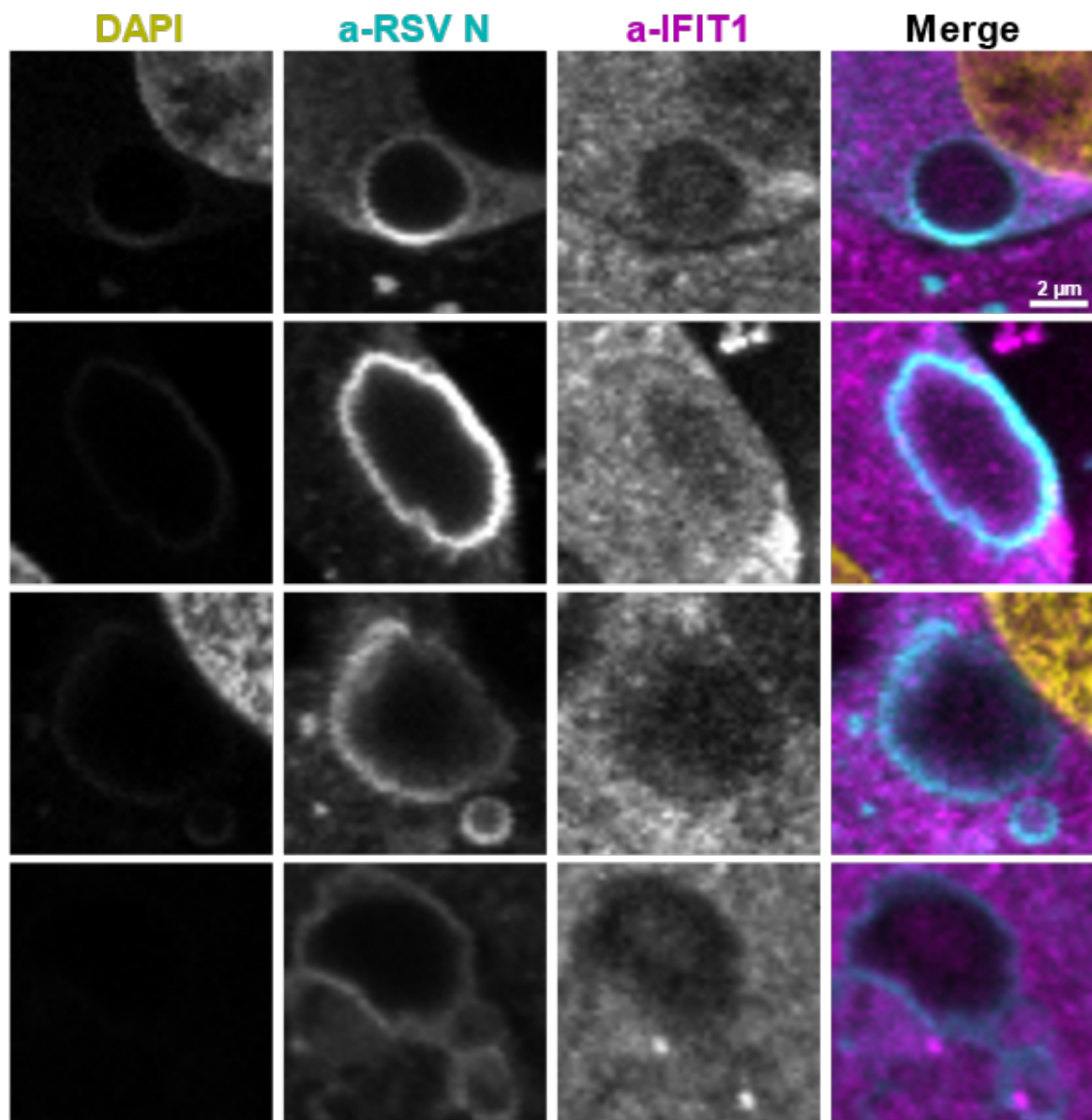


Figure 5.7: i1 mdbk brsv

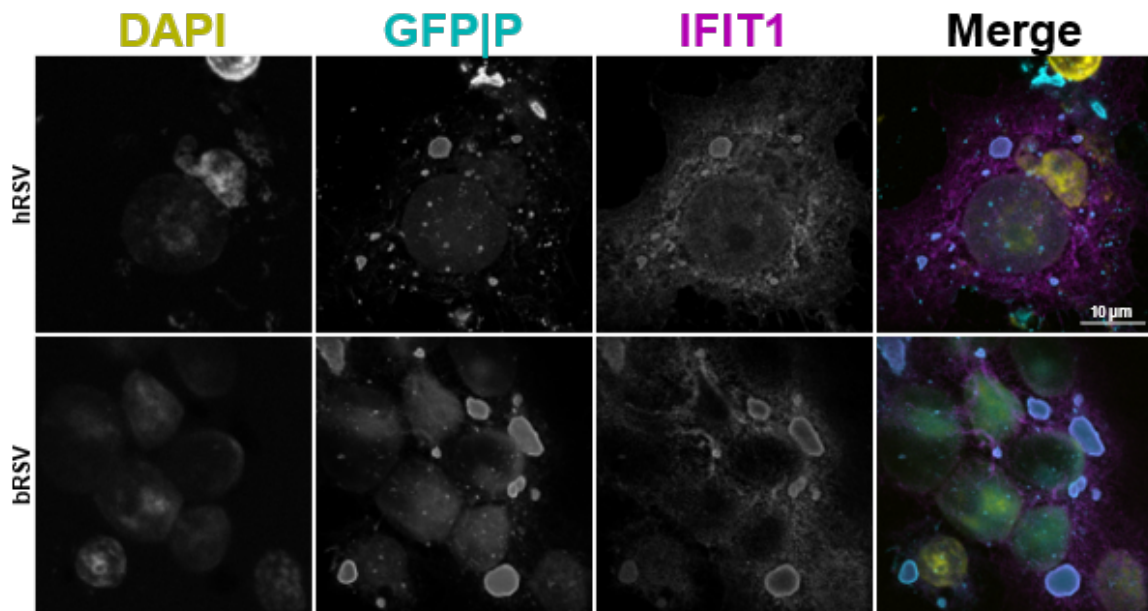


Figure 5.8: hi1 + hrsv brsv

5.2.1.3.1 hi1 + hrsv brsv

Detecting magenta: exogenous human IFIT1-FLAG

Detecting cyan: h/bIB

Cell Line: VERO

Treatment: h/bRSV-GFP

Overexpressed hIFIT1-FLAG colocalises with both human and bovine RSV IBs. This data is supported by evidence from z stacks.

5.2.1.4 Summary

Endogenous human IFIT1 seems to be diffused through the human pIB structure. On the other hand, endogenous monkey IFIT1 forms an inclusion in human pIBs, colocalises with the edge of human and bovine pIBs and is excluded from the filamentous pIB network. This suggests that the colocalization is not caused by mere interaction with N or P but its dependant on the integrity of pIBs. In the context of infection, endogenous human IFIT1 concentrates within the human RSV IB structure; colocalises to the edge of the IB; is diffused through the structure and cytoplasm equally; or is excluded from the structure. This suggests that the interaction between human IFIT1 and hRSV IB is dynamic and depends on factors that we do not understand yet. In the case of endogenous bovine IFIT1 in the context of

Detailed Analysis of Subcellular Localisation of Human and Bovine IFIT Proteins in the Context of RSV Inclusion Bodies

bRSV IBs, IFIT1 is either excluded from the structure; excluded from the IB inner edge but concentrated inside; or excluded from the centre of IB structure but concentrated on the inner edge of the structure. Overexpressed hIFIT1-FLAG in the context of h/bRSV infection colocalises to both human and bovine IB structures.

5.2.2 IFIT3

5.2.2.1 Nascent Human and Monkey IFIT3 in a Simplified System of pseudo-IBs

5.2.2.1.1 vero hnhp

Detecting magenta: endogenous monkey IFIT3

Detecting cyan: human pIB

Cell Line: VERO

Treatment: hNhP

Nascent monkey IFIT3 seems to behave a if he pIB was not here. This means I has diffused phenotype. One exception is the top panel (shown with the arrow) which hints at concentrated IFIT3 at the edge of the pIBs. We do not know the localisation with respect to the pIB filaments as none were found in the slides. This data is as well supported by z stack measurements.

5.2.2.2 Nascent Human and Bovine IFIT3 Localisation During h/bRSV Infection

5.2.2.2.1 hIFIT3 Localisation During hRSV Infection

5.2.2.2.1.1 a549 hrsv

Detecting magenta: endogenous human IFIT3

Detecting cyan: human IB

Cell Line: A549

Treatment: hRSV

Nascent human IFIT3 seems to have mainly diffused phenotype (top and bottom panel) with occasional exclusion without any marked IFIT3 concentration adjacent to the IB structure (middle panel).

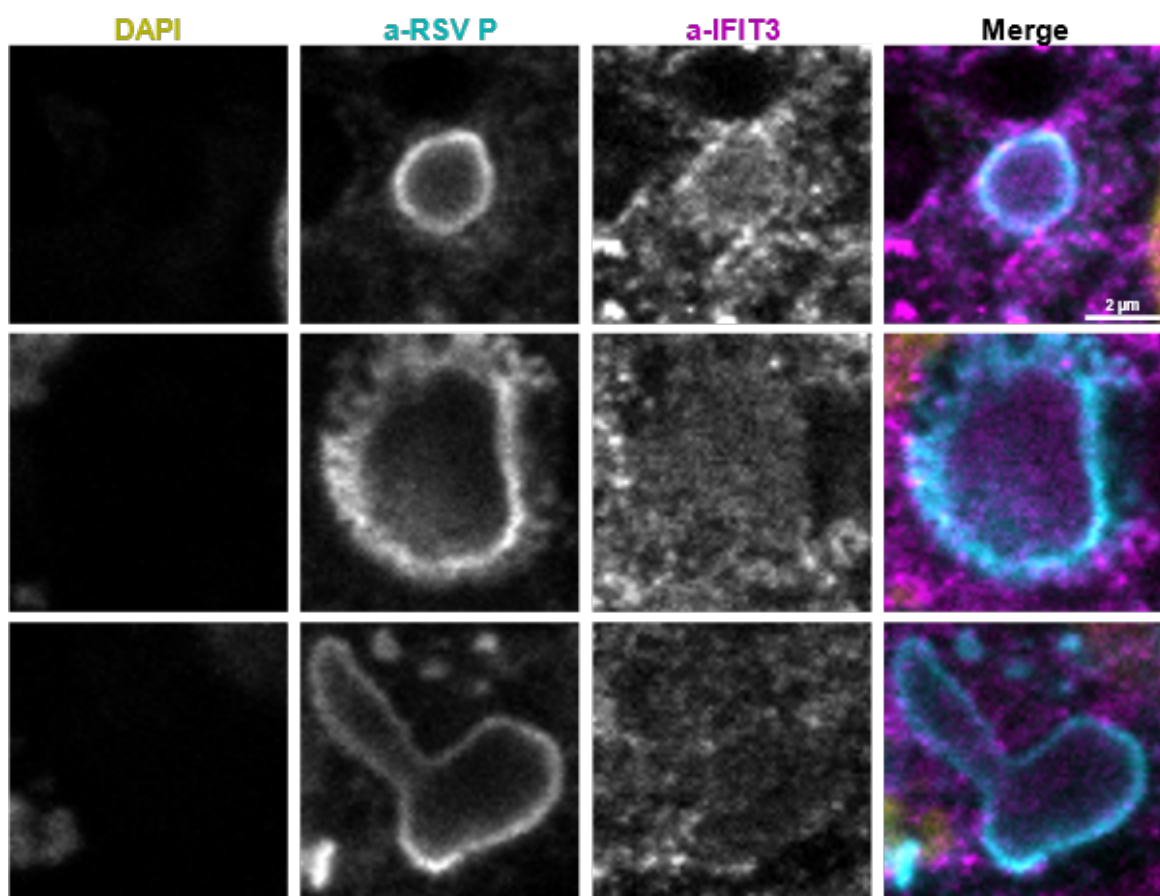


Figure 5.9: i3 vero hnhp

Detailed Analysis of Subcellular Localisation of Human and Bovine IFIT Proteins in the Context of RSV Inclusion Bodies

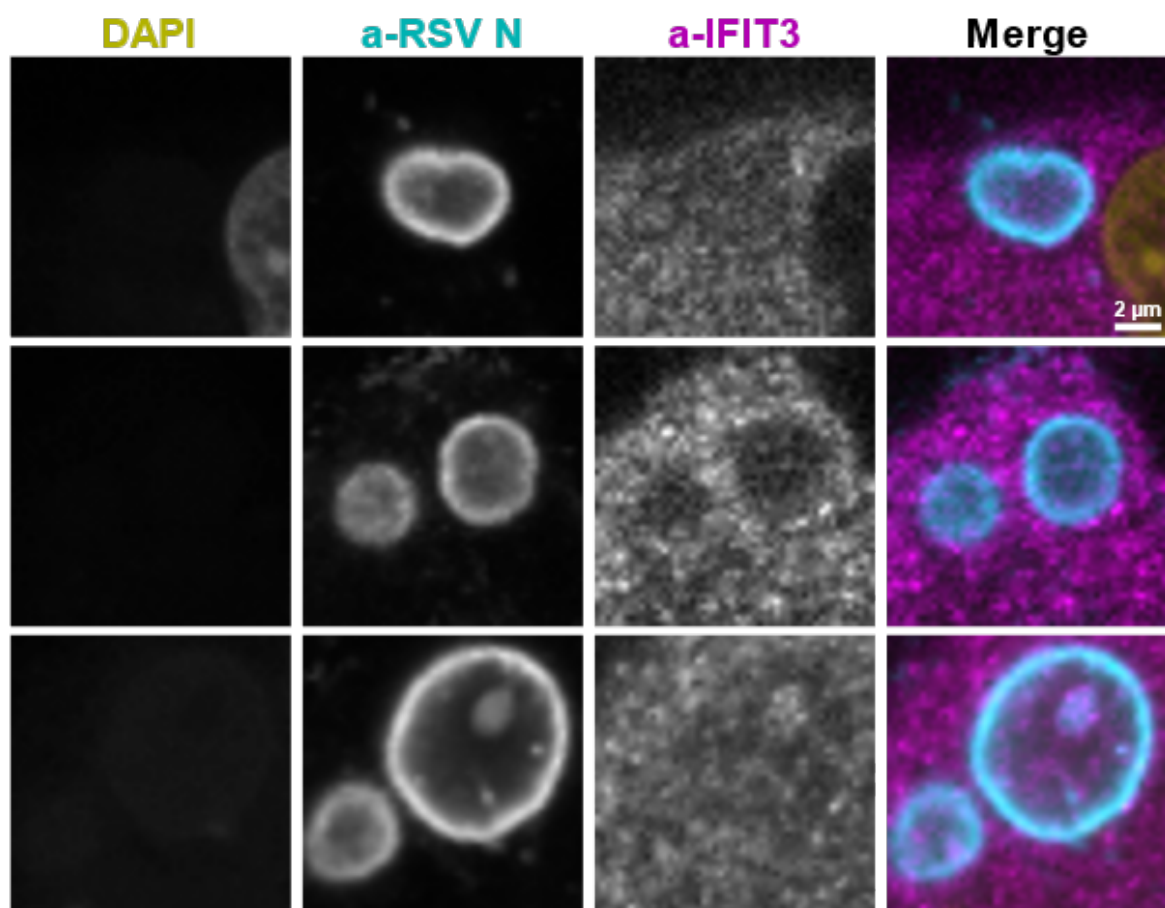


Figure 5.10: i3 a549 hrsv

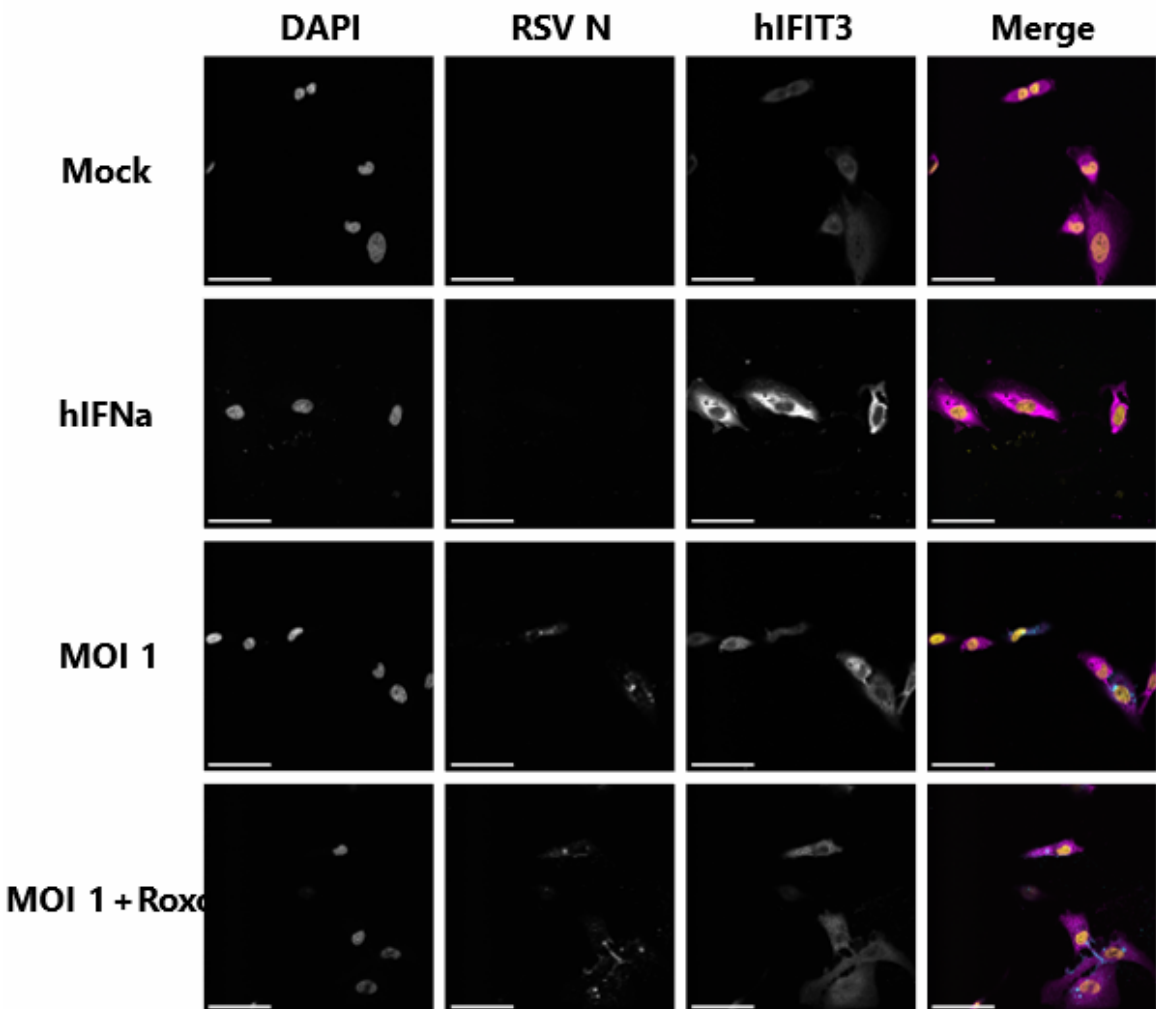


Figure 5.11: i3 beas2b hrsv

5.2.2.2.1.2 beas2b hrsv

Detecting magenta: endogenous human IFIT3

Detecting cyan: human IB

Cell Line: BEAS2B

Treatment: hRSV

5.2.2.2.2 bIFIT3 Localisation During h/bRSV Infection

Detailed Analysis of Subcellular Localisation of Human and Bovine IFIT Proteins in the Context of RSV Inclusion Bodies

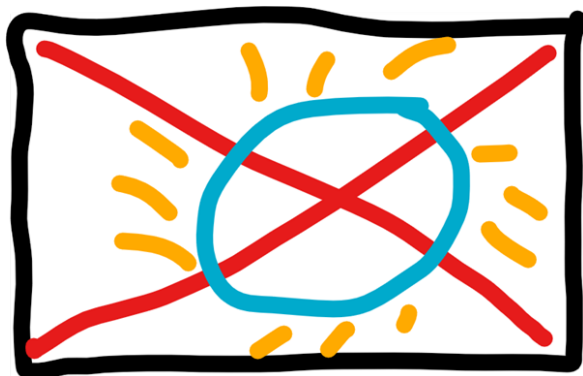


Figure 5.12: i3 mdbk hrsv

5.2.2.2.1 mdbk hrsv

some text

5.2.2.2.2 mdbk brsv

Detecting magenta: endogenous bovine IFIT3

Detecting cyan: bovine IB

Cell Line: MDBK

Treatment: bRSV dSH + bIFNa

In this experiment the nascent bovine IFIT3 was consistently concentrated inside IBs. In some IBs the IFIT3 signal showed signs of sub-concentrations within the inclusions (bottom panel; highlighted with arrows), resembling IBAGs (inclusion body associated granules).

Subsequent experiments did not recapitulate the IFIT3 inclusions. It however shows signal which is almost identical to what is observed with IFIT5 in MDBKs during bRSV infection i.e., decrease, but not complete abolition of IFIT3 signal inside the IB structure (top panel), and IB boundary exclusion while maintaining similar levels of signal intensity between cytoplasmic and intra IB stain.

5.2.2.3 Exogenously Expressed hIFIT3-FLAG During RSV Infection

5.2.2.3.1 bi3 + hrsv brsv

Cell Line: VERO

Treatment: hRSV-GFP

Detecting magenta: exogenous bovine IFIT3

Detecting cyan: human IB

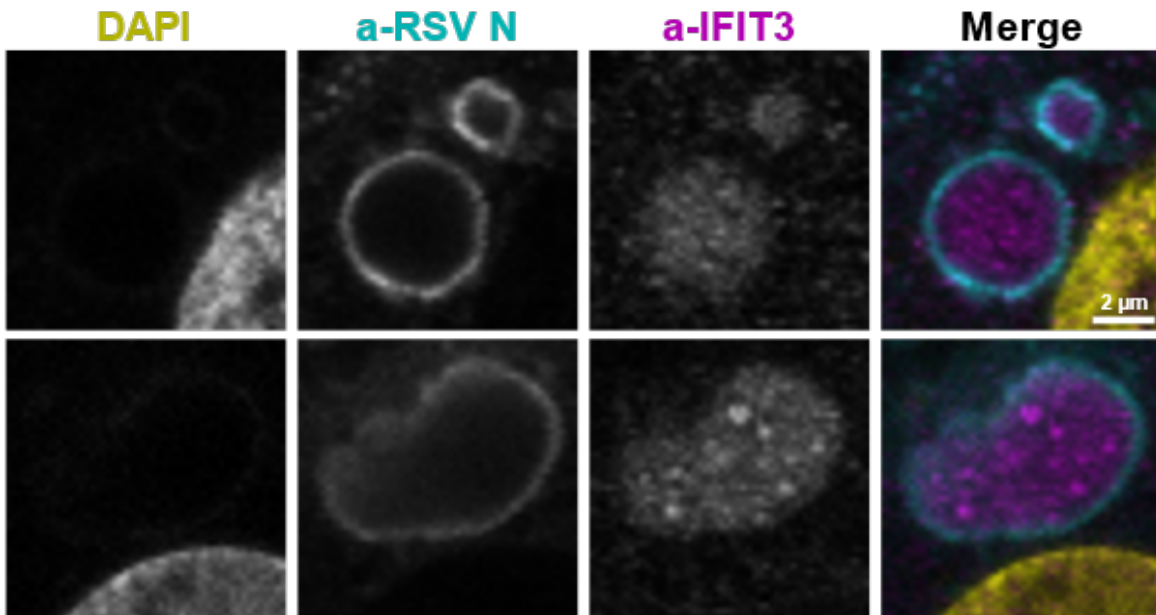


Figure 5.13: i3 mdbk brsv

Overexpressed bIFIT3-FLAG was observed to colocalise with hRSV inclusion bodies (top panel; highlighted with arrows), as well as being excluded from the hRSV IBs, without any signs of IFIT3 signal on the periphery of the IB structures (middle and bottom panel). This data is supported by z stack measurements.

Cell Line: VERO

Treatment: bRSV-GFP

Detecting magenta: exogenous bovine IFIT3

Detecting cyan: bovine IB

Very similar phenotype is observed for overexpressed bIFIT3-FLAG in bRSV infected cells. We see colocalization with IB (top panel) as well as exclusion from the structure without any signs of IFIT3 signal on the periphery of the IB structure (bottom panel). This data is as well supported by z stack measurements.

5.2.2.4 Summary

Endogenous monkey IFIT3 seems to be diffuse through the human pIB structures (with maybe a small hint of colocalization). Nascent human IFIT3 during hRSV infection is either excluded from IB structure or is diffused through the structure. Occasionally it colocalises to the IB ring. Nascent bIFIT3 during bRSV infection either siphons inside IBs and shows

Detailed Analysis of Subcellular Localisation of Human and Bovine IFIT Proteins in the Context of RSV Inclusion Bodies

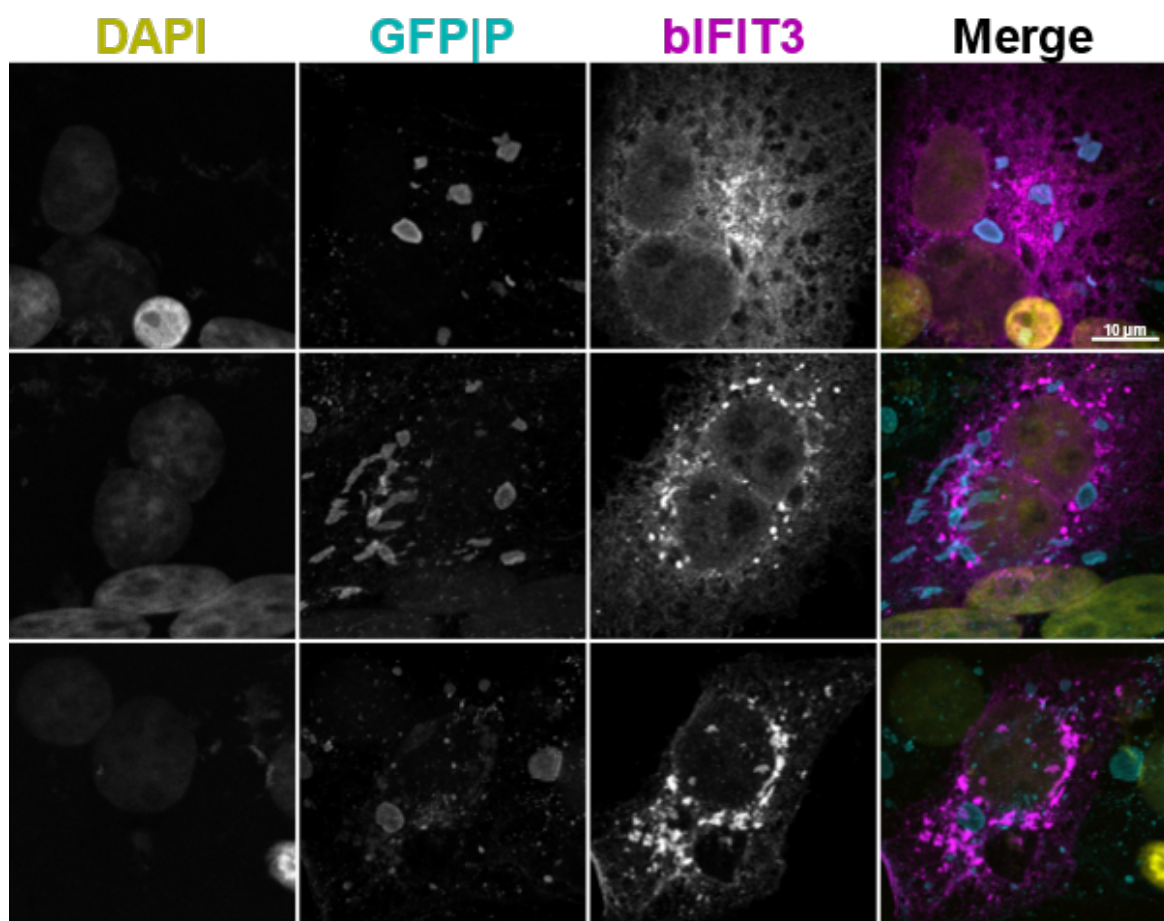


Figure 5.14: bi3 + hrsv

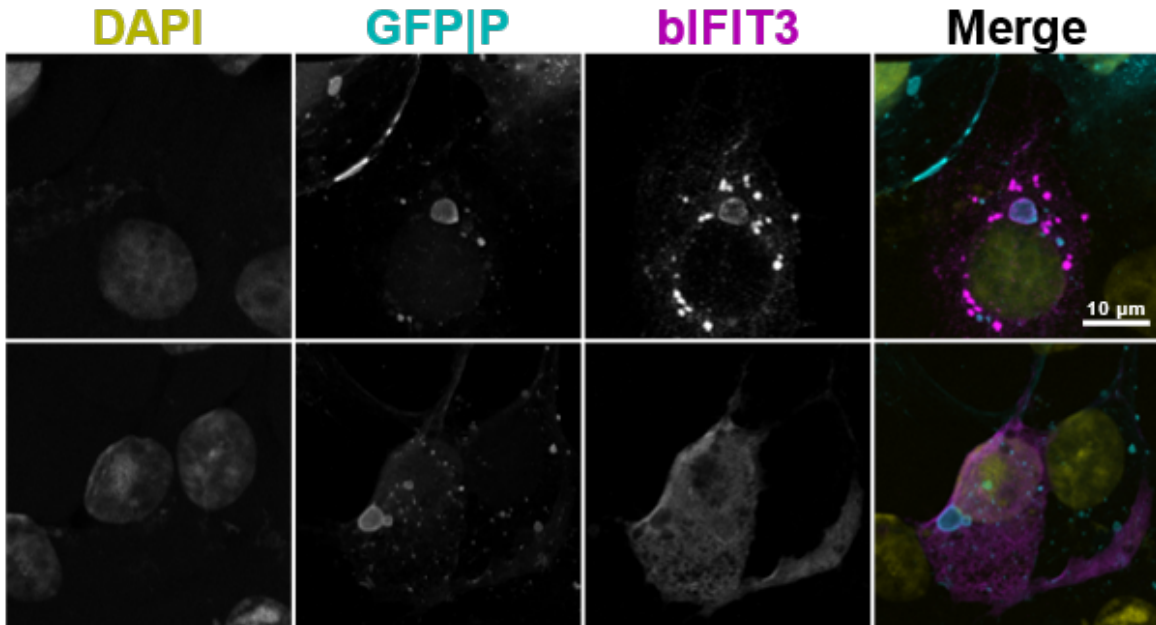


Figure 5.15: bi3 + brsv

sub-IB granules or is excluded from the IB boundary with slightly decreased signal inside of the IB. Overexpressed bIFIT3 behaves equally between hRSV and bRSV infection, that is it sometimes colocalises with the IB structure and sometimes is completely excluded from the structure.

5.2.3 IFIT5

5.2.3.1 Nascent Human and Monkey IFIT5 in a Simplified System of pseudo-IBs

5.2.3.1.1 vero hnhp

Detecting magenta: endogenous monkey IFIT5

Detecting cyan: human pIB

Cell Line: VERO

Treatment: hNhP

Nascent monkey IFIT5 colocalises with hRSV pseudo inclusion bodies (basically resembling the P staining). It also colocalises with pIB filamentous network. This network is only seen in cells that are co-transfected with RSV N and P proteins. We believe that they are an aftermath of a pIB breakdown. This data is as well supported by z stack measurements.

Detailed Analysis of Subcellular Localisation of Human and Bovine IFIT Proteins in the Context of RSV Inclusion Bodies

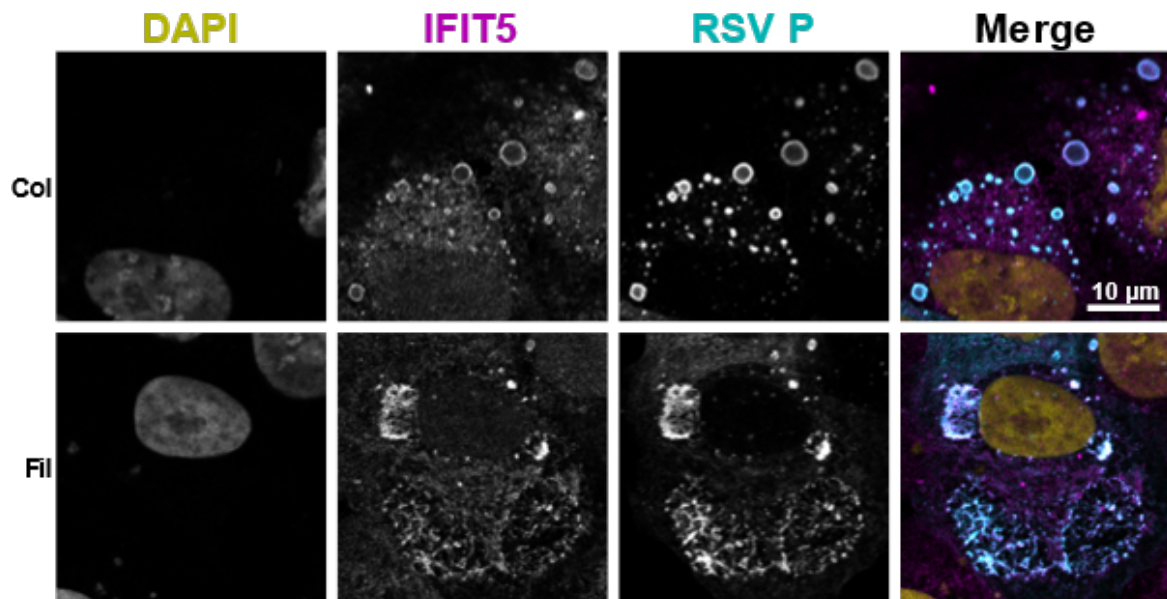


Figure 5.16: i5 vero hnhp

5.2.3.2 Nascent Human and Bovine IFIT5 Localisation During h/bRSV Infection

5.2.3.2.1 hIFIT5 Localisation During hRSV Infection

5.2.3.2.1.1 a549 hrsv

Detecting magenta: endogenous human IFIT5

Detecting cyan: human IB

Cell Line: A549

Treatment: hRSV

hIFIT5 seems to be excluded from hRSV IBs. There is a hint of accumulation of IFIT5 on the outside of IB (bottom panel; no z stacks to confirm this).

5.2.3.2.1.2 beas2b hrsv

Detecting magenta: endogenous human IFIT5

Detecting cyan: human IB

Cell Line: BEAS2B

Treatment: hRSV

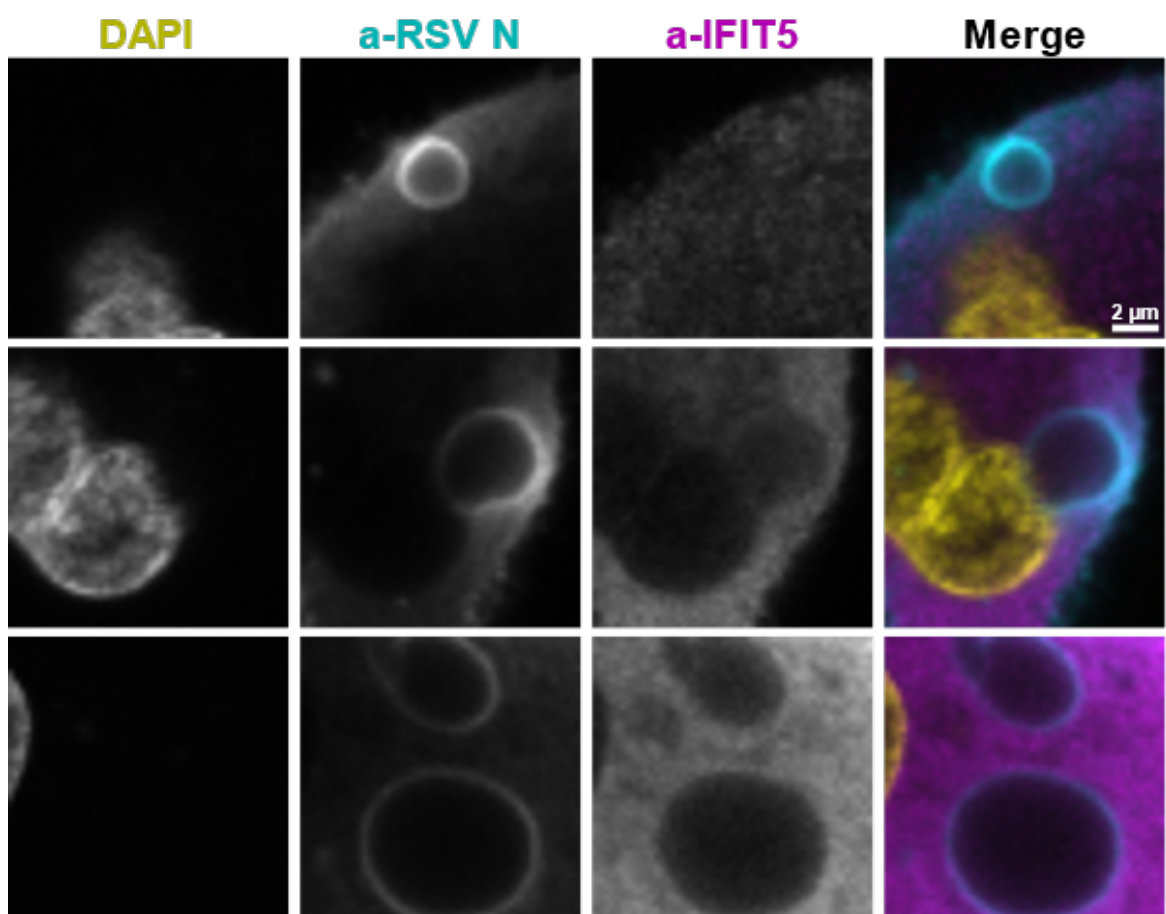


Figure 5.17: i5 a549 hrsv

Detailed Analysis of Subcellular Localisation of Human and Bovine IFIT Proteins in the Context of RSV Inclusion Bodies

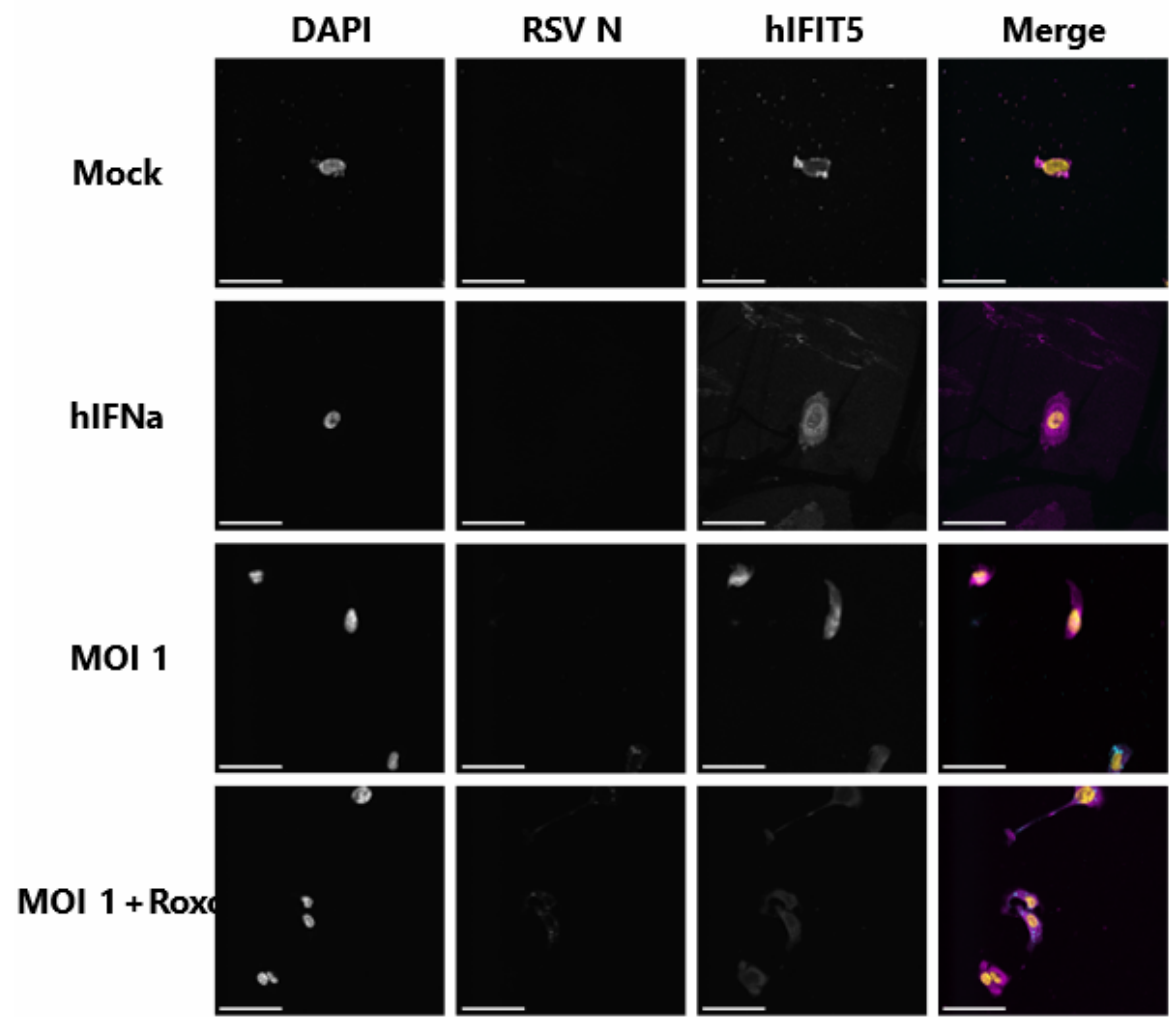


Figure 5.18: i5 beas2b hrsv

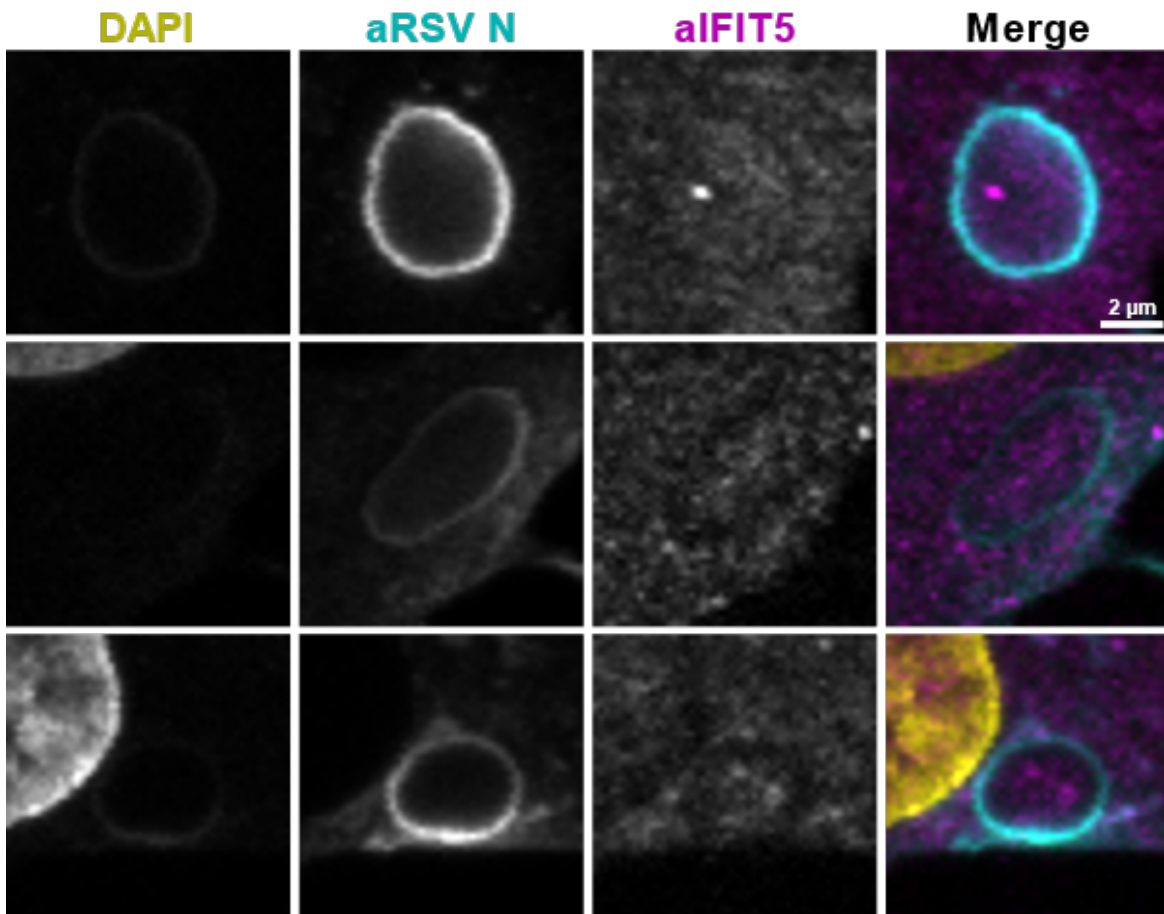


Figure 5.19: i5 mdbk brsv

5.2.3.2.2 bIFIT5 Localisation During h/bRSV Infection

5.2.3.2.2.1 mdbk brsv

Detecting magenta: endogenous bovine IFIT5

Detecting cyan: bovine IB

Cell Line: MDBK

Treatment: bRSV dSH + bIFNa

The distribution of bIFIT5 is equal between cytoplasmic stain and inside of the IB (with a hint of concentrations/substructures in top and bottom panel; no z stack data available). All 3 panels show a depression of IFIT5 signal at the side of IB boundary (highlighted by arrows).

Detailed Analysis of Subcellular Localisation of Human and Bovine IFIT Proteins in the Context of RSV Inclusion Bodies

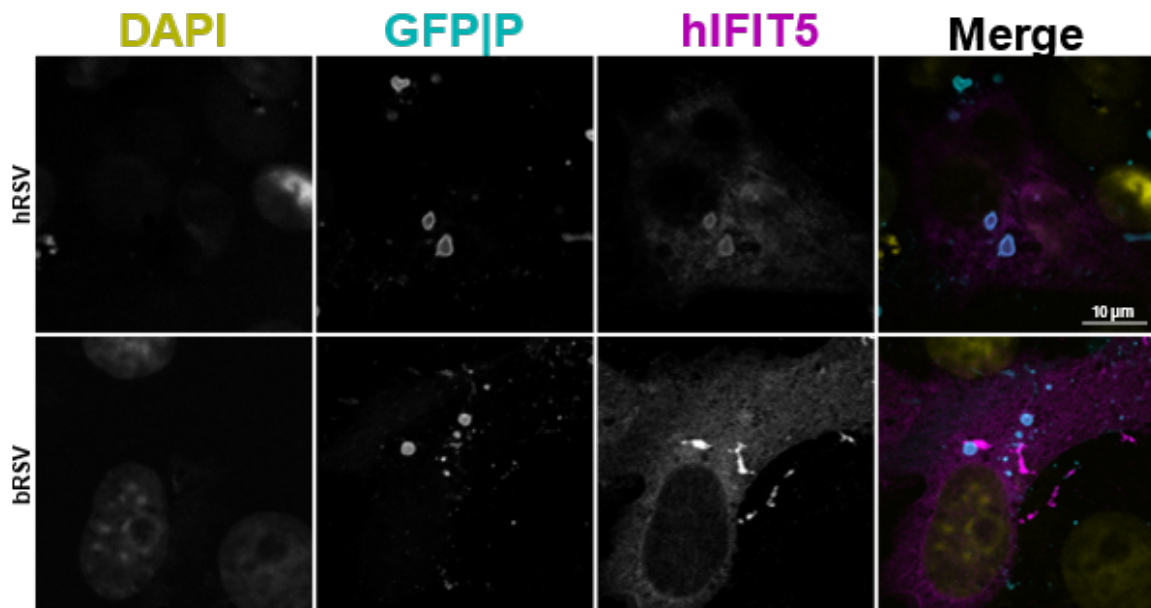


Figure 5.20: hi5 + hrsv brsv

5.2.3.3 Exogenously Expressed hIFIT5-FLAG During RSV Infection

5.2.3.3.1 hi5 + hrsv brsv

Detecting magenta: exogenous human IFIT5-FLAG

Detecting cyan: h/bIB

Cell Line: VERO

Treatment: h/bRSV-GFP

hIFIT5-FLAG is colocalising with hRSV inclusion bodies (basically resembling the P staining), while in bRSV infected cell there is a hint of IFIT5 signal concentration at the side of bRSV IB.

This data is by single cells per conditions as transfection did not work well. It is however supported by z stack measurements.

5.2.3.4 Summary

Endogenous monkey IFIT5 colocalises with human pIBs and with the NP network (this network is never present in infected cells, so we do not know how are other IFIT5s colocalising with it). In human cells during hRSV infection IFIT5 is mainly excluded from the IBs but seems to concentrate on their edge. Once we saw colocalization with the IB ring and a concentration of IFIT5 inside it. In bovine cells IFIT5 is always excluded from the IB

5.3 Discussion

boundary and the signal inside is either slightly decreased or equal compared to cytoplasmic IFIT5. Overexpressed hIFIT5 in hRSV infected cells colocalises with the IBs.

5.2.4 Liquid-Liquid Phase Separation

Add stuff about the likelihood of IFIT and viral proteins and their propensity to phase separate
This is using an online tool called PSPredictor

5.3 Discussion

pIBs and IBs are dynamic structures and that's why we see variable interactions within the same IFIT experiments.

Chapter 6

IFIT2 confocal story

6.1 Introduction and Aims

Talk about the two antibodies

6.2 IFIT2AB

6.2.1 IFIT2A

6.2.1.1 Human and Monkey IFIT2 in a Simplified System of pseudo-IBs

6.2.1.1.1 Nascent Human and Monkey IFIT2 in pIBs

6.2.1.1.1.1 i2a 293t hnhp

Cell Line: 293T

Treatment: hNhP

Detecting magenta: endogenous human IFIT2

Detecting cyan: human pIB

Nascent human IFIT2 strongly concentrates within the human RSV pseudo inclusion bodies.

6.2.1.1.1.2 i2a vero hnhp

Cell Line: VERO

IFIT2 confocal story

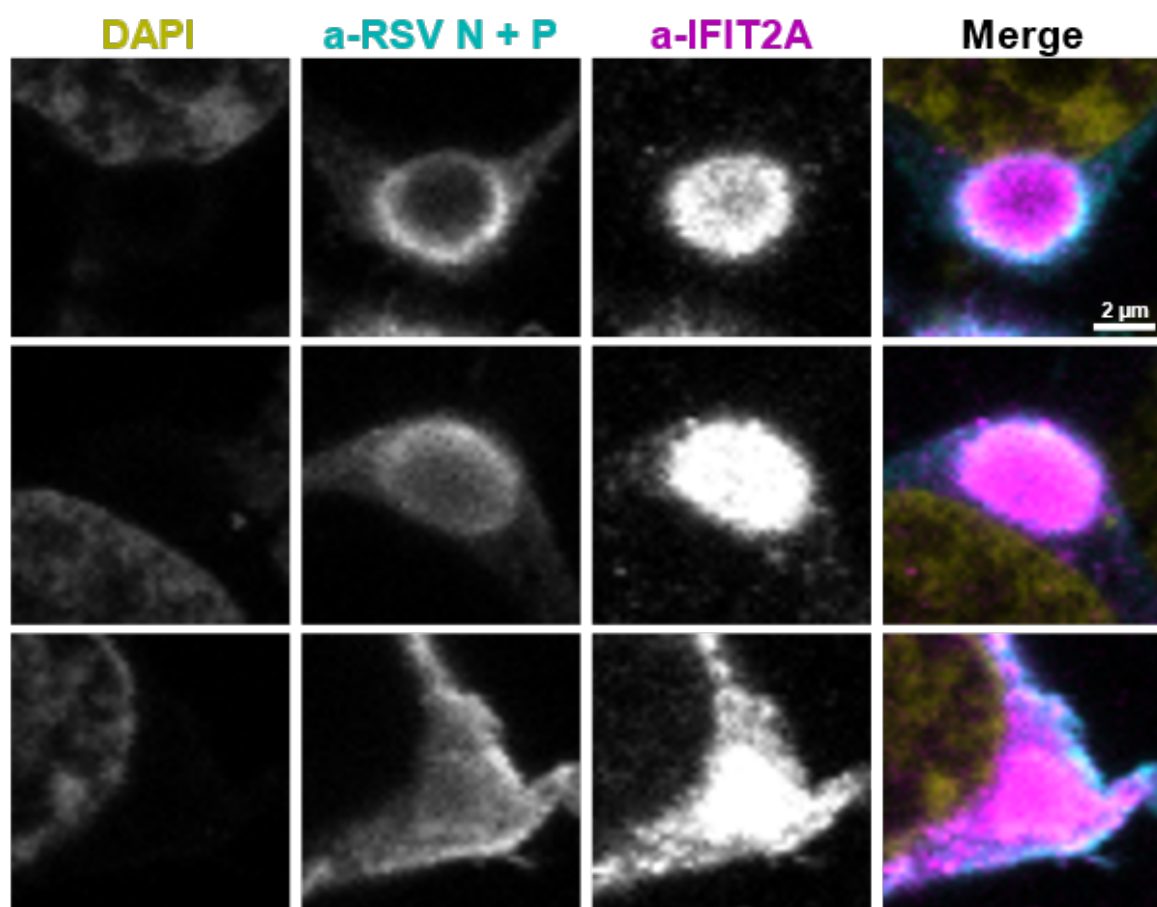


Figure 6.1: i2a 293t hnhp

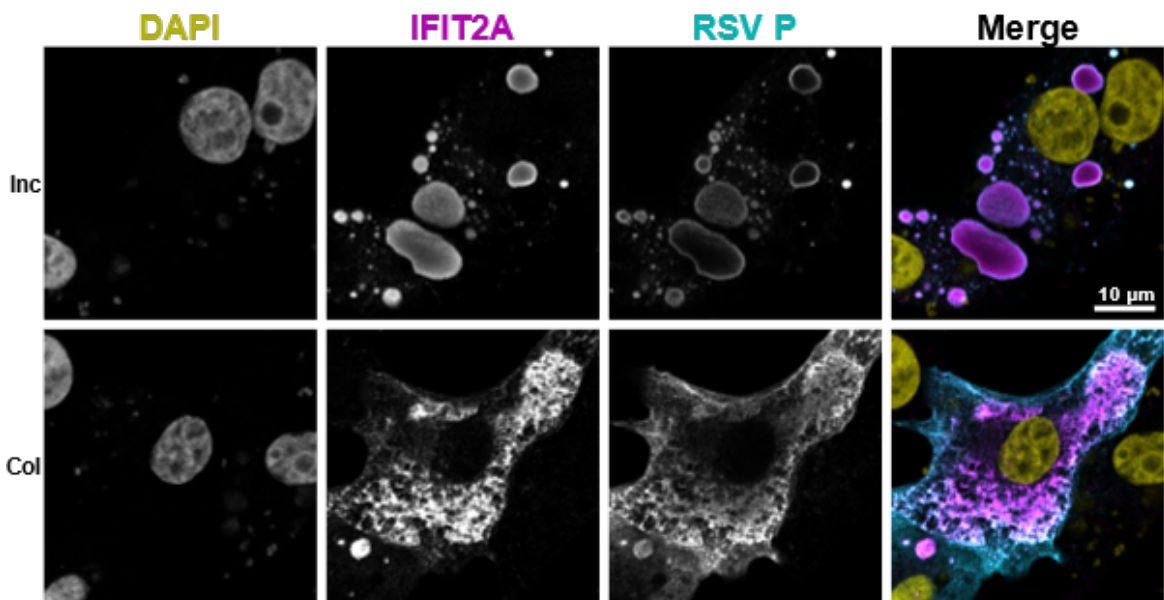


Figure 6.2: i2a vero hnhp

Treatment: hNhP

Detecting magenta: endogenous monkey IFIT2

Detecting cyan: human pIB

Endogenous monkey IFIT2 colocalises with the pIB structure (probably like an inclusion), as well as with the pIB filamentous network.

6.2.1.1.2 Exogenous Human and Bovine IFIT2 in pBs

6.2.1.1.2.1 i2a vero hi2 + hnhp

Cell Line: VERO

Treatment: hNhP + hIFIT2-FLAG

Detecting magenta: endogenous monkey IFIT2 + exogenous human IFIT2

Detecting cyan: human pIB

Monkey cells transfected with human RSV N and P, along with human IFIT2-FLAG show concentration within the pIB structures as well as the pIB filamentous network. In this experiment we are detecting both human and monkey IFIT2, however we can see a huge difference in IFIT2 expression between some cells (bottom panel; cells in the periphery

IFIT2 confocal story

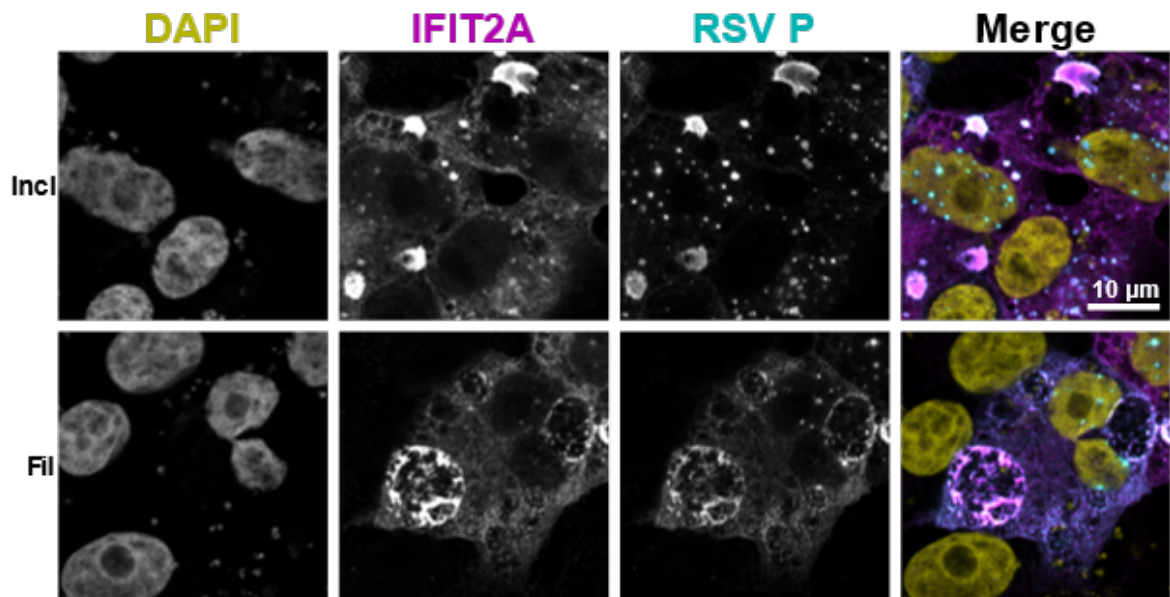


Figure 6.3: i2a vero hi2 + hnhp

of the picture), suggesting that what we are mainly detecting is the overexpressed human IFIT2-FLAG.

6.2.1.2 Nascent Human and Bovine IFIT2A Localisation During h/bRSV Infection

6.2.1.2.1 hIFIT2A localisation during hRSV Infection

6.2.1.2.1.1 i2a a549 hrsv

Cell Line: A549

Treatment: hRSV

Detecting magenta: endogenous human IFIT2

Detecting cyan: human IB

Nascent human IFIT2 shows 3 phenotypes with regards to colocalization with human RSV N. It seems to colocalise to the edge of the IB structure, with a partial signal also being detected in the inner edge of the structure (top panel); it completely colocalises to the N staining (middle panel; could be because the section is going through the top of the IB sphere); or forms inclusion inside the IB structure (bottom panel).

Cell Line: A549

Treatment: hRSV

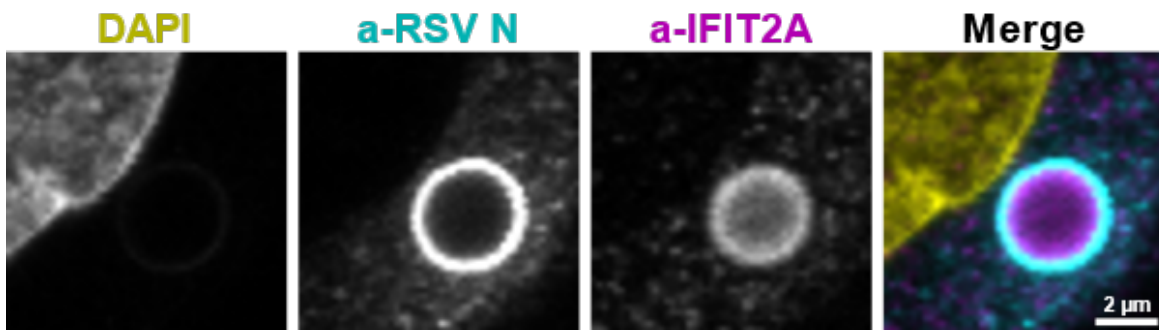


Figure 6.4: i2a a549 hrsv n

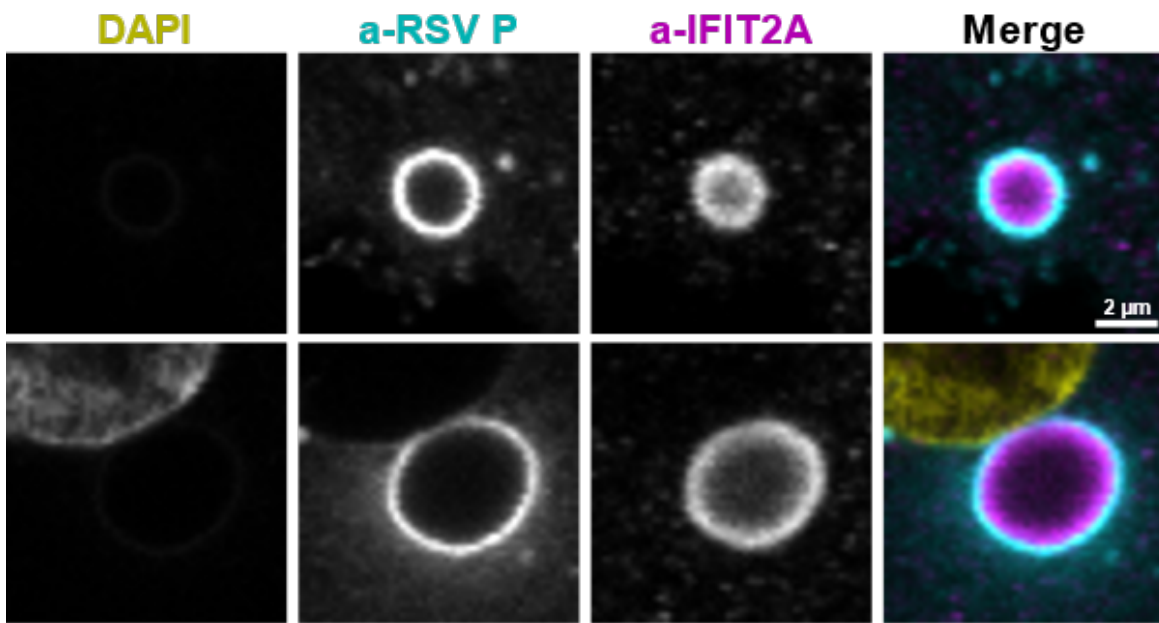


Figure 6.5: i2a a549 hrsv p

Detecting magenta: endogenous human IFIT2

Detecting cyan: human IB

Nascent human IFIT2 colocalises with the ring structure (outlined by RSV P staining) and to the inner edge of the IB.

Cell Line: A549

Treatment: hRSV

Detecting magenta: endogenous human IFIT2

Detecting cyan: human IB

With regards of colocalization with human RSV M2/1 protein, human IFIT2 seems to

IFIT2 confocal story

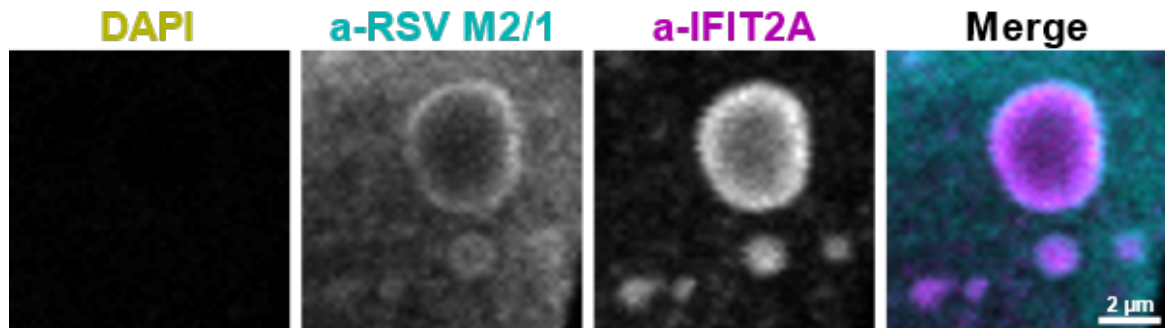


Figure 6.6: i2a a549 hrsv m21

either form inclusion, which has a signal decrease towards the middle of the IB structure (top panel), or seems to strongly colocalise with the ring structure highlighted by M2/1 staining (bottom 2 panels; there also seems to be IFIT2 signal concentration on the inner edge of the IB structure).

6.2.1.2.1.2 i2a beas2b hrsv

Cell Line: BEAS2B

Treatment: hRSV

Detecting magenta: endogenous human IFIT2

Detecting cyan: human IB

6.2.1.2.2 hIFIT2A localisation during bRSV Infection

6.2.1.2.2.1 i2a mdbk brsv

Cell Line: MDBK

Treatment: bRSV + bIFNa

Detecting magenta: endogenous bovine IFIT2

Detecting cyan: bovine IB

Nascent bovine IFIT2 colocalization with regards of N stained bRSV IBs seems to strongly associate with the ring of the structure.

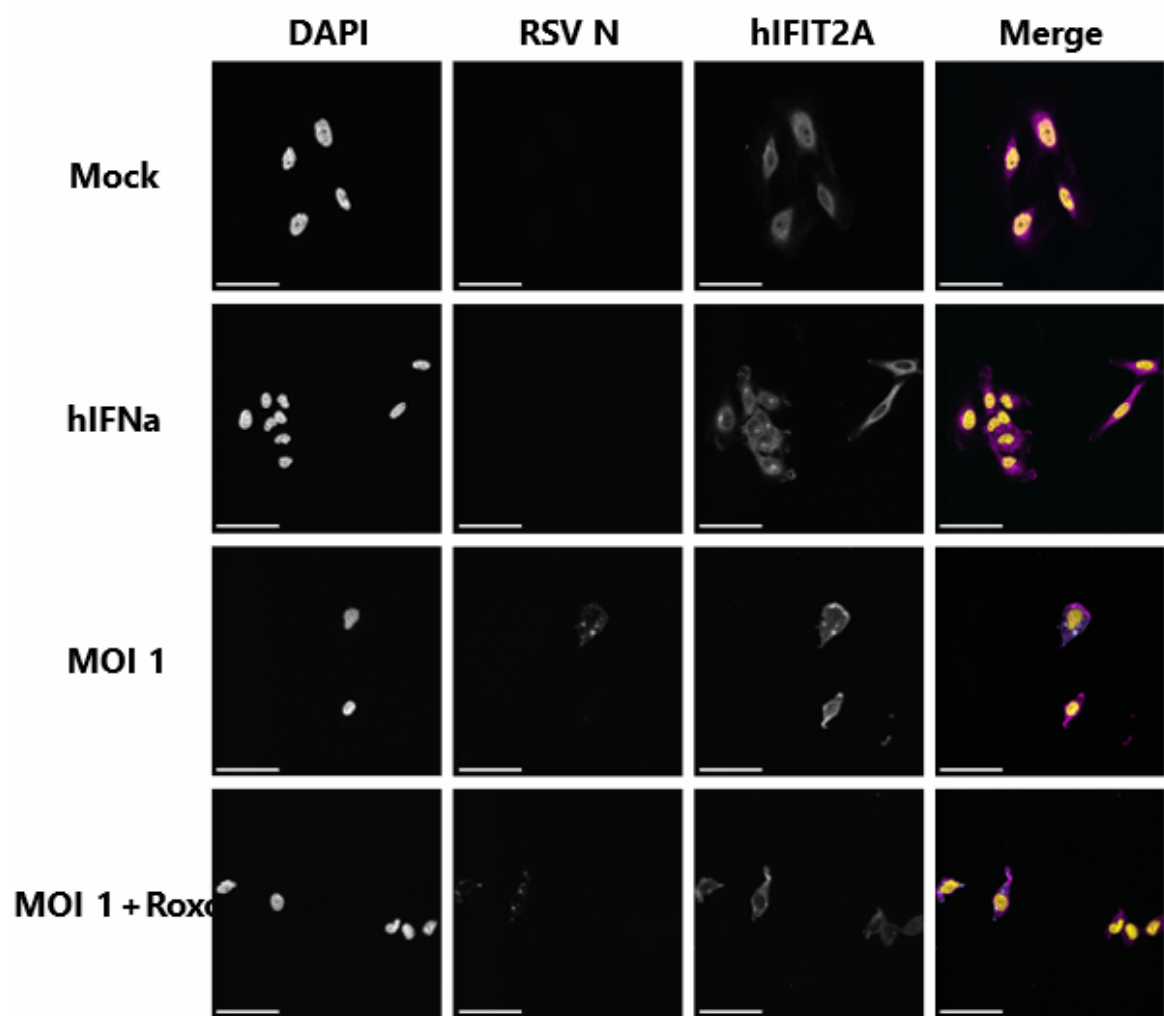


Figure 6.7: i2a beas2b hrsv

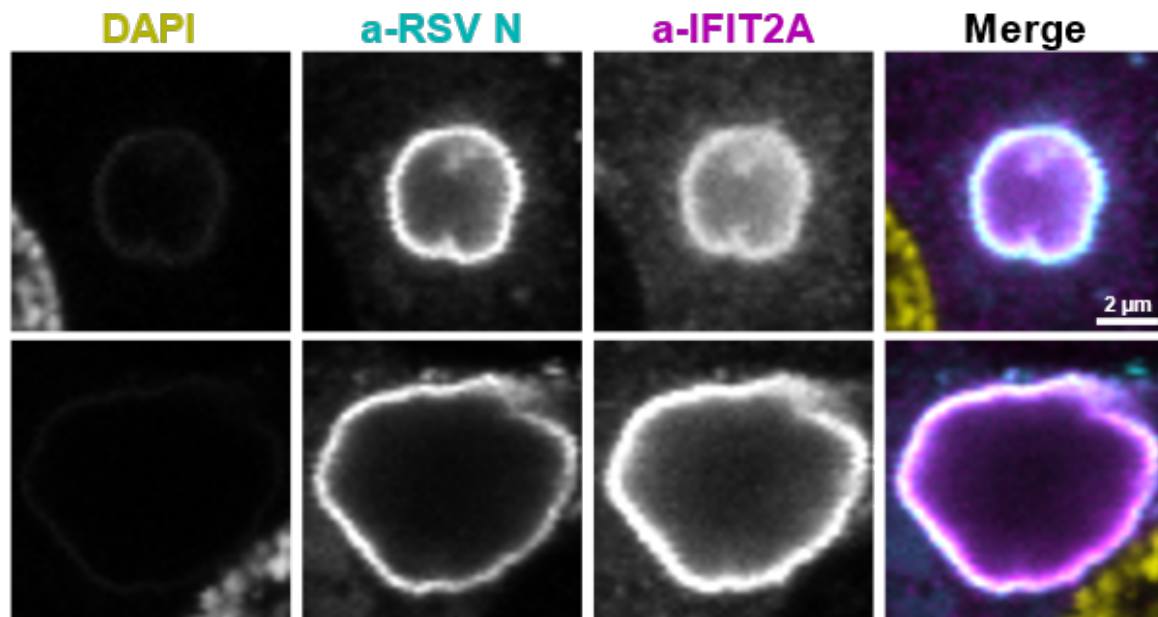


Figure 6.8: i2a mdbk brsv

6.2.2 Summary

Both endogenous human and monkey IFIT2 forms inclusions inside human RSV pseudo-IBs. Monkey IFIT2 also colocalises to the pIB filamentous network (this structure was not observed in the human experiment). The identical staining can be observed in monkey cells with overexpressed human IFIT2-FLAG. Nascent human IFIT2 during hRSV infection consistently localises to the IB structure. It seems to have preference for the ring and the inner edge of the structure; however, we have seen it as homogenous inclusion as well. Endogenous bovine IFIT2 colocalises to the ring of the IB during bRSV infection.

6.2.3 IFIT2B

IFIT2B -> stuff detected by anti-IFIT2 antibody B

Everything stated in this subchapter is only attributable to the staining seen with IFIT2 antibody B

6.2.3.1 Nascent Human and Monkey IFIT2 in a Simplified System of pseudo-IBs

6.2.3.1.1 Nascent Human and Monkey IFIT2 in pIBs

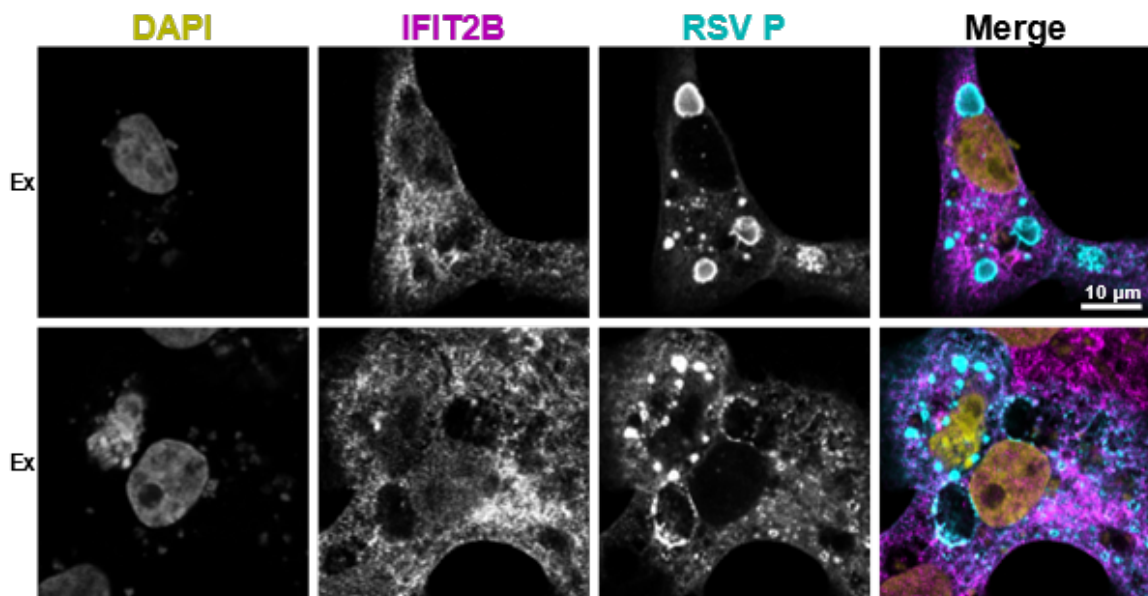


Figure 6.9: i2b vero hnhp

6.2.3.1.1.1 i2b vero hnhp

Cell Line: VERO

Treatment: hNhP

Detecting magenta: endogenous monkey IFIT2

Detecting cyan: human pIB

Nascent monkey IFIT2 is completely excluded from the human RSV pseudo-IBs and the pIB filamentous network.

6.2.3.1.2 Exogenous Human and Bovine IFIT2 in pBs

6.2.3.1.2.1 i2b vero hi2 + hnhp

Cell Line: VERO

Treatment: hNhP + hIFIT2-FLAG

Detecting magenta: endogenous monkey IFIT2 + exogenous human IFIT2

Detecting cyan: human pIB

Monkey cells transfected with human RSV N and P, along with human IFIT2-FLAG show concentration within the pIB structures but show exclusion from the pIB filamentous

IFIT2 confocal story

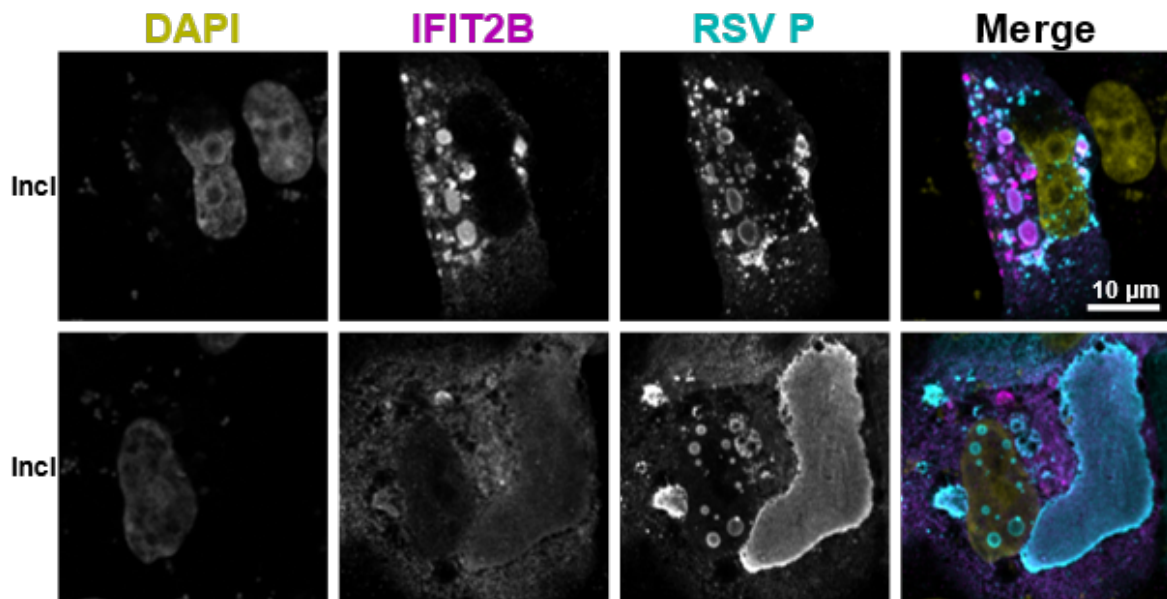


Figure 6.10: i2b vero hi2 + hnhp

network (or partial colocalisation?). This suggest that the IFIT2B antibody can indeed detect IFIT2 but the overexpressed IFIT2 observed between the inclusion and the one interacting with the filamentous network is somehow different (epitope masking?).

6.2.3.2 Nascent Human and Bovine IFIT2B Localisation During h/bRSV Infection

6.2.3.2.1 hIFIT2B localisation during hRSV Infection

6.2.3.2.1.1 i2b a549 hrsv

Cell Line: A549

Treatment: hRSV

Detecting magenta: endogenous human IFIT2

Detecting cyan: human IB

Endogenous human IFIT2 is either partially excluded (top panel; decrease of intra IB signal compared to cytoplasmic signal) or completely excluded (bottom panel) from the human IB structure.

Cell Line: A549

Treatment: hRSV

Detecting magenta: endogenous human IFIT2

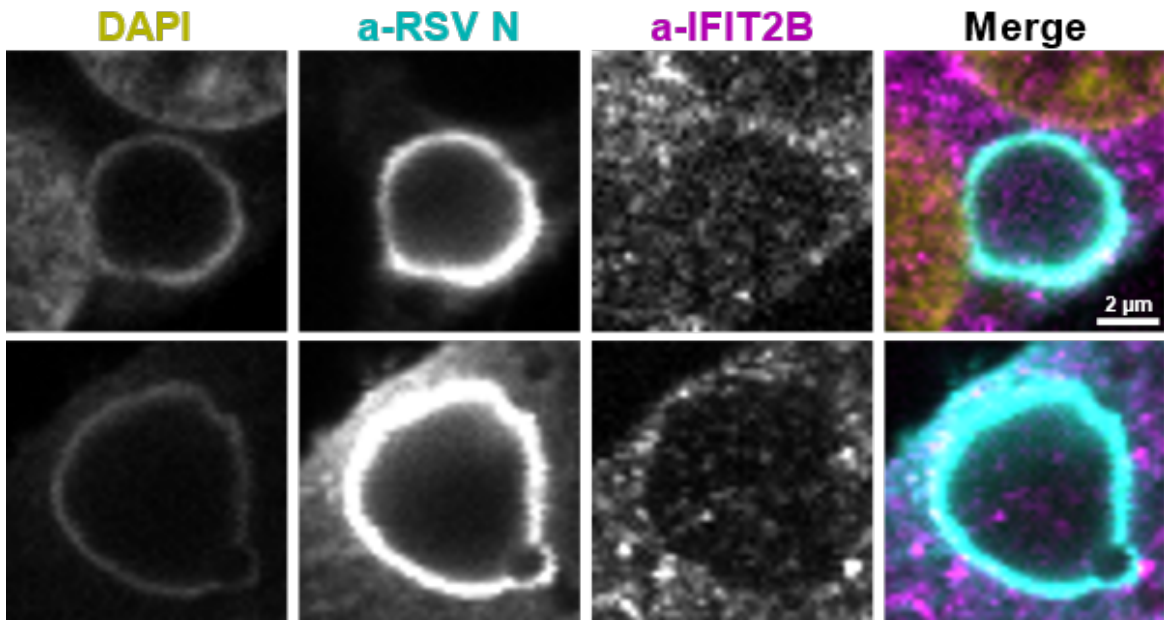


Figure 6.11: i2b a549 hrsv n

Detecting cyan: human IB

We observe similar pattern of staining to what was observed with N stained human IBs. IFIT2 signal is either partially or totally excluded from the IB structure.

Cell Line: A549

Treatment: hRSV

Detecting magenta: endogenous human IFIT2

Detecting cyan: human IB

Endogenous human IFIT2 seems to be excluded from hRSV IBs.

6.2.3.2.1.2 i2b beas2b hrsv

some text

6.2.3.2.2 hIFIT2B localisation during bRSV Infection

6.2.3.2.2.1 i2b mdbk brsv

Cell Line: MDBK

Treatment: bRSV + bIFNa

IFIT2 confocal story

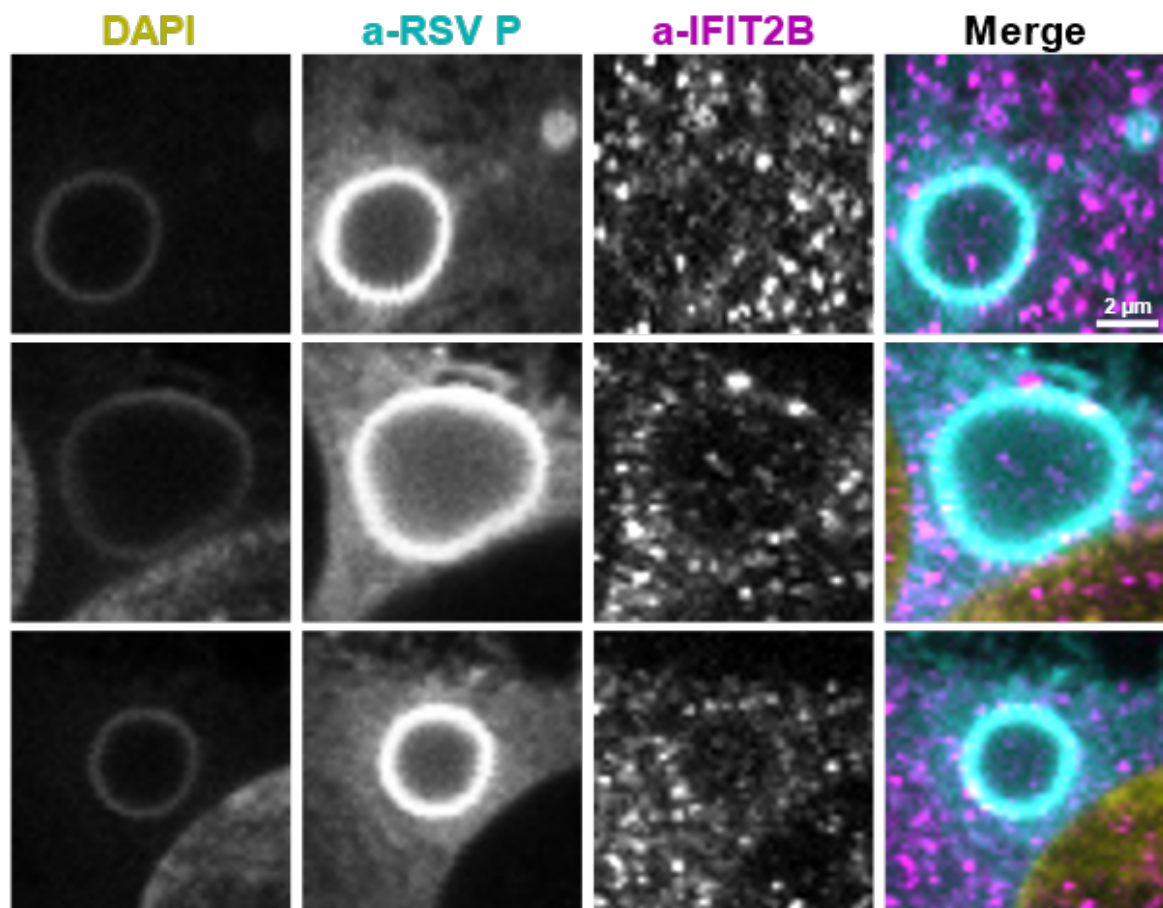


Figure 6.12: i2b a549 hrsv p

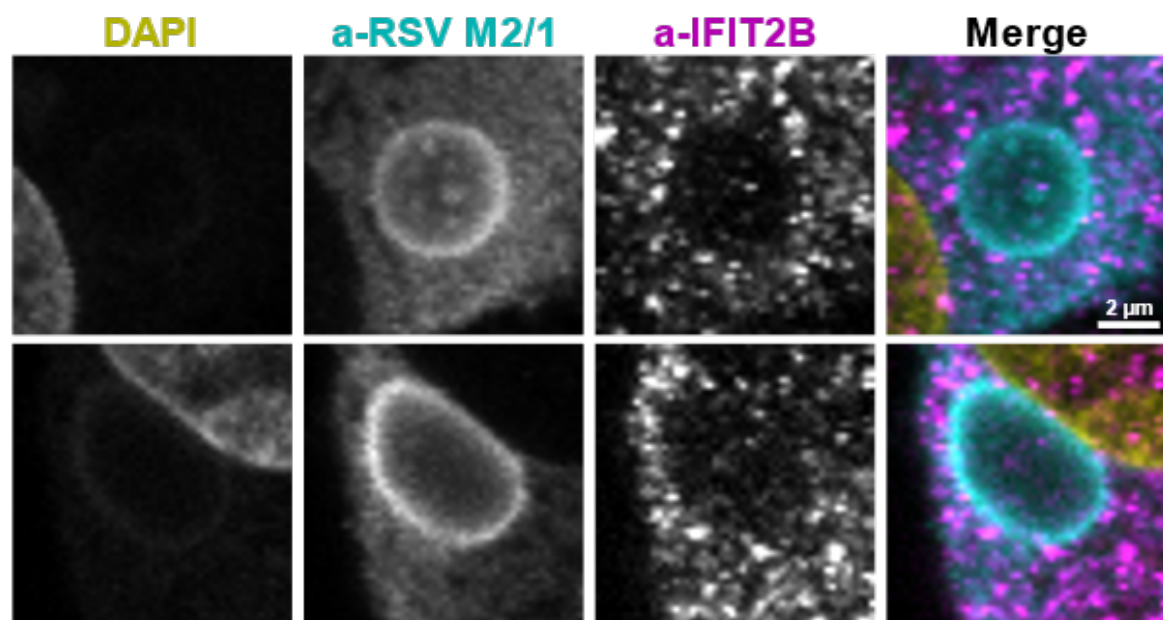


Figure 6.13: i2b a549 hrsv m21

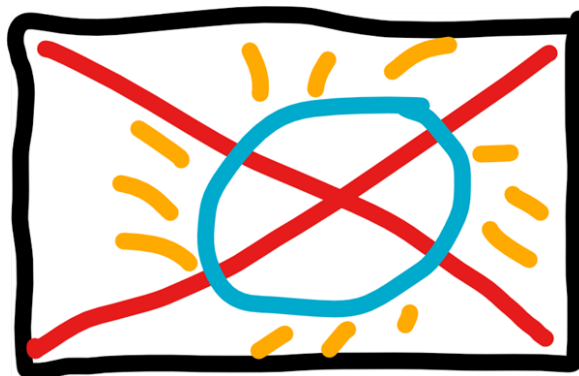


Figure 6.14: i2b beas2b hrsv

Detecting magenta: endogenous bovine IFIT2

Detecting cyan: bovine IB

Endogenous bovine IFIT2 localisation with respect to the bovine inclusion bodies shows a few different phenotypes. We see partial exclusion (top panel; signal still present in the middle of the IB structure), exclusion from IB ring and the inner IB edge (middle panel; highlighted with arrow) with IBAG-like concentrations inside the structure; and diffusion through the IB structure (bottom panel). These phenotypes are similar to what is observed during RSV infection of human but especially bovine IFIT3 and IFIT5.

6.2.4 Summary

Endogenous monkey IFIT2 is excluded from human pIB and the pIB associated filamentous network. Overexpressed human IFIT2-FLAG is detected by the antibody and shows inclusions inside the human pIB structures, which is consistent to data from IFIT2A staining and FLAG staining of IFIT2-FLAG overexpressed samples. Interestingly, IFIT2B antibody shows exclusion from the pIB filamentous network, which was colocalised by IFIT2A and FLAG antibodies. Nascent human IFIT2 shows full or partial exclusion from human IBs during human RSV infection. Nascent bovine IFIT2 during bRSV infections shows 3 different phenotypes. We observed partial exclusion; exclusion from the IB ring and inner edge with IBAG-like inclusions; and diffusion through the IB structure. This staining is similar to what is observed with bovine IFIT3 and IFIT5 during bRSV infection.

IFIT2 confocal story

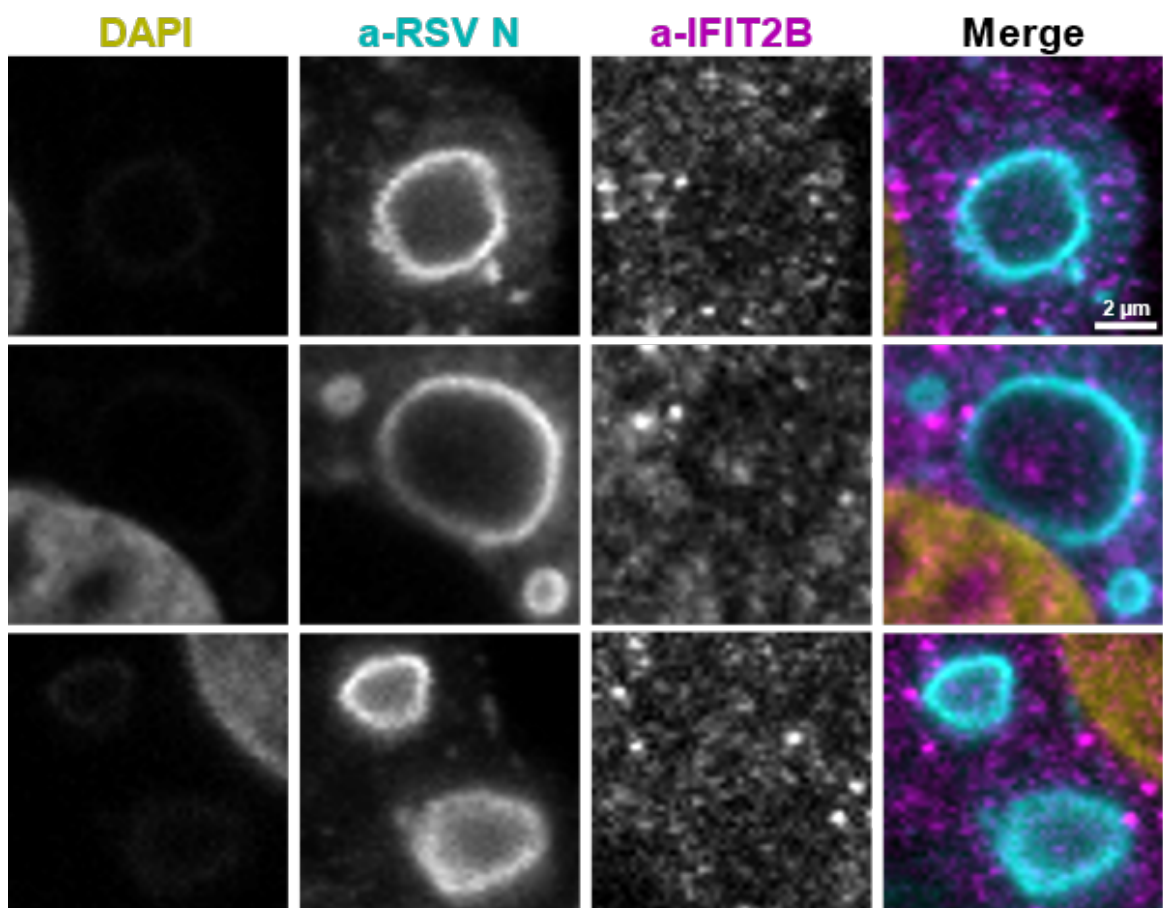


Figure 6.15: i2b mdbk brsv

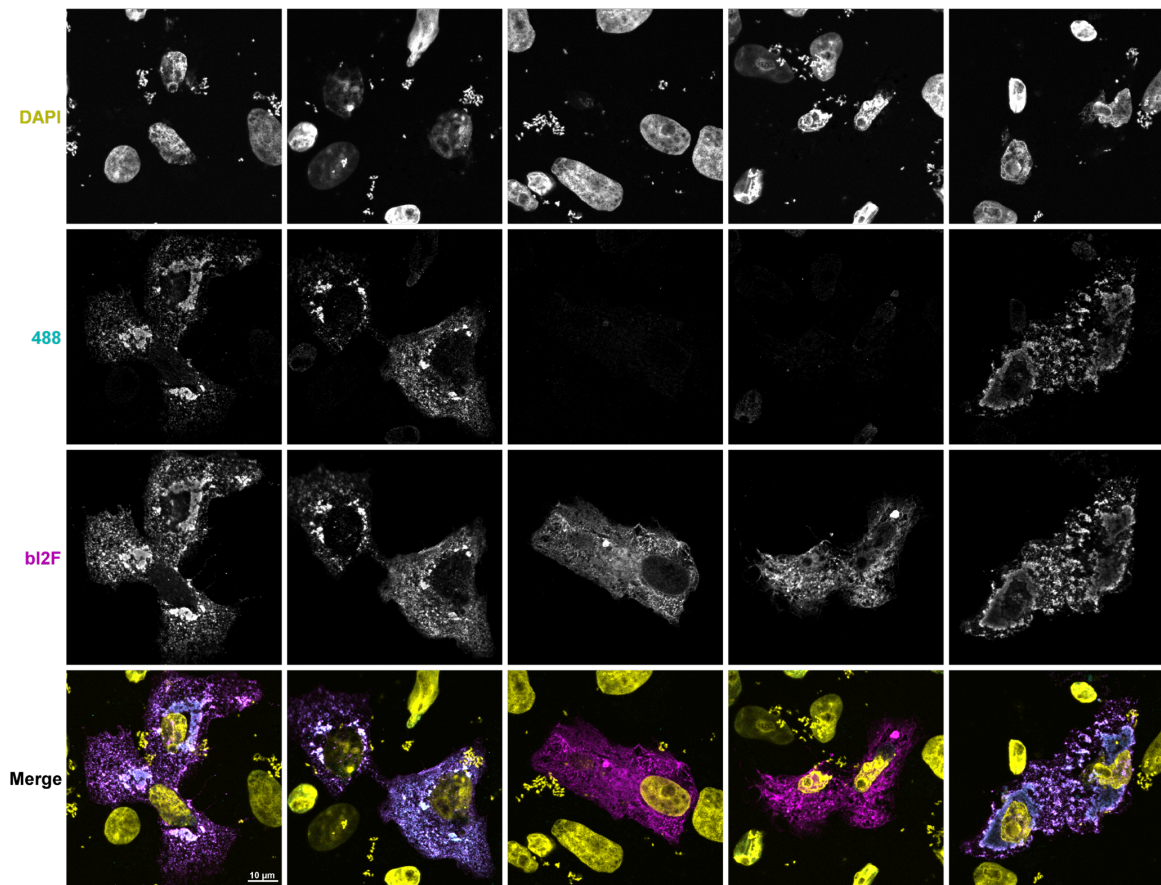


Figure 6.16: hi2f

6.2.5 IFIT2-FLAG

6.2.5.1 Impact of IFIT2-FLAG Expression in Mock Cells

6.2.5.1.1 hi2f

Cell Line: VERO

Treatment: hIFIT2-FLAG

Detecting magenta: exogenous human IFIT2

Detecting cyan: background

This data is for comparison with bIFIT2-RNA-binding mutant staining only. Some aggregations but the cells look reasonably healthy.

6.2.5.2 Exogenously Expressed IFIIT2-FLAG in a Simplified System of pseudo-IBs

IFIT2 confocal story

6.2.5.2.1 hi2f hnhp

Cell Line: VERO

Treatment: hNhP + hIFIT2-FLAG

Detecting magenta: exogenous human IFIT2

Detecting cyan: human pIB

Exogenously expressed human IFIT2 colocalises with the pIB associated filamentous net (top panel). It also forms inclusion inside the human pIB structures. This data is consistent with what we observed with IFIT2A antibody. IFIT2 also seems to occasionally form aggregates/spots (highlighted by arrows). These could be functional or just aggregates caused by overexpression, we do not know.

6.2.5.2.2 bi2f hnhp

Cell Line: VERO hSLAM

Treatment: hNhP + bIFIT2-FLAG

Detecting magenta: exogenous bovine IFIT2

Detecting cyan: human pIB

Exogenous bovine IFIT2 colocalises with the edge of human pIB structures. This is unusual as human IFIT2 data suggest inclusions with regards to pIBs.

6.2.5.3 Exogenously Expressed IFIT2-FLAG During RSV Infection

6.2.5.3.1 hi2f hrsv

Cell Line: VERO hSLAM

Treatment: hRSV + hIFIT2-FLAG

Detecting magenta: exogenous human IFIT2

Detecting cyan: human IB

Overexpressed human IFIT2 during hRSV infection shows several phenotypes (in this experiment). We see IFIT2 being excluded from the IB interior while being concentrated to the IB ring (top panel); IFIT2 forming concentrated inclusion inside the IB structure (2nd panel); IFIT2 being excluded from the IB interior but colocalising to the IB ring and forming spots inside of the IB (3rd panel); and IFIT2 being diffused evenly through the cytoplasm and the IB structure (last panel). The different phenotypes suggest that IBs are dynamic structures, and the localisation depends on factors we do not comprehend yet.

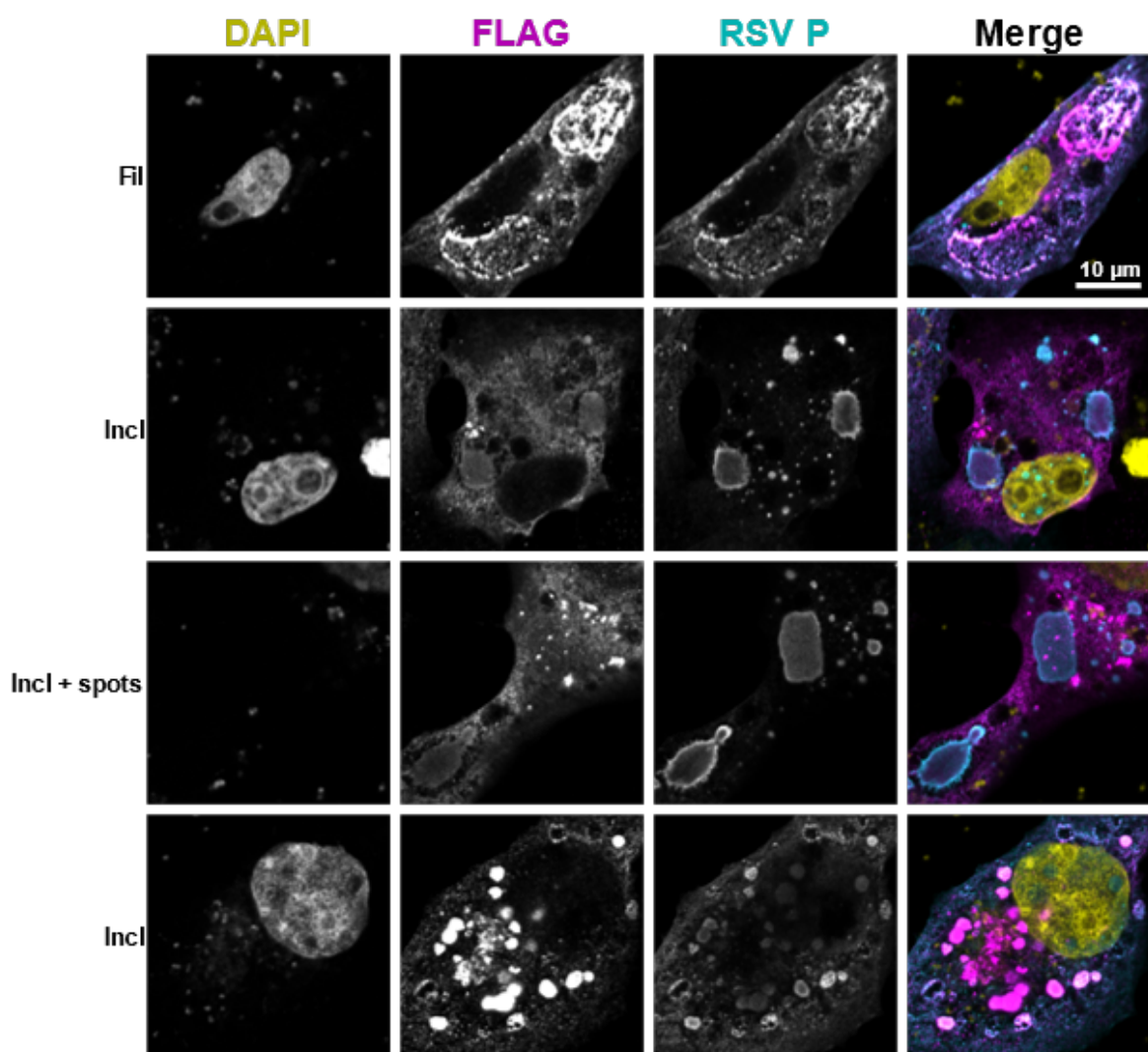


Figure 6.17: hi2f hnhp

IFIT2 confocal story

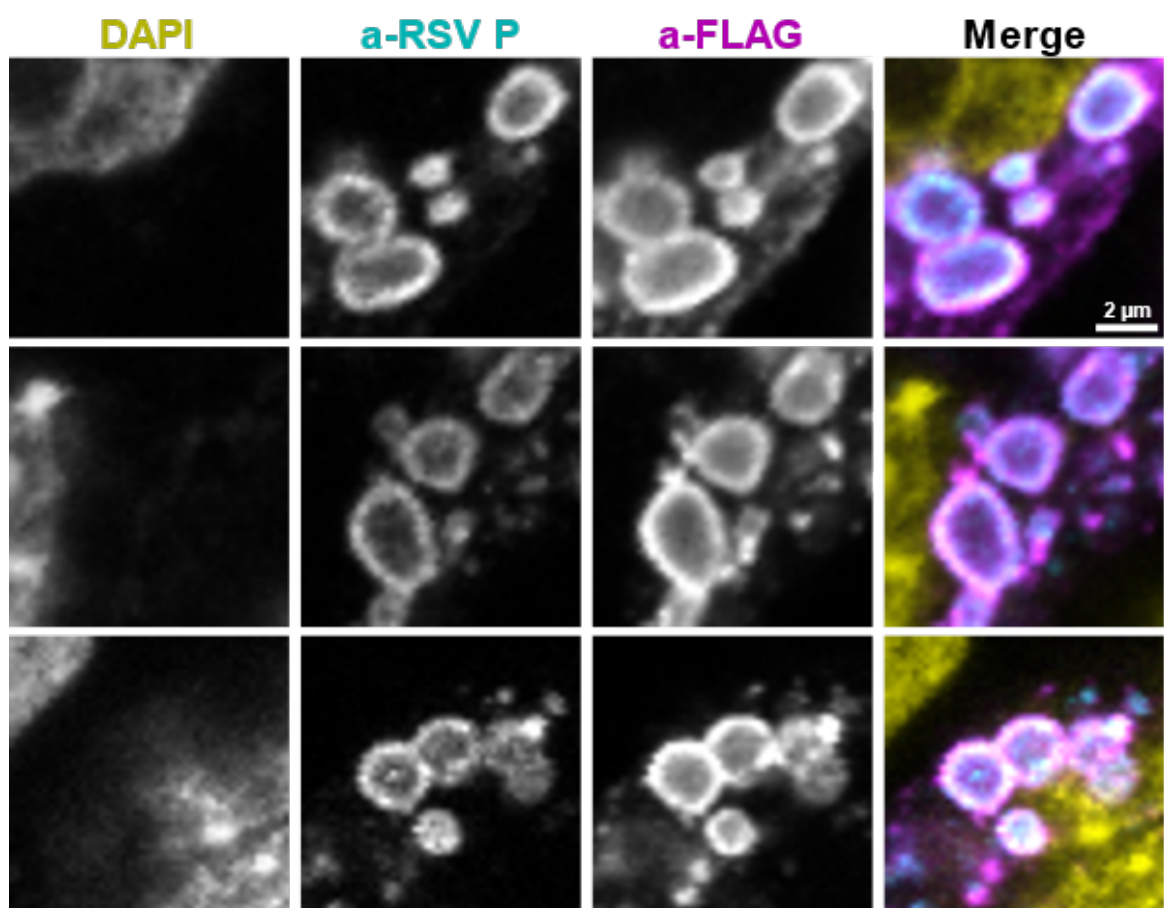


Figure 6.18: bi2f hnhp

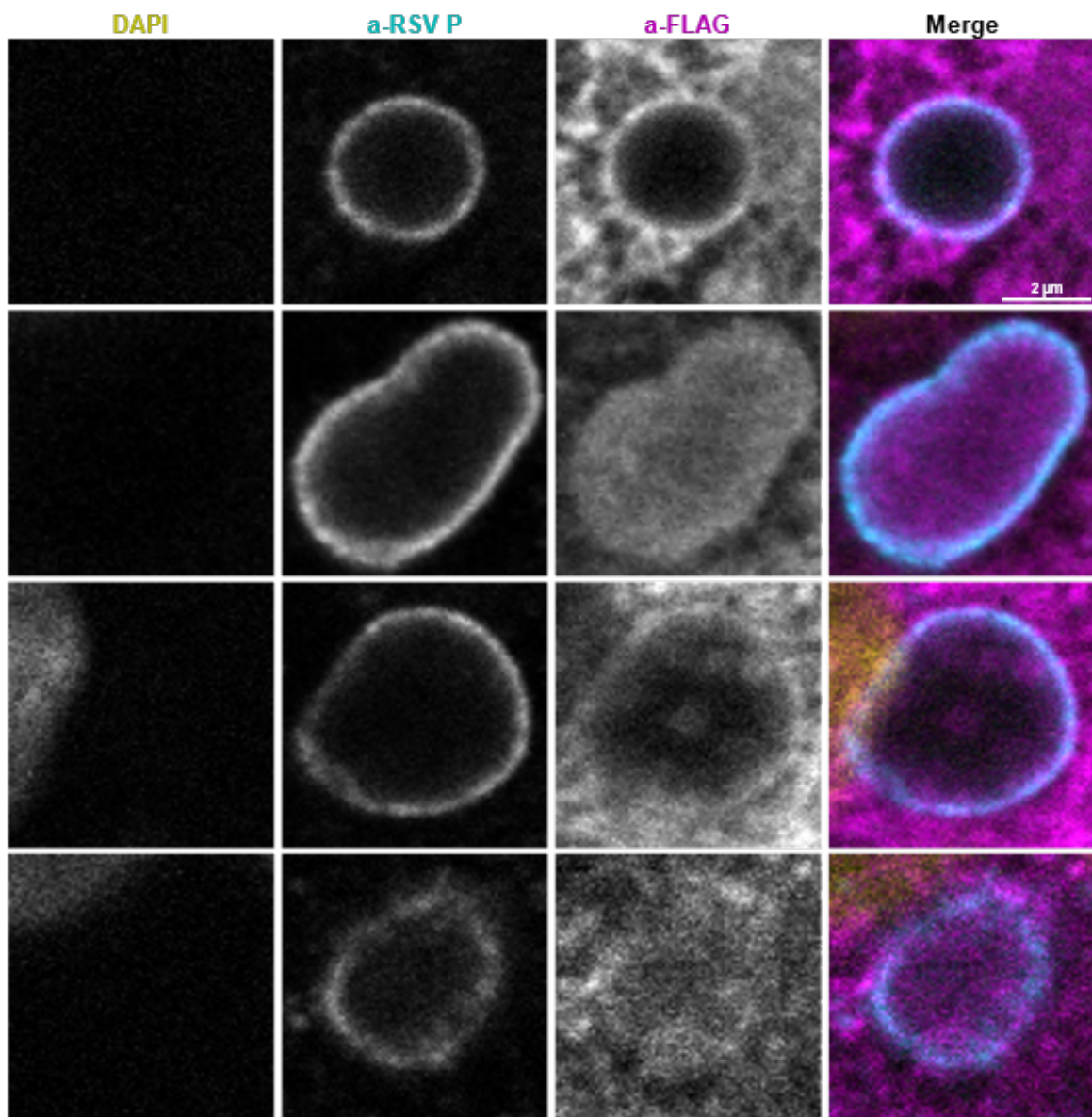


Figure 6.19: hi2f hrsv

IFIT2 confocal story

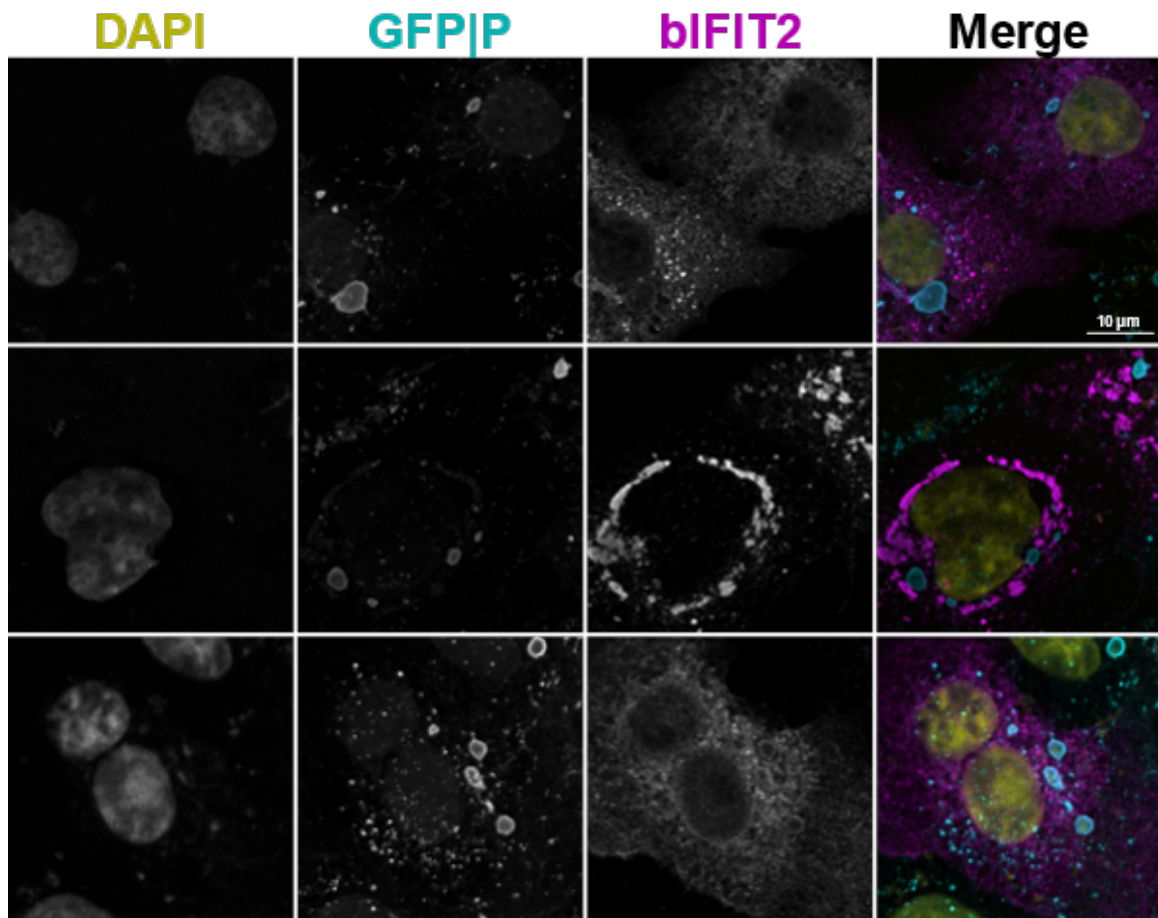


Figure 6.20: bi2f hrsV

6.2.5.3.2 bi2f hrsV

Cell Line: VERO

Treatment: hRSV + bIFIT2-FLAG

Detecting magenta: exogenous bovine IFIT2

Detecting cyan: human IB

In the follow up experiment, exogenous bovine IFIT2 in the context of human RSV infection shows the same two phenotypes. It is either excluded from the IBs (middle panel) or colocalises with the ring structure of the IBs (top and bottom panel; highlighted with arrows).

6.2.5.3.3 bi2f brsv

Cell Line: VERO

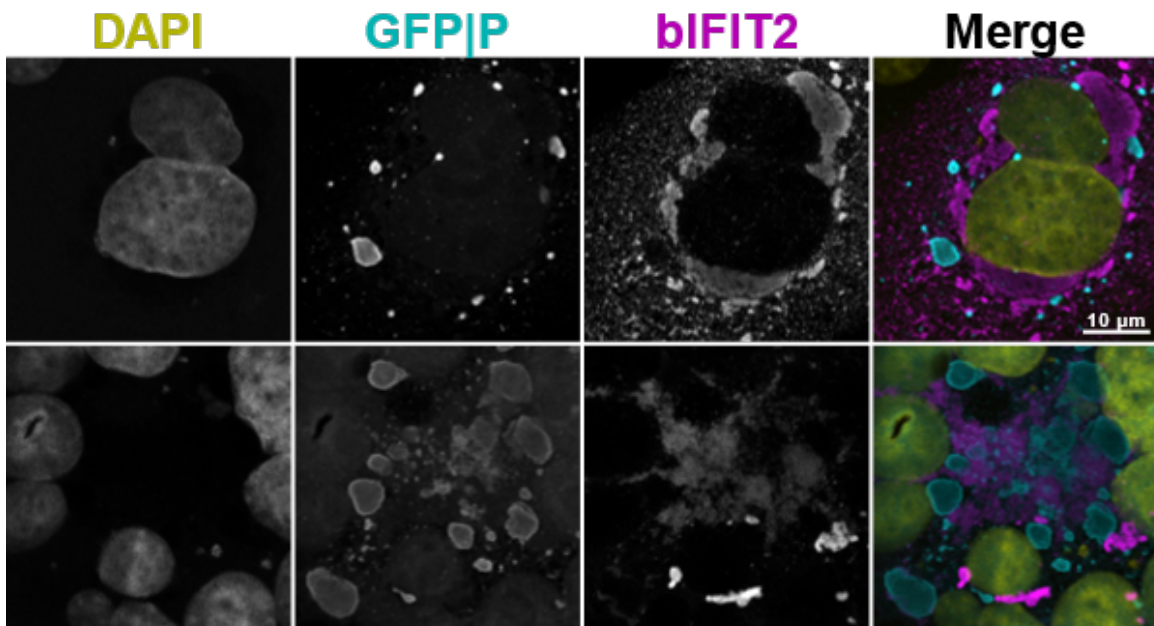


Figure 6.21: bi2f brsv

Treatment: bRSV + bIFIT2-FLAG

Detecting magenta: exogenous bovine IFIT2

Detecting cyan: bovine IB

Exogenous bovine IFIT2 during bovine RSV infection seems to be excluded from the inclusion bodies, although the data is not great and the IFIT2 is aggregated in both cells shown.

6.2.5.4 Summary

Overexpressing human IFIT2-FLAG does not seem to be detrimental to the cells. Exogenous human IFIT2 seems to form inclusions inside human pIB structures. It also colocalises with the pIB associated filamentous network. This data is consistent with IFIT2A antibody staining. IFIT2B staining showed inclusion inside pIB but failed to show the colocalization with the filamentous network. Exogenous bovine IFIT2 colocalises to the edge of human pIBs, which is in contrast to what we see with endogenous and exogenous human IFIT2 and its interaction with human pIBs. Exogenous human IFIT2 during human RSV infection showed different phenotypes in 2 different experiments. In the first experiment we observed it to: form inclusions inside the IB structure; be excluded from IB but colocalise to the IB ring; be excluded from the IB but colocalise to the ring and have spots inside the IB structure;

IFIT2 confocal story

or to be diffused through cytoplasm and IB equally. In the second experiment we observed it to be either completely excluded from the IBs or to colocalise with them. Exogenous bovine IFIT2 during human RSV infection was either completely excluded from the IB or was colocalised to the ring of the structure. This was consistently seen in both experiments conducted. Exogenous bovine IFIT2 during bovine RSV infection seems to be excluded from the IBs.

6.2.6 IFIT2AB Discussion

6.2.6.1 Discussion About Differences Seen Between the Two Antibodies in Previous Subchapter

IFIT2A shows monkey IFIT2 forming inclusion within the pIB structure, while also colocalising with the pIB-associated filamentous network. IFIT2B shows exclusion from both pIB and the filaments.

IFIT2A shows overexpressed hIFIT2-FLAG to form inclusion inside the pIBs and colocalization with the filamentous network. IFIT2B also shows inclusion inside the pIBs but shows potential exclusion from the filamentous network. IFIT2A shows colocalization to the ring and inner edge of human IBs with occasional inclusions. IFIT2B shows complete and partial exclusion from the human IB structures.

IFT2A shows bovine IFIT2 colocalisation to the with the ring structure of bovine IBs. IFIT2B shows partial exclusion; exclusion from the IB ring and inner edge with IBAG-like inclusions; and diffusion through the IB structure.

6.2.6.2 Differences Between the Two Antibodies Other Than IB Staining

6.2.6.2.1 Human Protein Atlas Show Cytoplasmic Localisation Similar to IFIT2B

IFIT2A antibody shows mainly cytoplasmic distribution (although some spots are visible)
IFIT2B shows mainly granular/vesicular distribution.

Human protein atlas shows vesicular distribution of IFIT2. Side note: second figure from section 1.1.1.2.3 shows cytoplasmic staining (like IFIT2A, but kinetochore microtubule staining (like IFIT2B).

6.2.6.2.2 P Transfection Induces IFIT2A Signal but not IFIT2B Signal

Cell Line: 293T

Treatment: hN and/or hP (EV – empty vector)

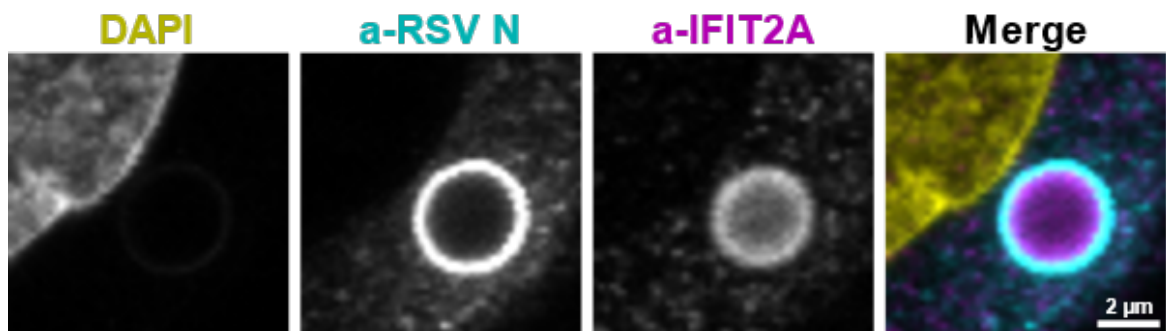


Figure 6.22: example ifi2a hrsv

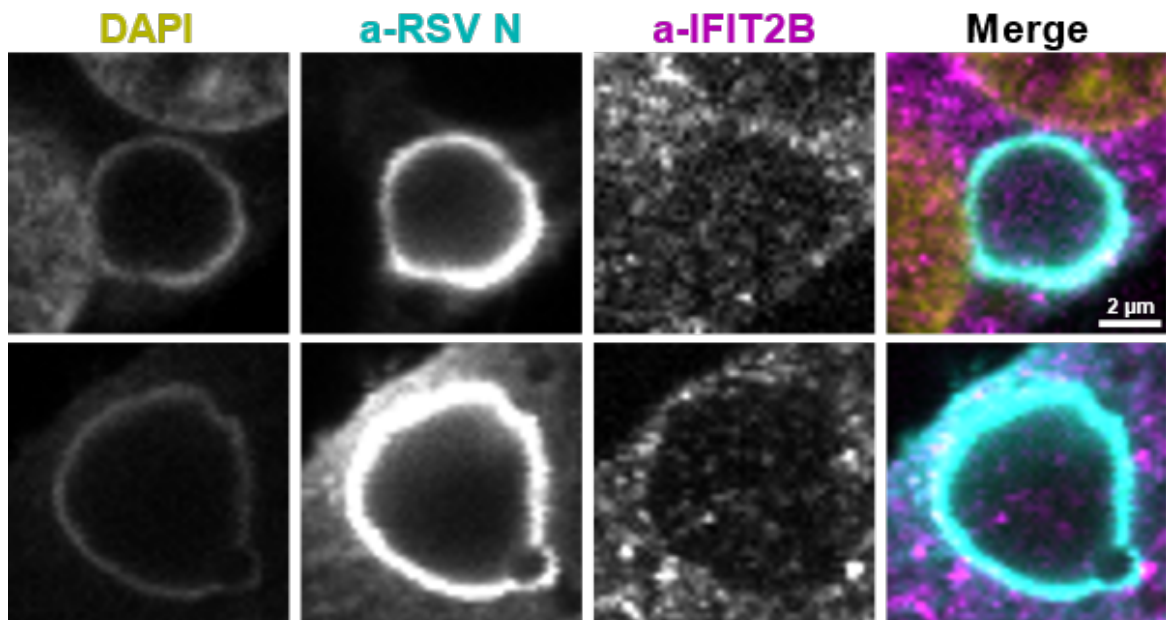


Figure 6.23: example ifi2b hrsv

IFIT2 confocal story

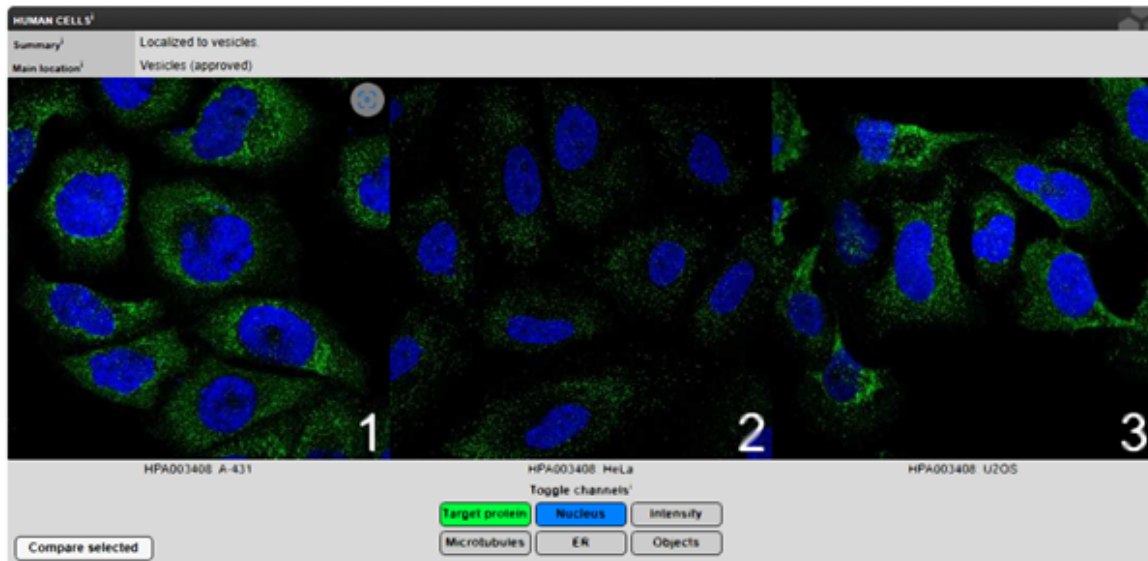


Figure 6.24: human protein atlas ifit2

Detecting magenta: endogenous human IFIT2 (A)

Detecting cyan: N and/or P

IFIT2 induction detected in hP and hP + hN conditions, suggesting that transfection of P induces IFIT2 expression (but this does not happen with IFIT1 or IFIT3 in the same cells). About the different genomic regulation landscape... why does IFIT2 get induced but not other IFITs (within human genome which is well annotated)? Side note: No kinetochore microtubule staining (especially in first panel)

Cell Line: 293T

Treatment: hN and/or hP (EV – empty vector)

Detecting magenta: endogenous human IFIT2 (B)

Detecting cyan: N and/or P

No detected IFIT2 induction in any of the conditions. Side note: We can see kinetochore microtubule staining, especially in the first row.

6.2.6.2.3 IFIT2B but not IFIT2A Stains Kinetochore Microtubules

Cell Line: MDBK

Treatment: bRSV + bIFNa

Detecting magenta: endogenous human IFIT2 (B)

Detecting cyan: bovine IBs

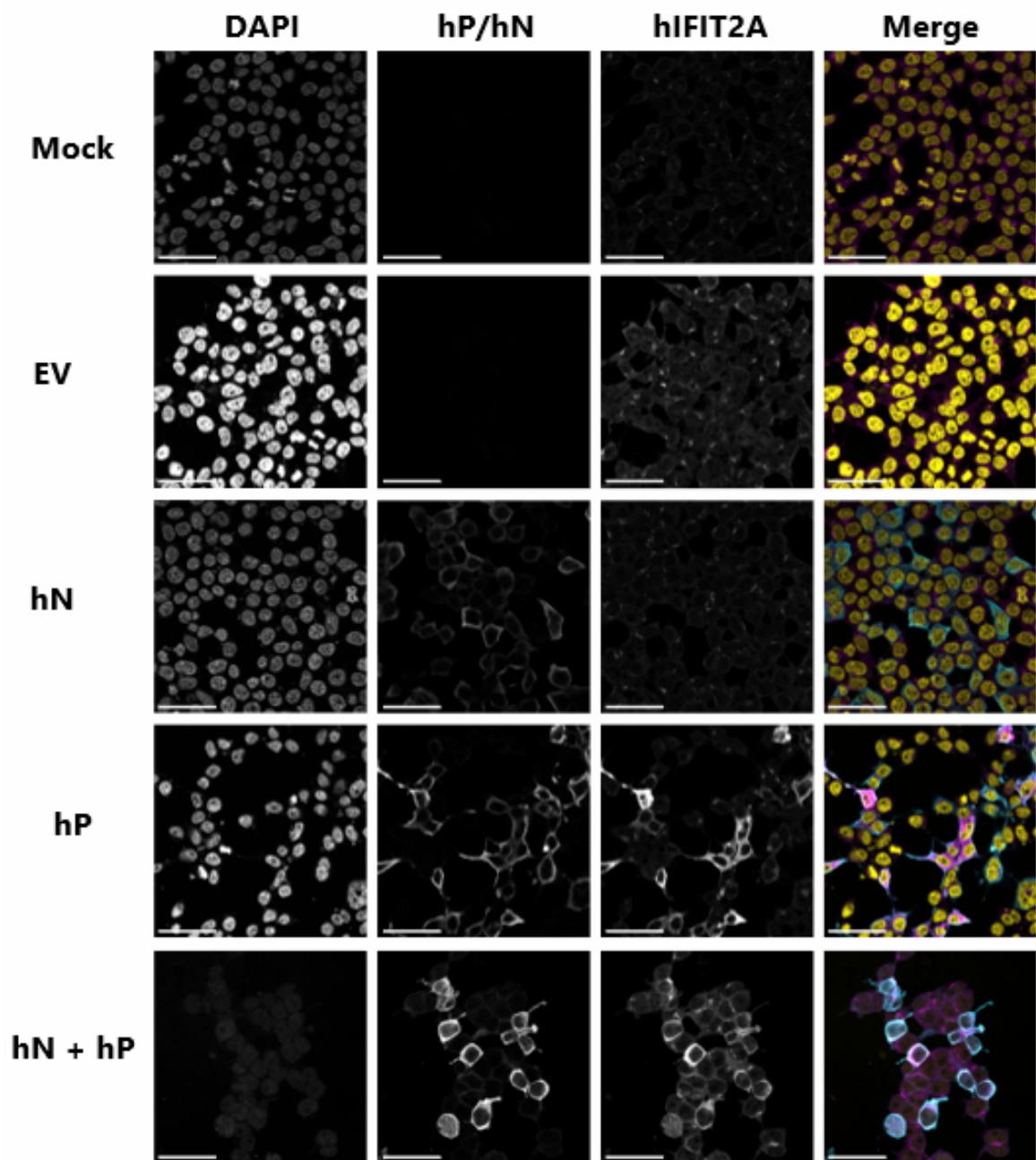


Figure 6.25: ifit2a p transfection

IFIT2 confocal story

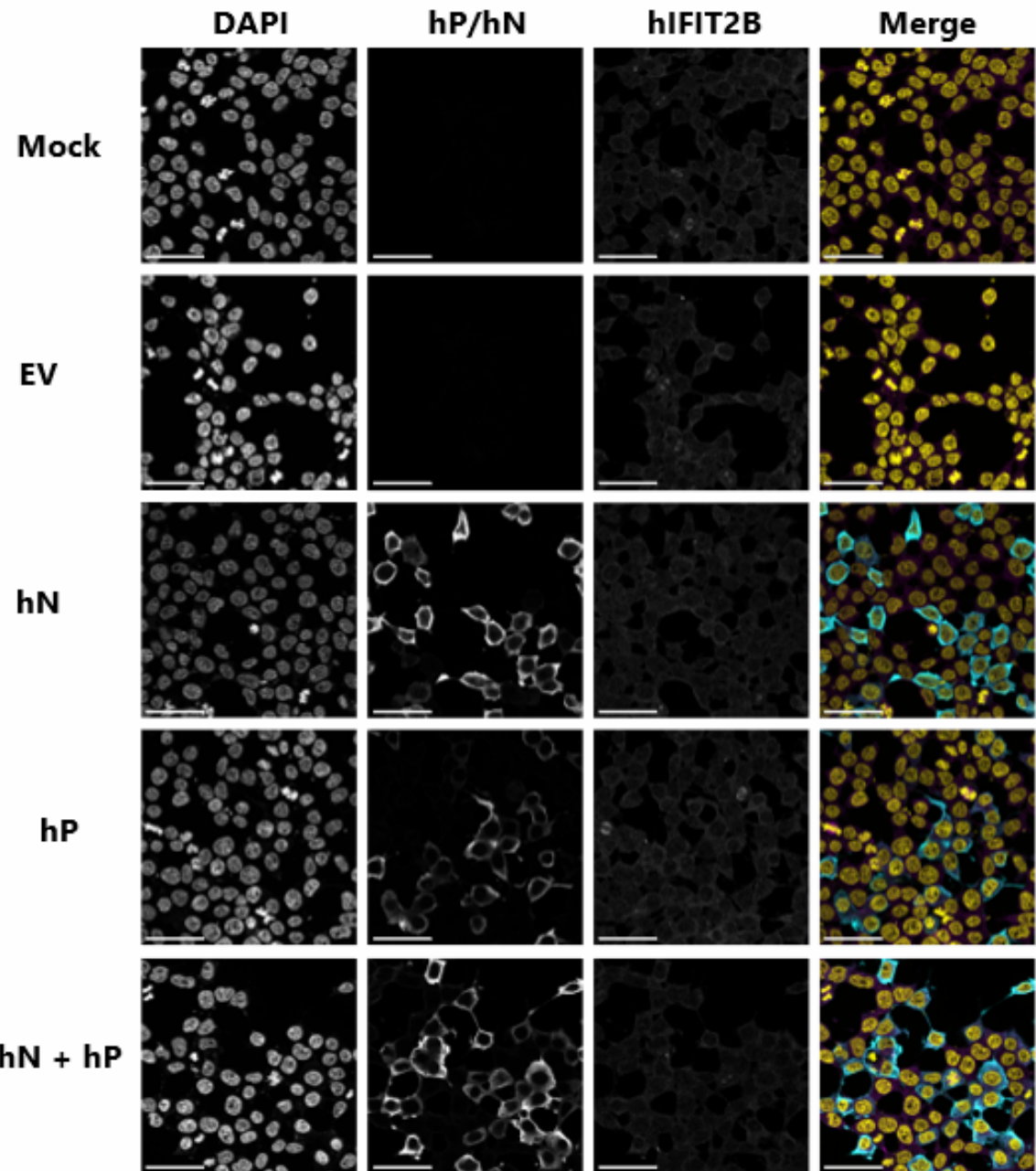


Figure 6.26: ifit2b p transfection

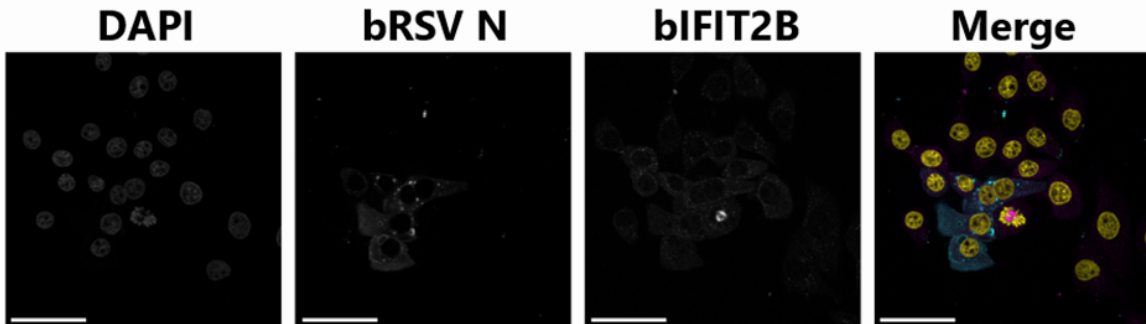


Figure 6.27: kinetochores

IFIT2B antibody consistently stains kinetochore microtubules in all cells regardless of the condition. This was figure that I had done already which had the kinetochore microtubule staining present, hence I included it here. I found only one minor paper about IFIT2 localisation that shows the same staining. Literature search looking at kinetochore proteomes never mentioned IFIT2, neither papers about anaphase/metaphase proteome.

This is figure from the paper that mentions mouse IFIT2 (GARG39) to be associated with microtubules during the different phases of cell cycle. Side note: The IFIT2 distribution is cytoplasmic and not vesicular, like human protein atlas suggests.

6.2.6.2.4 WB antibody validation

Western blots below are a validation of IFIT antibodies cross-reactivity. They are 293T cells transfected with empty vector or highlighted IFITs.

We see less material to be present in bovine samples, especially bovine IFIT3 sample.

IFIT2A antibody detects overexpressed human and bovine IFIT2, while also detecting overexpressed human and bovine IFIT3. We see differential staining between IFIT2A and IFIT3 antibody, hence we can conclude that IFIT2A is not detecting IFIT3 in IF analyses. IFIT2A is also detecting a moiety at 25 kDa, which we do not know the origin of (cellular sources as it is present in empty vector as well).

IFIT2B antibody detects human IFIT2. It fails to detect bovine IFIT2, however, this could be due to lower reactivity with the bovine IFIT2 and/or lower expression levels in that sample. Unlike in IFIT2A antibody, we see no reactivity with IFIT3. As with IFIT2A antibody, we are detecting 25 kDa moiety in all conditions.

IFIT2 confocal story

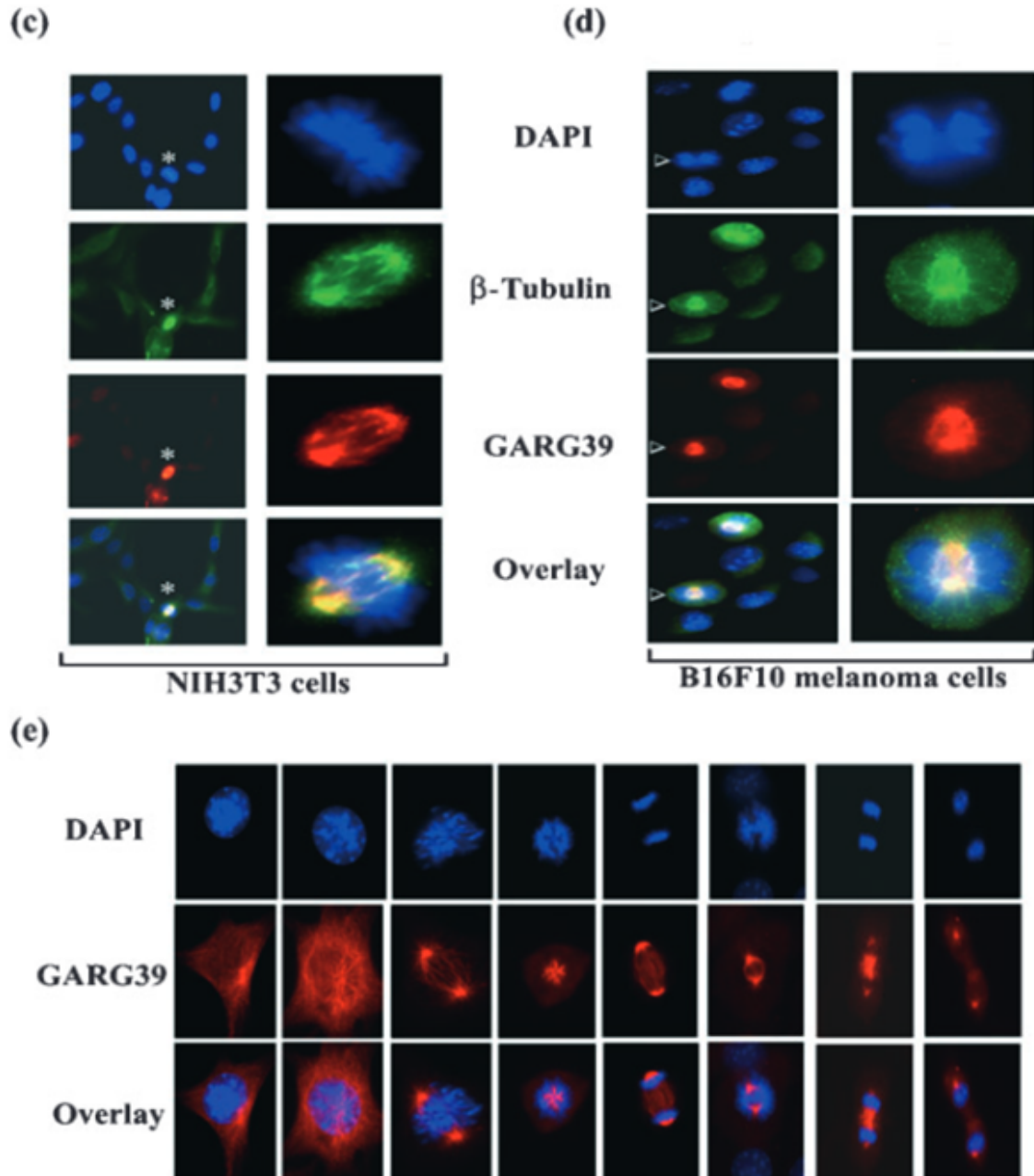


Figure 6.28: kinetochore published figure

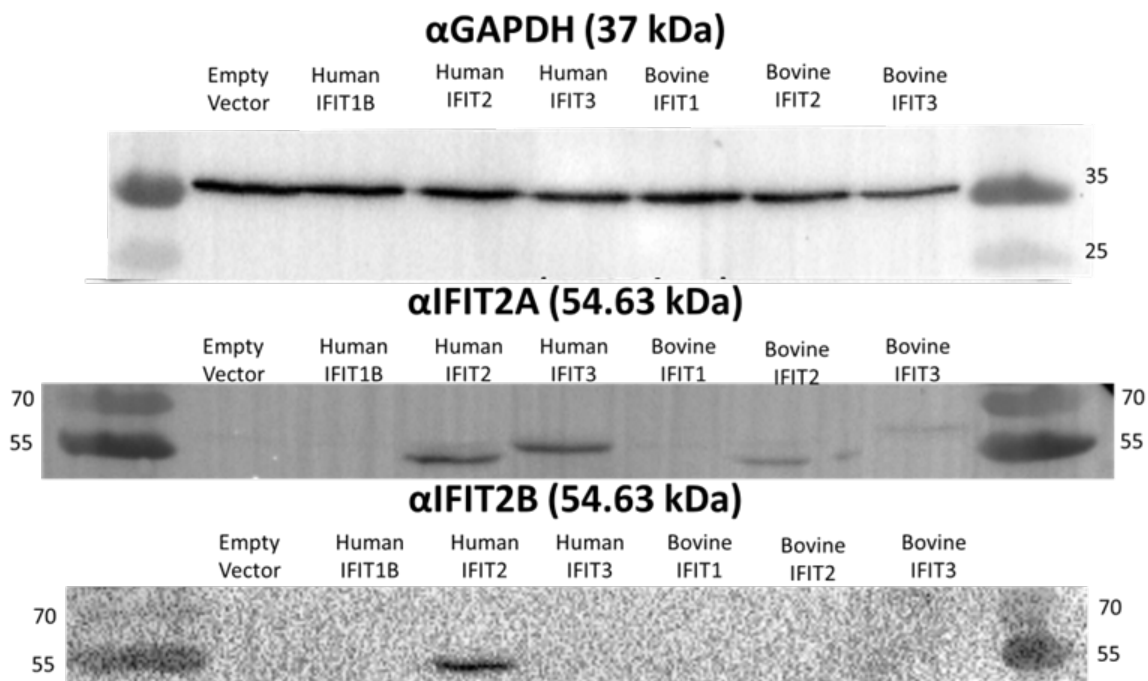


Figure 6.29: ifit2 antibodies figure

6.2.6.3 Summary

We were thinking that the differential staining between IFIT2A and IFIT2B antibodies could be due epitope masking (due to e.g. RNA interaction; interaction with other IFITs; interaction with other cellular proteins; interaction with viral proteins) but although both of the antibodies seem to detect IFIT2 in western blots, they differ quite substantially in other aspects. One fails to capture induction caused by P transfection, while the other fails to capture kinetochore microtubule staining.

6.2.7 Confocal of RNA-binding mutant

Using published data about hIFIT2 rna-binding mutant

Difficulty of using alpha-fold with IFIT2 due to the swap domain

Using SWISS-MODEL to predict bIFIT2 structure from published hIFIT2 structures

Alignment of both structures, assessment of electrostatic charges and establishment of residues to be mutated

Primer design and mutagenesis procedure based on published hIFIT2 RNA-binding mutant paper

IFIT2 confocal story

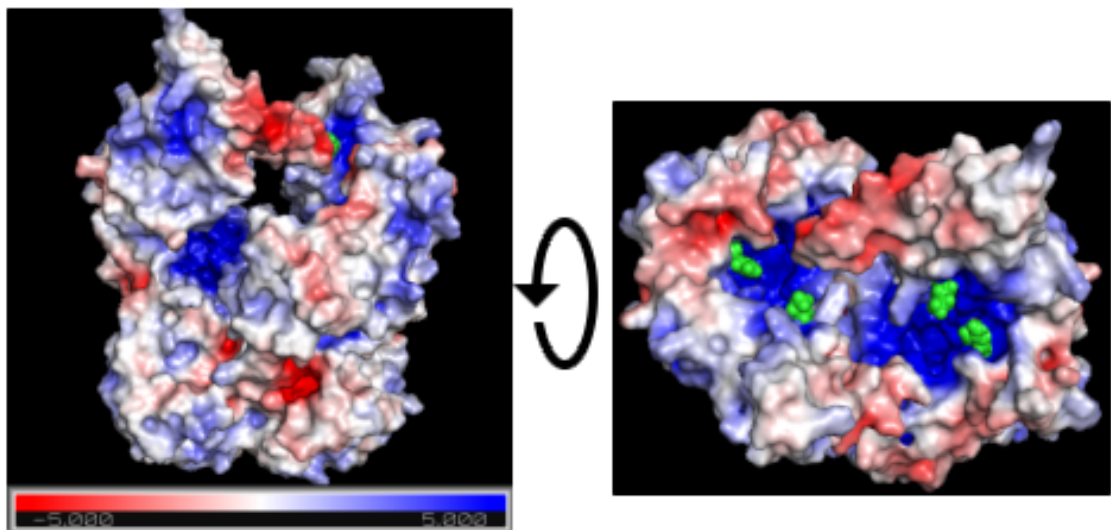


Figure 6.30: ifit2 mutant structure

6.2.7.1 i2f-24

6.2.7.1.1 bi2f24

Cell Line: VERO Treatment: bIFIT2-FLAG-RBM Detecting magenta: exogenous bovine IFIT2 RBM Detecting cyan: background

Exogenous bovine IFIT2 RNA-binding mutant (RBM) seems to have the same distribution and effect on the cell as human IFIT2-FLAG overexpression.

6.2.7.2 pIB

6.2.7.2.1 bi2f24 + hnhp

Cell Line: VERO Treatment: hNhP + bIFIT2-FLAG-RBM Detecting magenta: exogenous bovine IFIT2 RBM Detecting cyan: human pIB

In the second experiment we see consistent colocalization and/or inclusion of bovine IFIT2 RNA-binding mutant with human pseudo inclusion bodies.

6.2.7.3 Summary

We have described how bovine IFIT2 RNA-binding mutant was designed based on the published human IFIT2 RNA-binding mutant data (needs to be annotated more). Overexpression of bovine IFIT2 RNA-binding mutant yields cellular distribution and morphology similar to what was observed with overexpressing human IFIT2-FLAG, suggesting that the

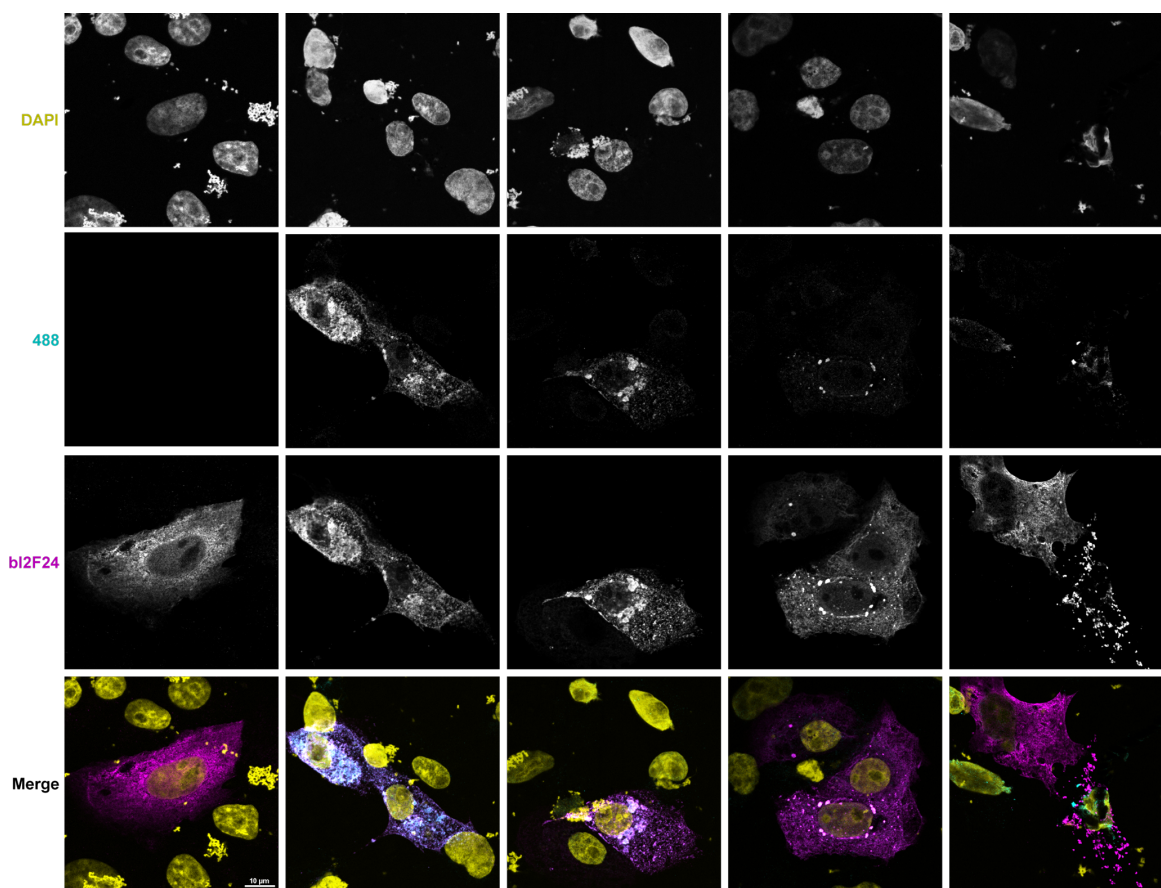


Figure 6.31: bi2f24

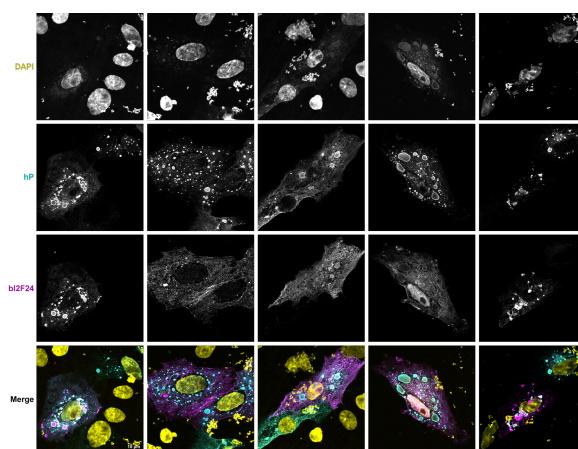


Figure 6.32: bi2f24 + hnhp

IFIT2 confocal story

mutant proteins are not toxic to the cells. In the first experiment where we were looking at interaction between bovine IFIT2 RNA-binding mutant and human pseudo inclusion bodies we saw several phenotypes. We observed bovine IFIT2 RNA-binding mutant being excluded from small and big pIBs and pIB associated filamentous network, while fully or partially colocalising with other pIBs. In a subsequent experiment we observed only colocalization and inclusion formation. When assessing the interaction between bovine IFIT2 RNA-binding mutant and human pIBs formed using wild-type human RSV P and GFP-tagged human RSV N, we observed consistently in two experiments that bovine IFIT2 RNA-binding mutant colocalises to the pIB structures.

6.2.8 Liquid-Liquid Phase Separation

Add stuff about likelihood of IFIT and viral proteins and their propensity to phase separate
This is using a online tool called PSPredictor

6.3 Discussion

asdfasdf

Chapter 7

Discussion and Conclusion

7.1 Discussion

lorem ipsum

7.2 Conclusion

lorem ipsum

7.3 Future Directions

to become a baker